2006

Characterization of the TCOF1 Gene Using a Neuroblastoma Cell Line and a Mouse Model

Lin Li
Virginia Commonwealth University

CHARACTERIZATION OF THE *TCOF1* GENE USING A NEUROBLASTOMA CELL LINE AND A MOUSE MODEL

A dissertation submitted in partial fulfillment of the requirements for the degree of Doctor of Philosophy at Virginia Commonwealth University.

by

LIN LI
Master in Genetics, Qingdao Medical School, China, 2000
Doctor in Medicine, Shandong Medical University, China, 1997

Director: Rita Shiang, Ph.D.
Associate Professor, Department of Human Genetics

Virginia Commonwealth University
Richmond, Virginia
June, 2006

Acknowledgement

I would like to express my gratitude to my advisor, Dr. Rita Shiang, for her support, advice and mentoring throughout my graduate studies, for teaching everything I learned in research. I truly appreciate that she made my graduate study a fun experience. And I am especially grateful for her patience and encouragement during difficult times.

I would like to express my special thanks to my committee members Dr. Joyce Lloyd, Dr. Jolene Windle, Dr. Shawn Holt and Dr. Shirley Taylor. I could not complete this dissertation without their guidance and great suggestions. Thanks for taking their time to help me with my research and all my questions. I would also like to thank all former and present Shiang's lab members, Dr. Kate Shows, Guangan Li, Dr. Sinitdhorn Rujirabanjerd, Dr. Michael Mogass, Christy Ward and Cindy Heisey for their friendship, encouragement and help. I am fortunate to have the opportunity to work with them.

I would like to thank Dr. Colleen Jackson-Cook and Dr. Catherine Rheder and for their help with cytogenetics techniques and Helen Zhang for her mouse expertise. I would like to thank Caroline Harding and Rex Scudder for treating me like a family member. I thank Sami Amr, Mariam Fida and Sarah Bergen for their friendship, support and encouragement.

Finally, and most importantly, I would like to thank my parents Yuhua Li and Qiuting Yuan, my brother Bing Li, and my boyfriend Rong Zuo for their love, support and trust. I would also like to thank Rong for his help with figures. I could not have done this without my friends and family.

Table of Contents

List of Tables

Page

List of Figures

Page

List of Abbreviations

BA ..... Branchial arch

bHLH-Zip ..... Basic helix-loop-helix leucine zipper

BMP ..... Bone morphogenetic protein

BrdU ..... Bromodeoxyuridine

CAT ..... Chloramphenicol acetyl transferase

CD ..... Cytosine deaminase

Cnbp ..... Cellular nucleic acid binding protein

CNC ..... Cranial neural crest

DFC ..... Dense fibrillar component

DMEM ..... Dulbecco's minimal essential medium

EMT ..... Epithelial to mesenchymal transition

FBS ..... Fetal bovine serum

FC ..... Fibrillar centers

FGF ..... Fibroblast growth factor

GC ..... Granular component

KD ..... Knockdown

NB ..... Neuroblastoma

NC ..... Neural crest

NLS ..... Nuclear localization signal

NoLS ..... Nucleolar localization signal

NOR ..... Nucleolar organizing regions

OE ..... Overexpression

PAGE ..... Polyacrylamide gel electrophoresis

PCNA ..... Proliferating nuclear antigen

PKC ..... Protein kinase C

Pol I ..... Polymerase I

PVDF ..... Polyvinylidene fluoride

rRNP ..... .ribosomal ribonucleoprotein

SDS ..... Sodium Dodecyl Sulfate

snRNP ..... .Small nuclear ribonucleoprotein

snoRNP ..... Small nucleolar ribonucleoproetin

TCS ..... Treacher Collins syndrome

TGF ..... Transforming growth factor

TK ..... Thymidine kinase

TUNEL ..... TdT-mediated dUTP-X nick end labeling

UBF ..... Upstream binding factor

UTR ..... Untranslated region

ZNF ..... Zinc finger protein

Abstract

Characterization of the *Tcof1* gene using a neuroblastoma cell line and a mouse model

By Lin Li, M.S.

A dissertation submitted in partial fulfillment of the requirements for the degree of Ph.D. at Virginia Commonwealth University.

Virginia Commonwealth University, 2006

Major Director: Rita Shiang, Ph.D.
Associate Professor, Department of Human Genetics

Treacher Collins syndrome (TCS) is an autosomal dominant craniofacial development disorder and is caused by mutations in the *TCOF1* gene. The TCOF1 protein treacle is a nucleolar protein and may function in ribosome biogenesis.

Previously, we identified downstream candidate genes using microarray analysis after manipulating Tcof1 levels in a murine neuroblastoma (NB) cell line. The list of genes includes cell cycle genes as well as the transcription factors Cnbp and Tbx2, which are known to affect the cell cycle through the c-myc and p19-Mdm2-p53-p21 pathways respectively. To further characterize the cellular effects of Tcof1, stably transfected NB cell lines with overexpression or knockdown of Tcof1 were generated. Growth curves

were generated by counting cell numbers. BrdU incorporation and TUNEL assays were used to determine proliferation and apoptosis levels. Western blot analysis was used to detect protein level changes of candidate downstream pathway genes. Both overexpression and knockdown of Tcof1 are detrimental to cell growth. Overexpression of Tcof1 causes increased apoptosis and knockdown of Tcof1 causes reduced cell proliferation and increased apoptosis. Western blot analysis shows that Cnbp and Tbx2 protein levels change with Tcof1, c-myc level is decreased in Tcof1 knockdown cells and p19 (Cdkn2d), p53 and p21 (Cdkn1a) levels are increased in Tcof1 overexpressing cells. Our results suggest that an optimal Tcof1 level is required for cell proliferation and survival, and that overexpression and knockdown of Tcof1 may affect cell proliferation and apoptosis through the p19-Mdm2-p53-p21 and Cnbp-c-myc pathways respectively.

Heterozygous Tcof1 knock out mice are neonatal lethal, which circumvents further analysis of the heterozygous and homozygous mice. In this study, we generated Tcof1 conditional allele mice with loxP sites flanking exon 1. These mice were crossed with Wnt1-Cre transgenic mice to generate a conditional knockout of Tcof1 specifically in neural crest (NC) cells. Homozygous conditional knockout mice show craniofacial abnormalities resembling TCS patients. Heterozygous conditional knockout mice are phenotypically normal, which suggests that Tcof1 functions in tissues other than NC cells during development. Cnbp expression is decreased in a proportion of the homozygous conditional knockout mouse embryos. Our results suggest that Tcof1 may affect craniofacial development through Cnbp by maintaining cell growth.

Chapter 1: Background and literature review

Introduction

Treacher Collins syndrome (TCS), alternatively called mandibulofacial dysostosis (MFD), is an autosomal dominant craniofacial development disorder (Rovin et al., 1964). TCS is generally characterized by bilateral symmetric abnormalities in facial skeleton structures derived from the first and second branchial arches. In 1846, A. Thomson reported the first case of TCS, and in 1900, Dr. Edward Treacher Collins described the essential components of this syndrome (Collins, 1900). TCS has an incidence of approximately one in 50,000 live births, with 60% of cases arising from *de novo* mutations (reviewed by Gorlin et al., 1990; Jones et al., 1975).

The main features of TCS include hypoplastic facial bones, especially the mandible and zygomatic arches, and lateral downward slanting palpebral fissures with colobomas of the lower eyelids and a lack of eyelashes medial to the defect. Moderate to severe conductive hearing loss and cleft palate are sometimes present. Conductive hearing loss is usually caused by deformities of the external or middle ear, including absent, malformed or malposed external ears, closed external auditory canals and malformed middle ear ossicles (reviewed by Dixon, 1996). The degree of malformation present at birth is believed to be relatively stable and not progressive with age (Posnick and Ruiz,

2000). However, patients with TCS exhibit extreme variation in the severity of craniofacial characteristics both within and between families. While nonpenetrance is rare, the variation in the phenotype, coupled with high new mutation rate, makes diagnosis and genetic counseling challenging. Current treatment for TCS involves a series of surgical procedures staged with facial growth patterns, visceral function, and psychosocial needs. Because of the variable expressivity, the treatment plan needs to be tailored to patient's specific problems (Marszalek et al., 2002).

Craniofacial development

The tissues affected in TCS arise from the first and second branchial arches (BAs, also called pharyngeal arches) during early embryogenesis. The first arch gives rise to the maxillary and mandibular processes, the incus and malleus bones of the middle ear ossicles, the zygomatic bone and the upper and lower lips. The second arch gives rise to the external ear, the tongue and the stapes bone of the middle ear (Moore and Persaud, 1993).

1. Neural crest cells

Neural crest (NC) cells have been shown to make a major contribution to the mesenchymal component of BAs in vertebrates. NC cells are multipotent migratory embryonic cells that form by inductive interactions at the border of the neural and epidermal ectoderm (Figure 1A). Neural ectoderm derived neural plate cells invaginate to form the neural fold. The neural fold later fuses at the midline to form the neural tube.

A

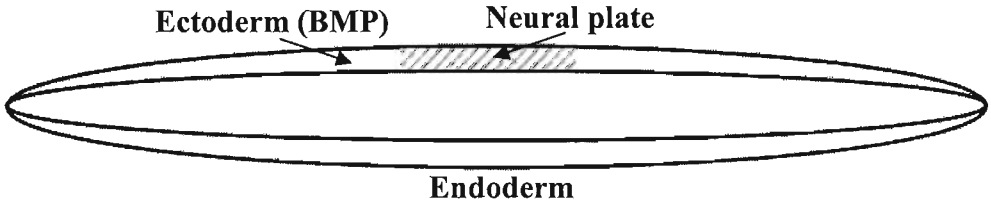

B

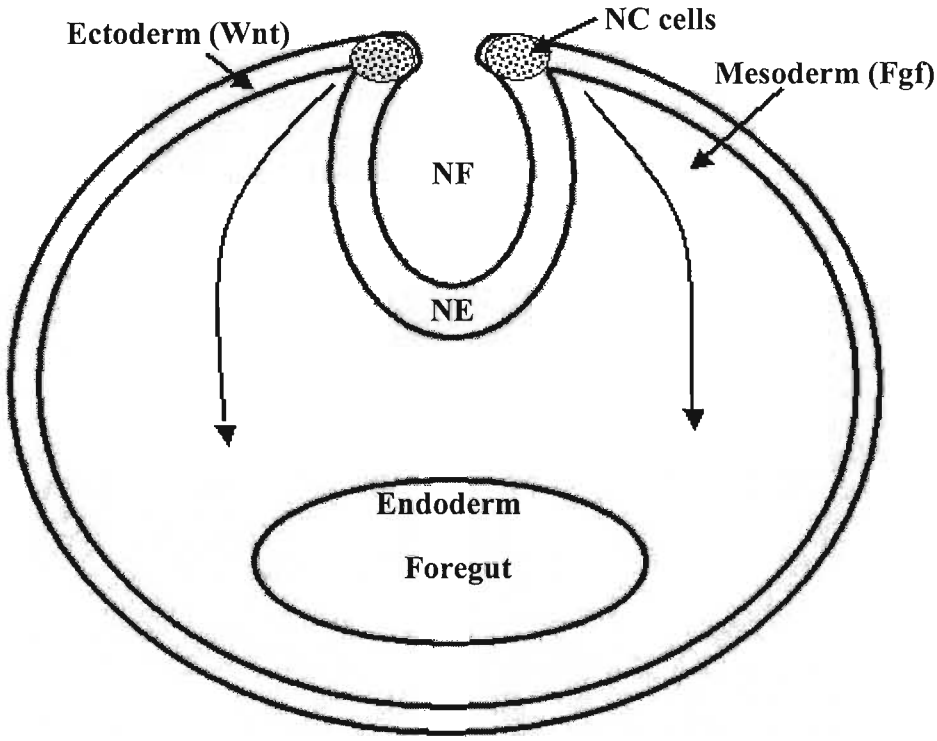

Figure 1 NC cell induction involves signals from both the ectoderm and mesoderm. A: Ectoderm secreted BMP family members are critical for positioning the border of the neural plate and function in the induction and migration of NC cells. B: Ectoderm secreted Wnt family members and mesoderm secreted Fgf family members are believed to be involved in NC cell induction. NF represents the neural fold that is formed by invaginating of the neural plate. NE represents neural ectoderm.

Around the time of neural tube closure, NC cells undergo an epithelial to mesenchymal transition, which enables their delamination and extensive migration.

The craniofacial skeleton forms primarily from cranial neural crest (CNC) cells that migrate away from the neural tube in the posterior midbrain and hindbrain regions (Figure 2) (Nichols, 1986). CNC cells from the posterior midbrain region migrate into the anterior part of the first branchial arch and later contribute to the formation of maxillary prominence (Osumi-Yamashita et al., 1994). The hindbrain is composed of seven distinct segmental structures called rhombomeres. CNC cells that migrate through the hindbrain travel ventrolaterally away from the neural tube in three segregated streams predominantly adjacent to even numbered rhombomeres (r2, r4 and r6). The three distinct streams of CNC cells populate the first, second and third BA respectively (Figure 2). CNC cells from odd numbered rhombomeres (r3 and r5) undergo elevated levels of apoptosis and those that survive migrate anteriorly or posteriorly to join the adjacent even numbered rhombomere CNC cell migrating streams (Trainor and Tam, 1995; Serbedzija et al., 1992). After reaching their final destination, NC cells differentiate and give rise to a wide range of derivatives including facial bone structures, neurons, glia, melanocytes, cardiac cells and endocrine cells (Chai et al., 2000; Jiang et al., 2002).

Molecular mechanisms underlying NC cell induction, delamination and migration are very complicated and still not completely understood despite extensive research. NC cell induction involves signals from both the ectoderm and mesoderm (Figure 1). Three signaling pathways (BMP, FGF, and Wnt) are critical for NC cell induction. During gastrulation, ectoderm secreted BMP4/7 (bone morphogenetic protein, transforming

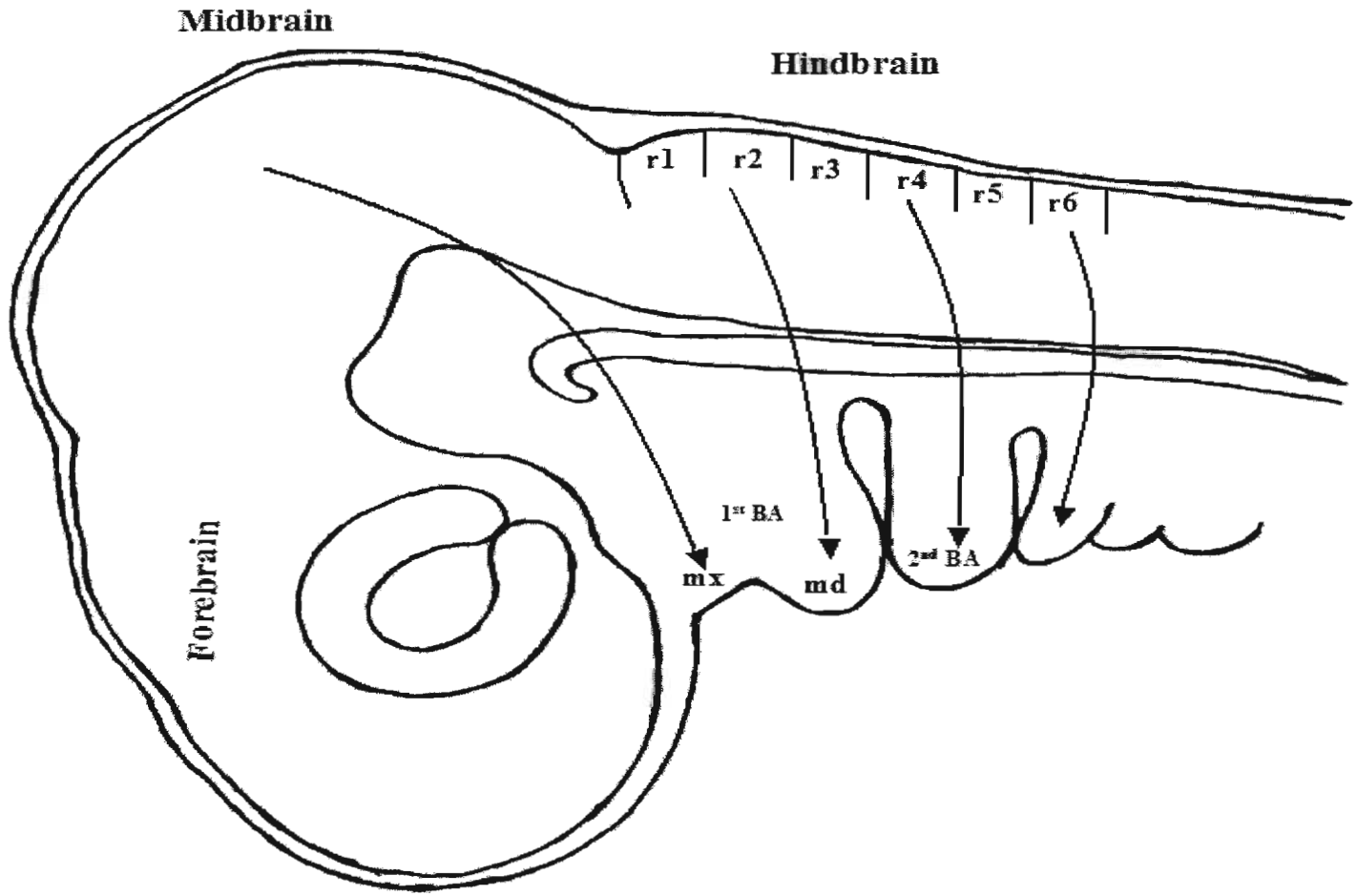

Figure 2 NC cell migration pattern. Solid arrows show the major NC cell migration streams. r1-r6: rhombomere1-6; mx: maxillary prominence; md: mandible prominence. BA: branchial arch.

growth factor TGF-β family members) signaling in the form of a morphogen gradient was considered critical for positioning the border of the neural plate and function in the induction and migration of NC cells in Xenopus and Zebrafish (Marchant et al., 1998; Mayor et al., 1995; Neave et al., 1997; Wilson et al., 1997).

More recently, ectoderm signals from Wnt (wingless/INT) family members are favored as prominent signaling factors for NC cell induction and act directly on NC cells in Avian, Xenopus and Zebrafish (Figure 1B) (Garcia-Castro et al., 2002; Lewis et al., 2004; LaBonne and Bronner-Fraser, 1998). In avian, Wnt6 is expressed in the ectoderm adjacent to the neural folds, which is consistent with an ectodermal inducer expression pattern. Injection of dominant negative Wnt inhibitors adjacent to the neural folds disturbs the formation and migration of NC cells *in vivo*. Wnts rather than BMPs can induce the formation of NC from cultured neural plates *in vitro* without other additives (Garcia-Castro et al., 2002). In zebrafish, injection of Wnt8.1 Morpholino oligonucleotides results in loss of expression of early NC cell markers Foxd3, Pax3 and Sox10 (Lewis et al., 2004). In Xenopus, overexpression of dominant negative xWnt8 also inhibits the expression of NC cell marker Xslug. Overexpression of β-catenin, a Wnt signal downstream mediator, results an expansion of NC forming region and increased expression of NC cell marker Xslug (LaBonne and Bronner-Fraser, 1998).

In Xenopus, mesodermal signals from FGF (fibroblast growth factor) family members are also shown to act on NC cell induction (Figure 1B) (LaBonne and Bronner-Fraser, 1998; Monsoro-Burg et al., 2003; Monsoro-Burg et al., 2005). Overexpression of Fgf8 *in vivo* and *in vitro* results in overexpression of NC cell markers Foxd3, Sox9 and

Zic5. Injection of Fgf8 Mopholino abolishes the expression of a NC cell marker Slug (Monsoro-Burg et al., 2003; Monsoro-Burg et al., 2005).

NC cell delamination involves an epithelial to mesenchymal transition (EMT). The EMT is a complex process involving loss of basolateral polarity, disruption of basal lamina components, dissociation of intercellular adhesive junctions, changes in extracellular matrix and directed migration. The Snail family of zinc finger transcription repressors (Snail/Slug) are believed to play pivotal roles in the EMT by down regulating cell adhesion molecules such as E-cadherin (Savagner et al., 1997; Batlle et al., 2000; Cano et al., 2000). Stable transfection of mouse Slug in rat bladder carcinoma cells induces morphological changes including looser cell contact and decreased expression of Cadherin family members (Savagner et al., 1997). Exogenous expression of mouse Snail in epithelial cell lines result in a fibroblastoid phenotype and decresed E-cadherin expression. Gel retardation and reporter assays show that Snail binds to E-cadherin promoter region and directly represses its transcription (Batlle et al., 2000; Cano et al., 2000). BMP signaling has also been shown to directly regulate *Slug* transcription by luciferase reporter assay (Sakai et al., 2005).

After reaching their final destination, the BAs, CNC cells differentiate to generate an impressive array of cell and tissue types including the craniofacial skeletons affected in TCS patients. The first BA cartilage, Meckel's cartilage, provides the template for mandible development. The majority of Meckel's cartilage disappears in the mandible as the bone forms while a persisting portion forms the malleus and incus middle ear ossicles. The ossification in the maxillary process of the first BA forms the zygomatic bone and

maxilla. The second BA cartilage, Reichert's cartilage, gives rise to the third middle ear ossicle (stapes) and the styloid process of the temporal bone and part of the hyoid bone.

The differentiation of CNC cells also involves complex signaling pathways. Transcription factors Sox9 and Runx2 are known to be important for cartilage and bone formation (Eames et al., 2004). Wnt signaling also appears to be important for NC cell differentiation. Overexpression of Wnt or β-catenin in neural tube explants results in expansion, differentiation, and pigmentation of NC cell derived melanocytes (Dunn et al., 2000). In mouse and chicken, Hox gene family members Hoxa2, Hoxa3 and Hoxa4 are important for defining craniofacial bone structures. Only skeletogenic NC cells that do not express Hox from the first BA respond to grafted endoderm and develop into facial and jaw skeleton structures (Couly et al., 2002; Creuzet et al., 2002). The removal of the Hox-negative NC domain abolishes facial bone structure development as well as Fgf8 expression in surrounding tissues. Exogenous Fgf8 expression in the presumptive BA region partly rescues this phenotype, which indicates Fgf8 is another signaling molecule important for facial skeletogenesis (Creuzet et al., 2004).

2. Paraxial mesoderm and pharyngeal endoderm

The other main mesenchymal component of the BAs arises from paraxial mesoderm, which is the part of the mesoderm adjacent to the neural tube. Unlike the paraxial mesoderm of the trunk, cranial paraxial mesoderm does not form segmented somite structures. Cranial paraxial mesoderm cells migrate away from surface ectoderm along

with neural crest cells into the BAs and generate the precursors of all voluntary muscles in the head and posterior part of the skull (Noden, 1983; Trainor et al., 1994).

Even with limited contribution to the craniofacial structure, the pharyngeal endoderm is believed to play an important role in directing branchial arch patterning and development. The branchial arches are separated by endodermal lined structures called branchial pouches (also known as pharyngeal pouches). *In situ* hybridization with branchial pouch marker Bmp-7 and migratory NC cells marker AP-2α shows that the formation of branchial pouches does not depend on the arrival of NC cells. With the correct formation of branchial pouches, the BAs can form and express corresponding branchial pouch markers Bmp-7, Fgf8 and Shh, and BA marker Dlx2 in the NC-ablated chick embryos (Veitch et al., 1999). In zebrafish mutants with endoderm defects, the disruption in branchial pouch formation results in disturbance in NC cells migration and disorganized BAs (Piotrowski and Nusslein-Volhard, 2000). It has been shown in the avian system that removal of foregut endoderm disrupts facial bone development. Grafts of quail foregut endoderm induces an extra lower jaw skeleton in chick embryos and the direction of the grafted endoderm determines the orientation of the facial skeleton development (Couly et al., 2002).

In brief, craniofacial development is a very complex process and needs the contribution and interaction of all three germ layers. NC cells and paraxial mesoderm provide the basic structure for craniofacial development but can only correctly develop when the coordinated reciprocal signals from the ectoderm, mesoderm and endoderm are present.

Pathogenesis

It has been proposed that TCS may result from a defect of NC cell induction, migration or improper cellular differentiation (Poswillo, 1975; Sulik et al., 1987). However, phenocopies of TCS have been produced in mice by acute maternal exposure to 13-cis-retinoic acid at 9.0-9.5 days post-fertilization (d.p.c.) (Sulik et al., 1987). Maternal retinoids overexposure is known to cause birth defects almost exclusively affecting CNC-derived tissues (Lammer et al., 1985). At 9.0-9.5 d.p.c., migration of the NC cells is completed (Hogan et al., 1994). This indicates that TCS may be caused by abnormal development of the first and second branchial arches rather than abnormal NC cell induction or migration. On the other hand, TUNEL assays in Tcof1 heterozygous knockout mice show a massive increase in the levels of apoptosis in the prefusion neural folds, which are the site of the highest levels of Tcof1 expression (Dixon et al., 2000). The relationship between this high level apoptosis and the phenotype is not clear. The high levels of apoptosis may cause a reduction in the number of NC cells migrating into the branchial arches or lead to reduction or ablation of structures that secrete other key regulators of NC cells migration and craniofacial development.

***TCOF1* gene structure, homologues and expression**

TCOF1 was mapped to human chromosome 5q32-33.1 in 1993 and identified by positional cloning in 1996 (Dixon et al., 1993; Treacher Collins Syndrome Collaborative Group, 1996). In 1997, the coding sequence of the *TCOF1* gene and its genomic organization was reported (Dixon et al., 1997; Wise et al., 1997). *TCOF1* contains an

open reading frame of about 4.3 kb, a 93 bp 5' untranslated region (UTR) and a 507 bp 3' UTR. The *TCOF1* gene has 28 exons, ranging from 49 to 561 bp in size. Exon 1 contains the translation initiation signal. Exon 25 contains the last 24 bp of the coding sequence, the termination codon and the first 22 bp of the 3' UTR. The remainder of the 3' UTR is encoded by exon 26. A series of repeated units have been identified within the gene and these have been shown to map onto individual exons, exons 7 to 16. Two alternatively spliced exons, exon 6A (between exons 6 and 7) and exon 16A (between exons 16 and 17) were identified in 2004 by aligning the previous version of the *TCOF1* cDNA with the human EST database (Figure 3) (So. et al., 2004). Exon 6A is present in the major isoform of *TCOF1*. Exon 6A shows homology with exons 7 to 16. Exon 16A is only present in the minor isoform and shows poor homology with exons 7 to 16. Exon 19 has also been identified as alternatively spliced, in which a smaller proportion of the transcripts excludes exon 19 (Figure 3). Whether differentially spliced transcripts have a specific function in different development stages and/or different tissues still needs further investigation.

Northern hybridization shows that *TCOF1* is widely expressed at a low level in all adult and fetal tissues examined. A 5.8 kb transcript was detected in placenta, adult heart, adult pancreas and fetal and adult brain, lung, liver and kidney; an additional 6.3 kb transcript was also detected in adult skeletal muscle (Treacher Collins Syndrome Collaborative Group, 1996).

The murine homologue of *TCOF1* was isolated in 1997. The mouse *Tcof1* is mapped to mouse chromosome 18 and is 74.3% identical to human *TCOF1*. The mouse

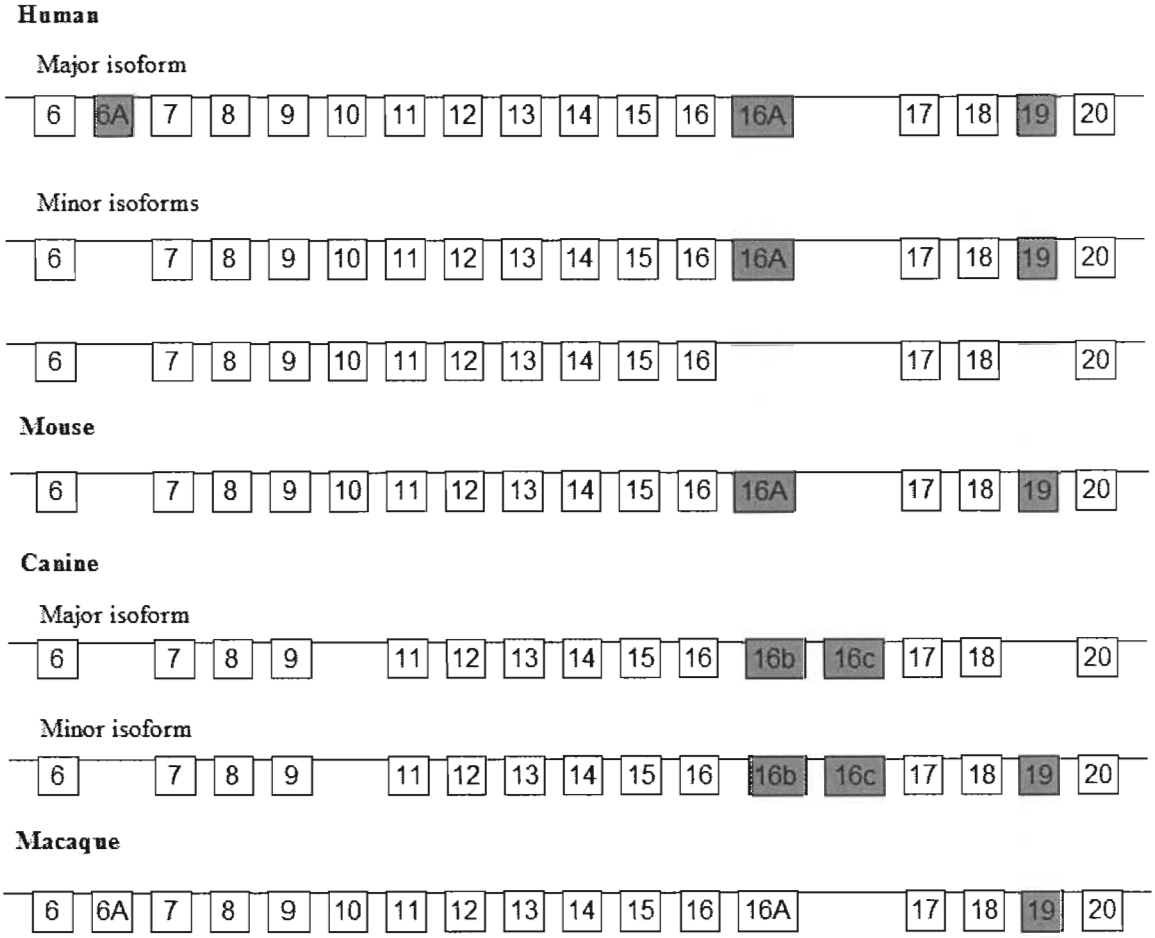

Figure 3 Human, mouse, canine and macaque *Tcof1* splice variants. Shaded boxes are alternatively spliced exons.

Tcof1 gene contains an open reading frame of 3906 nucleotides, a 48 bp 5'UTR and 450 bp 3'UTR (Dixon et al., 1997; Paznekas et al., 1997). There is no evidence for the existence of exon 6A in mouse. Exon 16A and exon 19 are also identified as alternatively spliced exons in mouse (Figure 3). Whole mount *in situ* hybridization in mice indicated that the *Tcof1* gene is expressed in a wide variety of embryonic and adult tissues, albeit at apparently different levels. Peak levels of expression were observed at the edges of the neural folds immediately prior to fusion, and also in the developing BAs at the times of critical morphogenetic events (Figure 4, provided by Dr. Rita Shiang), which is consistent with a fundamental role for *Tcof1* in the development of the craniofacial complex during embryonic development (Dixon et al., 1997).

In 2001, canine *TCOF1* was identified and cloned by screening a canine craniofacial cDNA library using a human *TCOF1* cDNA (Haworth et al., 2001). Dog *TCOF1* was located to the short arm of chromosome 4, which is syntenic with the part of human chromosome 5 where *TCOF1* is located. With 81% identity with the human sequence, canine *TCOF1* cDNA contains an open reading frame of 4269 bp, 47 bp of 5'UTR and 498 bp of 3' UTR. Canine *TCOF1* does not contain the equivalent of human *TCOF1* exon 10, but contains two extra exons 16b and 16c. Exon16b and 16c together encodes one single repeat and shows homology with exon 7-16. As in human and mouse genes, exon 19 is also differently spliced in the dog. Unlike human *TCOF1*, splicing out of exon 19 is the more common form in most tissues in dog (Figure 3). As in human and mouse, canine *TCOF1* is also widely expressed in all the neonatal tissues examined including brain, gut, heart, kidney, liver, spine and muscle. One polymorphism, C396T,

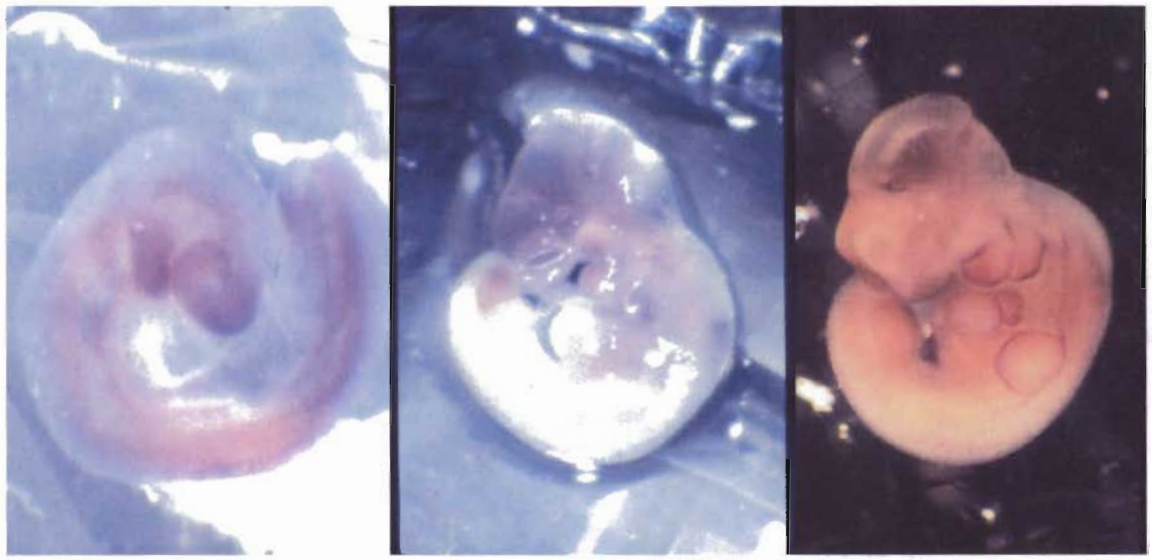

Figure 4 *Tcof1* gene expression patterns in mouse embryos by whole mount *in situ* hybridization. From left to right: E8.5, E9.5 and E10.5 embryos. At E8.5, *Tcof1* has a general high level of expression and particularly high level in the frontonasal and BAs regions. At E9.5, Tcof1 expression level is still high but more restricted to the BAs region and limb buds. At E10.5, general Tcof1 expression is greatly reduced and restricted only to the edges of BAs and limb buds.

within exon 4, which leads to a Pro117Ser substitution, is found to be associated with dog skull/face shape. Significantly more T alleles (Ser117) were found in short, broad head shapes in dog, which gives further evidence for the vital role of the *TCOF1* gene for normal craniofacial development (Haworth et al., 2001).

Recently, we cloned the rhesus macaque *TCOF1* gene by RT-PCR using degenerate primers designed from conserved human and mouse *TCOF1* sequences (Shows et al., 2006). Macaque *TCOF1* contains 28 exons including exons 6A and 16A, and alternatively spliced exon 19 (Figure 3). Macaque *TCOF1* shows 91.6% identity in cDNA sequence and 93.8% identity in amino acid sequence to human *TCOF1*. A newborn female rhesus macaque in the California National Primate Research Center displayed the typical phenotype of TCS, including smaller maxilla and mandible, poor feeding, abnormal palpebral fissures, webbed neck and low-set ears. Although direct PCR sequencing and Southern blot analysis did not find mutations or deletions in coding region, quantitative real-time PCR showed a reduced *TCOF1* expression level in affected macaque total RNA from spleen when compared to RNA from a normal animal. This finding gives further evidence for haploinsufficiency being the underlying mechanism of TCS.

TCOF1 mutations

The identification of the *TCOF1* gene structure has permitted the identification of more than 200 mutations including deletions, insertions, splicing mutations, nonsense mutations and three missense mutations. In 2005, Splendore et al. reported the

development of an online *TCOF1* mutation database (www.genoma.ib.usp.br/TCOF1_database). Most mutations are family specific, except for a 5 bp deletion in exon 24, which accounts for about 17% of all identified mutations, and a guanine insertion in exon 23. The most common mutations are small deletions, followed by insertions, nonsense mutations and splice mutations (Splendore et al., 2005). A total of 3 missense mutations have been reported, all in exon 2 (Tyr50Cys, Trp53Arg, Trp53Cys), suggesting an important functional domain (www.genoma.ib.usp.br/TCOF1_database). Exon 24 is indicated as a mutation hot spot, accounting for roughly 1 out of 5 known mutations. This may be due to the highly repetitive structure of exon 24, which has 60% adenines. Pathogenic mutations were also identified in the alternatively spliced exons 6A and 19 (Splendore et al., 2005).

The majority of the mutations introduce a premature stop codon into the *TCOF1* product treacle. The most amino terminal nonsense mutation would truncate the protein after the first 36 amino acids. Since most identified mutations cause premature termination, the most likely result of these mutations is a severe reduction in the level of mRNA produced from the mutant allele through the nonsense mediated mRNA decay mechanism (reviewed by Behm-Ansmant I and Izaurralde E, 2006). The reduced transcript level will cause a reduction in the protein product level. If the protein product level is below a critical threshold or the change affects the stoichiometry of treacle and its binding partners, then haploinsufficiency would be the pathogenic mechanism. Heterozygous knockout mice show an overlapping, although much more severe,

phenotype with TCS patients (Dixon et al., 2000), which also indicates that TCS results from haploinsufficiency of treacle.

Protein structure

The *TCOF1* gene encodes a 1488 amino acid protein, treacle, of approximately 152 kD molecular weight (Wise et al., 1997, So et al., 2004). Treacle is of very low complexity. Five amino acids, alanine (15%), serine (14%), lysine (11%), glutamic acid (9%), and proline (9%) account for about 60% of the amino acid residues (Treacher Collins Syndrome Collaborative Group, 1996).

Database sequence comparison shows weak but significant homology between treacle and a rat nucleolar phosphoprotein Nopp140. Nopp140, like treacle, is a low complexity protein which contains 10 repeat units of alternating acidic and basic regions, with each repeat unit containing numerous casein kinase phosphorylation sites. Nopp140 contains seven potential NLSs (Nuclear localization signals). Nopp140 is a highly phosphorylated protein and migrates as a band of about twice its theoretical molecular weight on Western blots mostly due to its high degree of phosphorylation (Meier and Blobel, 1992; Meier, 1996). Coimmunoprecipitation shows direct interaction between CKII (formerly casein kinase II) and Nopp140 in different cell lines. CKII can phosphorylate recombinant Nopp140 *in vitro*, which suggests CKII as the kinase responsible for the high degree of phosphorylation of Nopp140 (Meier, 1996; Li et al., 1997). Nopp140 shuttles between the nucleus and the cytoplasm and is thought to act as a chaperone in transporting proteins in and out of the nucleus and to be involved in the

ribosome assembly process by either importing ribosomal proteins or exporting preribosomal subunits (Meier and Blobel, 1992; Isaac et al., 1998). Nopp140 has been identified to interact with transcription factor C/EBPβ by immunoaffinity chromatography using a rat liver nuclear extract and by immunoprecipitation using different cell lysates. Chloramphenicol Acetyl Transferase (CAT) assays show that Nopp140 interacts with C/EBPβ and synergistically activates the alpha-1 acid glycoprotein gene, which suggests it acts as a transcription factor (Miau et al., 1997). Human Nopp140 has been shown to colocalize and interact with the large subunit of RNA polymerase I (Pol I) by immunofluorescence microscopy and coimmunoprecipitation. Overexpression of hNopp140 or ectopic expression of dominant negative hNop140 in Hela cells results in altered nucleolar structure, mislocalized RNA Pol I and disrupted rDNA transcription, which indicates hNopp140 plays a role in nucleolar integrity and rRNA transcription (Chen et al., 1999).

Treacle has a 213 residue N-terminal domain followed by 13 repeating units of alternating acidic and basic residues, and a C-terminal domain. The N-terminus of treacle contains a LisH (LIS1-homologous) motif, which is also found in nucleolar protein Nopp140 and other disease genes characterized by defective cell migration (Emes and Ponting, 2001). Each repeat unit, except for the one encoded by exon 14, contains a number of potential sites for CKII (S/T-XX-D/E) and protein kinase C (PKC) (S/T-X-K/R) phosphorylation. Similar to Nopp140, human treacle migrates as a band larger than its predicted 152 kD molecular weight (Isaac et al., 2000). GST-treacle fusion constructs containing exon 9, exon 14, or 20 can be phosphorylated *in vitro* by CKII and PKC

respectively. CKII is a multi-functional second messenger-independent eukaryotic serine/threonine kinase present in the nucleus and cytoplasm of all eukaryotic cells. CKII phosphorylates a large number of proteins including enzymes involved in nucleic acid synthesis, transcription and protein synthesis factors, structural proteins, and signal transduction proteins, suggesting a global role in the regulation of cellular processes (reviewed by Allende and Allende, 1995). Tissue extracts from avian embryonic BAs I and II show a kinase activity that could phosphorylate GST-treacle exon 9 fusion peptide *in vitro* (Jones et al., 1999). The treacle C-terminus contains multiple putative NLSs (K-R/K-X-R/K) and a single NoLS (nucleolar localization signal). Indirect immunofluorescence shows that treacle is localized to nucleolus in Hela cells and fibroblasts from healthy individuals (Isaac et al., 2000). Alternatively spliced exon 6A contains an extra nuclear localization signal which does not affect the nucleolar localization of treacle (So et al., 2004).

The mouse *Tcof1* encodes a serine/alanine-rich protein of 1302 amino acids with a molecular weight of 133kD, which is 186 amino acids shorter than its human counterpart. The sequence is also of low complexity with five amino acids (serine, alanine, lysine, proline and glutamic acid) accounting for almost 60% of the residues. The mouse and human treacle protein display 61.5% identity and 71.7% similarity. The homology between the two genes is greatest in the N- and C- terminal regions of the proteins. The area corresponding to the repeated region is less homologous with the exception of the potential CKII phosphorylation sites which are well conserved (Dixon et al., 1997; Paznekas et al., 1997). The predicted NLSs at the C-terminus are also well conserved.

GFP-treacle fusion construct shows that the normal cellular localization of treacle is the nucleolus. At least two functional NLSs from residues 1176 to 1302 have been shown to be sufficient for nuclear localization. The most C-terminal 41 amino acids contain a NoLS and are necessary and sufficient to direct GFP-treacle construct to the nucleolus (Winokur and Shiang, 1998).

Mouse treacle has been shown to migrate as a single band of ~220 kD on Western blots while the predicted molecular weight is 133 kD. The mobility of treacle was increased to ~180 kD after incubation with alkaline phosphatase in the absence but not the presence of phosphatase inhibitors, which indicates a high degree of phosphorylation in treacle. Coimmunoprecipitation using antibodies to the C terminus of treacle and CKII indicated interaction between treacle and CKII (Rujirabanjerd et al., 1999; Isaac et al., 2000; Rujirabanjerd, 2003).

Xenopus *TCOF1* was identified by blasting the Xenopus EST database using mouse *Tcof1*. Xtreacle contains 11 repeats in the central region and only shows 19% identity with human treacle, 21% identity with dog treacle and 20% identity with mouse treacle. Xtreacle is also of low complexity with five amino acids, alanine, serine, lysine, glutamic acid, and proline account for about 60% of the amino acid residues. Xtreacle was shown to colocalize with nucleolin in the nucleolus of Xenopus kidney cells. Xtreacle does not migrate slower on a Western gel than its predicted size of 154 kD as does the human or mouse treacle (Gonzales et al., 2005A).

Nucleolus and ribosome biogenesis

Human, mouse and Xenopus treacle are all localized to the nucleolus. The nucleolus is a complex and dynamic substructure in the eukaryotic nucleus. It is the site for synthesis of ribosomal RNA (rRNA) and ribosome biogenesis. The ribosome contains a small 40S subunit and a large 60S subunit. The small subunit contains a single 18S rRNA and 30 to 50 ribosomal proteins and the large subunit contains 5S, 5.8S and 23S rRNAs and 40-50 ribosomal proteins. The 18S, 5.8S and 23S rRNAs are transcribed as a single large precursor rRNA (pre-rRNA) by RNA Pol I in the nucleolus. The 5S rRNA is transcribed by RNA polymerase III (Pol III) in the nucleoplasm and later imported into the nucleolus (reviewed by Nazar, 2004).

The nucleolus contains three morphologically distinct structures: fibrillar centers (FC), dense fibrillar component (DFC) and granular component (GC). The FC contains rRNA genes located on the chromosomal nucleolar organizing regions (NORs). rDNA transcription occurs at the boundary of the FC and DFC. The DFC contains newly transcribed rRNA and is believed to be the location of early rRNA processing. The GC contains late processed rRNA and pre-ribosomal particles and is the ribosomal subunit assembly location (Reviewed by Spector, 1993). Treacle has been shown to localize to the DFC of the nucleolus. Unlike other nucleolar proteins localized to the DFC, treacle does not localize to the Cajal bodies (Isaac et al., 2000). Cajal bodies, previous known as coiled bodies, are involved in small nuclear and nucleolar RNA processing, small nuclear ribonucleoprotein (snRNP) biogenesis and trafficking of snRNP and snoRNP (small nucleolar ribonucleoprotein) (Reviewed by Gall, 2000).

Except for 5S rRNA, the synthesis of rRNAs is transcribed by RNA Pol I as a large pre-rRNA. Pre-rRNA is then cleaved and modified to generate mature 18S, 5.8S and 23S rRNAs. The rDNA gene promoter contains an upstream control element and core promoter. Besides Pol I, the Pol I initiation complex in mammalian cells also contains upstream binding factor (UBF) and selectivity factor 1 (SL1), which binds to the upstream control element and the core promoter respectively (Voit et al., 1992; Heix et al., 1997). DNA methylation is important for regulating ribosomal gene activity *in vitro*. DNase footprinting shows that UBF cannot bind to a methylated promoter and inhibits subsequent rDNA transcription (Santoro and Grummt, 2001). After transcription and splicing, rRNAs need to be further modified to form mature rRNAs. The modifications, methylation and pseudouridine synthesis, are performed by snoRNPs. Mutations in yeast that blocking these modifications inhibit cell growth and ribosome assembly (Tollervey et al., 1993; Zebarjadian et al., 1999).

Recent studies also suggest that the nucleolus is involved in other cellular functions as well, including cell growth and cell cycle control, tumorigenesis and nucleolar sequestration of nonribosomal proteins (Pederson, 1998; Tsai and McKay, 2002; Bernardi and Pandolfi, 2003). Ribosome biogenesis is essential for cell metabolism and determining cell growth. Dormant or differentiated cells usually contain one small nucleolus while proliferating cells usually contain one or several large neucleoli. Ribosome biogenesis is suppressed during mitosis and reaches high levels in S and G2 phases. During mitosis, SL1 is inactivated by CDK1 phosphorylation and UBF is inactivated by changes in its phosphorylation pattern (Heix et al., 1998; Klein and

Grummt, 1999). The MAP kinase and TOR (target of rapamycin) pathways are involved in the regulation of rRNA transcription by regulating the phosphorylation of UBF (Stefanovsky et al., 2001; Hannan et al., 2003). Phosphorylation of UBF *in vitro* enhances the initiation by increased recruitment of SL1 (Tuan et al., 1999). Tumor suppressor gene p53 is also suggested to be involved in the regulation of Pol I transcription. Immunofluorescence studies have shown that p53 is localized to both nucleoplasm and nucleolus (Rubbi and Milner, 2000). Immunoprecipitation shows that p53 binds to SL1 and inhibits SL1 and UBF interaction. *In vitro* transcription assays show that p53 inhibits human Pol I transcription activity (Zhai and Comai, 2000).

TCS mouse model

In 2000, Tcof1 heterozygous knockout mice were generated by replacing exon 1 of *Tcof1* with a neomycin-resistance cassette via homologous recombination in embryonic stem cells (Dixon et al., 2000). Tcof1 heterozygous mice with a mixed 129 and C57BL/6 background exhibit a generalized developmental delay and severe structural craniofacial anomalies throughout development (Dixon et al., 2000). The phenotype of heterozygous mice overlaps TCS patients, including malformation of the maxilla, secondary palate, nasal complex and external ear and hypoplasia of the zygomatic arch, tympanic ring, middle ear ossicles and mandible, though affected structures observed in Tcof1 heterozygous mice are much more severe. The heterozygous mice die shortly after birth because they are unable to establish an airway due to severe craniofacial abnormalities, the lack of nasal passages and exencephaly (neuroepithelium protruding out of the skull).

Abnormally high levels of apoptosis are detected by TUNEL assay in the prefusion neural tube, from which NC cells arise and which has the highest *Tcof1* expression level, and in the post fusion neural tube.

The penetrance and severity of craniofacial and other defects of Tcof1 heterozygous mice varies in different genetic backgrounds (Dixon and Dixon, 2004). Phenotypic variation includes severe facial defects and neonatal lethality in C57BL/6 or CBA/Ca and 129 mixed backgrounds to mostly phenotypically normal in BALB/c or DBA/1 and 129 mixed backgrounds. This finding might explain the highly variable expressivity and the lack of genotype-phenotype correlation in TCS patients. Heterozygous knockout mouse embryos from a neonatal lethal background DBA×CBA or DBA× C57BL/6 show reduced methylation level at C_{463} of 18S rRNA compared to wildtype. Heterozygous knockout mouse embryos from a phenotypically normal background DBA× BALB/c show no difference in the methylation level. This suggests that the pre-rRNA methylation level may be a contributing factor to the different phenotypes, and treacle most likely affects pre-rRNA methylation by interacting with Nop56 (Gonzales et al., 2005B).

Protein function

Human nucleolar protein hNop56p is a member of snoRNP complexes and directs pre-rRNA methylation during early stages of pre-rRNA processing. Treacle has been shown to interact directly with hNop56p in the pre-rRNP (pre-ribosomal ribonucleoprotein) complex using protein identification by LC-MS/MS (liquid chromatography-tandem mass spectrometry analysis), which indicates the involvement of

treacle function in ribosome biogenesis (Hayano et al., 2003). During telophase when rDNA transcription and pre-rRNA methylation occurs, mouse treacle colocalizes with Nop56p and fibrillarin, a putative methyl transferase, which suggests treacle may be involved in rDNA transcription and pre-rRNA modification (Gonzales et al., 2005B).

Treacle has also been shown by indirect immunofluorescence to colocalize with UBF, a RNA Pol I transcription factor, in all stages of cell cycle, which suggests that they are components of an RNP complex that associates with condensed chromosomes. Immunoprecipitation assays show direct physical interaction between treacle and UBF. RNase protection assay shows that siRNA mediated down-regulation of treacle expression inhibits rRNA production by almost 50 percent (Valdez et al., 2004). As shown in human cell lines, down regulation of Xtreacle also inhibits rDNA transcription in Xenopus (Gonzales et al., 2005B).

Treacle is localized to the nucleolus and interacts with Nop56 and UBF. Down regulation of treacle inhibits rDNA transcription in human and Xenopus and reduces the rRNA methylation level in mouse. Ribosome biogenesis is essential for cell metabolism and cell growth. The fast growing craniofacial region in development may require high cellular metabolism. In TCS patients, reduced treacle level could affect development through inhibition of rDNA transcription and/or ribosome assembly.

Objectives of this study

Although the *TCOF1* gene has been cloned, many questions remain unanswered, specifically about the cellular effects of treacle including expression changes of any

specific genes. Previously, we manipulated Tcof1 levels in an NC derived mouse neuroblastoma (NB) cell line as an *in vitro* model and identified candidate *Tcof1* downstream genes using microarray analysis (Mogass et al., 2004). In this study, we generated stably transfected NB cell lines with overexpression or knockdown of Tcof1 levels and analyzed cell growth, proliferation and apoptosis. Western blot analysis was used to confirm protein level changes for downstream candidate genes. The identification of *Tcof1* downstream genes and pathways gave us further insight into Tcof1 function on cell growth and survival.

The creation and use of a murine model of human disease can provide a powerful tool for the analysis of gene function. Partial elimination of the *Tcof1* gene in the mouse causes neonatal lethality, which circumvented further analysis of the heterozygous and homozygous mice. The heterozygous knockout mice have an increased level of apoptosis in regions that normally express high levels of *Tcof1* (Dixon and Dixon, 2004). However, it was not clear whether the elevated apoptosis occurred in NC cells or other types of cells. The potential effect on NC migration was also not examined in these mice. Thus as the second part of this study, we generated a conditional knockout mouse using the Cre-lox system, a model which might more closely resemble human TCS. Analysis of the phenotype, changes in the distribution of treacle and downstream genes in this model as compared to control animals gave us further insights into the protein product function. Any future therapies can also be tested in this model.

Chapter 2: Cellular effects of Tcof1 in a neuroblastoma cell line

Introduction

The TCS disease gene *TCOF1* encodes for a 152 kD nucleolar phosphoprotein treacle which has an N-terminus followed by 13 repeating units of alternating acidic and basic residues and a C-terminus with multiple putative NLSs (nuclear localization signals) and a single NoLS (nucleolar localization signal) (Dixon et al., 1997; Wise et al., 1997). Treacle has been shown to be highly phosphorylated by CKII and PKC (Isaac et al., 2000; Rujirabanjerd, 2003). The mouse and human treacle share 61.5% identity and 71.7% similarity (Dixon et al., 1997; Paznekas et al., 1997). Heterozygous Tcof1 knockout mice have severe craniofacial abnormalities and increased apoptosis in the regions that normally express *Tcof1* at the highest levels (Dixon et al., 2000). This indicates that treacle expression is indispensable for development of the craniofacial region. Human and mouse treacle has been shown to interact directly with nucleolar protein hNop56p, a member of snoRNP (small nucleolar ribonucleoprotein) complexes which direct pre-rRNA methylation during early stages of pre-rRNA processing (Hayano et al., 2003; Gonzales et al., 2005). Treacle colocalizes and directly interacts with upstream binding factor (UBF), a RNA polymerase I transcription factor, in all stages of the cell cycle. Down regulation of treacle inhibits rDNA transcription in human and Xenopus and

reduces the rRNA methylation levels in mouse (Valdez et al., 2004; Gonzales et al., 2005B). These results indicate the involvement of treacle function in ribosome biogenesis, which is known to be essential for cell metabolism and cell growth. During development, the fast growing craniofacial region may require high cellular metabolism. In TCS patients, reduced treacle levels could affect development through inhibition of rDNA transcription and/or ribosome assembly.

The tissues affected in TCS arise from the first and second BAs during early embryogenesis (Moore and Persaud, 1993). NC cells have been shown to make a major contribution to the mesenchymal component of BAs. NC cells are multipotent migratory embryonic cells that form by inductive interactions at the border of the neural and epidermal ectoderm. Around the time of neural tube closure, they undergo an epithelial to mesenchymal transition, which enables their delamination and extensive migration into the BAs. After reaching their final destination, NC cells differentiate and give rise to a wide range of derivatives including facial skeletal structures, neurons, glia, melanocytes, cardiac cells and endocrine cells. Neuroblastoma (NB) cells used in this study are NC derived tumor cells and are suitable as an *in vitro* model to study NC cell proliferation, apoptosis, differentiation, transcription regulation and signal transduction (Smith et al., 1998; Bachetti et al., 2005; Cesi et al., 2005).

Previously, we generated Tcof1 overexpression clones by transfection of full length *Tcof1* cDNA into a murine NB cell line N1E-115. Tcof1 expression was down regulated in N1E-115 cells using the siRNA technique. Wildtype N1E-115, Tcof1 overexpression or knockdown cells were used to perform microarray analysis to identify downstream

candidate genes (Mogass et al., 2004). Downstream candidate genes include cell cycle genes and transcription factors *Cnbp* (Cellular Nucleic Acid Binding Protein, zinc finger 9) and *Tbx2* (T-box 2), which are known to affect the cell cycle through c-myc and p19-Mdm2/p21$^{WAF/CIP}$ pathways respectively (Figure 5). Our hypothesis is that Tcof1 is required for cell growth and survival. Tcof1 raises the level of Cnbp and/or Tbx2 expression and regulates the cell cycle and assists cell proliferation by inhibiting cell cycle arrest and apoptosis (Figure 5). Knockdown of Tcof1 will cause decreased cell growth and/or increased apoptosis while overexpression of Tcof1 will cause increased cell growth and/or decreased apoptosis. The research objectives of this study are to confirm candidate downstream gene expression changes including *Cnbp* and *Tbx2* by real-time quantitative PCR; to generate stably transfected NB cell lines with overexpression or knockdown of Tcof1; to analyze cell growth, proliferation and apoptosis of these cells; and to perform Western blot analysis to confirm protein level changes for downstream candidate genes.

Materials and methods

Cell culture

The NB cell line N1E-115 was a gift from Dr. Elliot Richelson (obtained from Dr. John Bigbee). The cell cultures are the same as described previously (Mogass et al., 2004). Briefly the cells were maintained in Dulbecco's minimal essential medium (DMEM) supplemented with 10% fetal bovine serum (FBS), and 1% penicillin and streptomycin at 37°C in 5% CO_2 incubator. Transfected cells with neomycin resistance

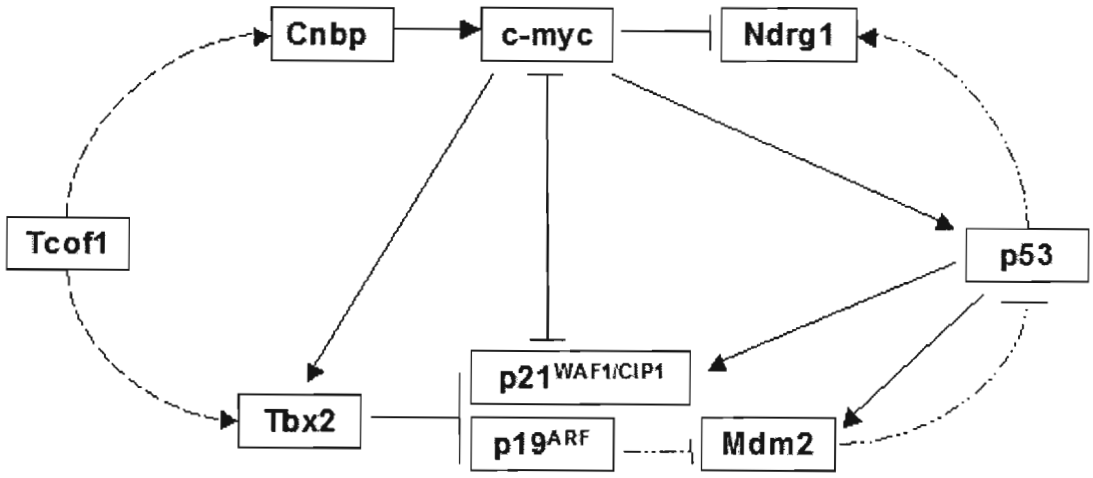

Figure 5 Schematic Tcof1 downstream genes and pathways affecting the cell cycle. Tcof1 raises the level of Cnbp and/or Tbx2 expression and may regulate the cell cycle and assist cell proliferation by inhibiting cell cycle arrest and apoptosis. Knockdown of Tcof1 should cause decreased cell growth and/or increased apoptosis while overexpression of Tcof1 should cause increased cell growth and/or decreased apoptosis. An arrow represents the increased expression or activation of the gene; vertical bar represents inhibition of the gene. - - - - - - - : Unknown mechanism; ——— : Regulates transcription directly; -·-·-·- : Regulate through mechanisms other than affecting transcription (degradation, change of localization, etc.).

were maintained under selection in DMEM with 10% FBS and 300 μg/ml Geneticin (concentration titration showed that this is the lowest Geneticin level that effectively killed 100% of wildtype NB cells in two weeks).

Creation of stable transfectants for overexpression and knockdown of Tcof1 in NB cell line

Stable Tcof1 overexpression cell lines (OE9 and OE39) were generated as described previously (Mogass et al., 2004). Briefly, the *Tcof1* full length cDNA clone pDEST12.2-N2 was generated using the Gateway cloning system (Invitrogen) and transfected into NB cells using lipofectamine 2000 following manufacturer's protocol (Invitrogen). pDEST12.2 vector was used to generate the control cell line DT3.

Tcof1 expression was suppressed in the NB cell line using the pSUPER RNAi system (OligoEngine, a gift from Dr. Holt). Oligo nucleotide inserts (mTcof1tar2oligoF: GATCCCCGCGATGAGACAGATGTCGATTCAAGAGATCGACATCTGTCTCATC GCTTTTTGGAAA and mTcof1tar2oligoR: AGCTTTTCCAAAAAGCGATGAGACAGATGTCGATCTCTTGAATCGACATCTG TCTCATCGCGGG) were designed following the manufacturer's protocol using the previously identified siRNA target sequence, target 2 (Mogass et al., 2004). The forward and reverse oligo nucleotides at a concentration of 3 μg/μl in 48 μl universal buffer (100 mM NaCl and 50 mM Tris, pH 7.4) was denatured at 100°C for 10 minutes, transferred to a 70°C water bath and incubated for 10 minutes, and then annealed overnight as water cooled to room temperature after turning off the water bath. The annealed oligo insert

was ligated to pSUPER.retro.neo+GFP (pSP) vector linearized with HindIII and BglII. The correct construct pSP-Tcof1 was confirmed by sequencing and used to transfect into NB cells by lipofectamine 2000. The original pSP vector was used to generate the control cell line SP21.

One day before transfection, 1×10^5 cells were plated in 6-well plates with 2 ml DMEM with 10% FBS so that cells would be 70-75% confluent at the time of transfection. Four micrograms of DNA was diluted in 250 μl of media without antibiotics. Twelve microliters of lipofectamine 2000 was diluted in 250 μl of DMEM without antibiotics and incubated at room temperature for 5 minutes. The diluted DNA and lipofectamine 2000 were combined and incubated at room temperature for 20 minutes, then added to the cells, which were incubated at 37°C in 5% CO_2 incubator. After 24 hours, the cells were replated into 100 mm tissue culture dishes with selection media. Clonal populations were isolated and maintained in selection media.

Semi-quantitative RT-PCR and quantitative real-time PCR

Semi-quantitative RT-PCR was used to screen Tcof1 overexpression or knockdown cell lines. Tcof1 and microarray identified candidate downstream genes level changes were confirmed by quantitative real-time PCR. GAPDH was used as an endogenous control (Table 1). Total RNA was isolated using Trizol (Invitrogen) following the manufacturer's protocol. RNA concentration was determined by measuring UV absorbance at 260 nm. First strand cDNA was reverse-transcribed from 200 ng of total RNA using M-MLV reverse transcriptase in a 20μl reaction according to manufacturer's

Table 1 Primers used for semi-quantitative RT-PCR and quantitative real-time PCR

Gene	Primer	Sequence	Product size
GAPDH	Forward	5' AGCCTCGTCCCGTAGACAAAA 3'	111 bp
	Reverse	5' TGGCAACAATCTCCACTTTGC 3'	
Tcof1	Forward	5' CAGGCTGTGAACACCACAAAGA 3'	132 bp
	Reverse	5' CGTCACACTGGTTCTGAGAGCA 3'	
Cnbp	Forward	5' CCTTCTTGGTTCTTCGTCCGA 3'	106 bp
	Reverse	5' CAGATCGTCCACACTTGAAGCA 3'	
Tbx2	Forward	5' TTCATCGCTGTCACTGCCTA 3'	116 bp
	Reverse	5' TGCTTCCTTTTCTCCCGAC 3'	
Ndrg1	Forward	5' AGTTCGATGTTCAGGAGCAGGA 3'	101 bp
	Reverse	5' ATACGTGAGGATGACAGGACGG 3'	
Ddx42	Forward	5' GGTTTCGGAAATCTCGCTTCA 3'	114 bp
	Reverse	5' TTCCTCGGTCCGAATTCTCAG 3'	
Mapk14	Forward	5' AGTCCATCATTCACGCCAAAAG 3'	118 bp
	Reverse	5' AATTCCTCCAGTGACCTTGCG 3'	
Nolc1	Forward	5' CGGAGGTGGCCAGTAAATTTG 3'	101 bp
	Reverse	5' GGTGGACTTGAGCCAGAAGCTA 3'	

instructions (Invitrogen). PCR was performed with 1× PCR buffer, 0.4 mM dNTP, 0.1 pmol/μl primers and 1 μl cDNA product. The 12.5 μl reaction was denatured at 94°C for 2 min, then cycled at 94°C for 30 sec, 60°C for 30 sec, and 72°C for 30sec for 20/23 cycles, and then at 72°C for 7 min. Exponential phase amplification was determined by performing PCR at different cycle numbers. Tcof1 and GAPDH were amplified at 23 and 20 cycles respectively. PCR products were separated on polyacrylamide gels and quantified using spot densitometry.

Real-time quantitative RT-PCR was performed in triplicate using Applied Biosystems (ABI) PRISM 7900HT with the standard temperature (60°C) protocol. The primers were designed using the Primer Express program version 2.0 (ABI), and the sequences of the primers are shown in Table 1. Reactions were run with 1.5 μl cDNA, 0.1 pmol/μl primers and iTaq SYBR Green Supermix with ROX (Bio-Rad) in a total volume of 15 μl. Acquired data were analyzed using SDS software version 2.2 (ABI). Gene expression levels were normalized with GAPDH.

Cell growth curve and proliferation assay

Cell growth curves were generated in triplicate by counting cell numbers using a hematocytometer. Cell viability was assessed by trypan blue exclusion. About 1×10^4 cells were plated in T25 flasks and harvested and counted for six continuous days. Cell numbers were plotted against days in culture. Growth curves were also generated for cells growing in log phase. About 5×10^4 cells were plated in T25 flasks and harvested and counted every three days for 18 days total in culture. Population doublings were

calculated as [log (number of cells collected/number of cells plated)]/0.3 (Compton et al., 2006).

Bromodeoxyuridine (BrdU) incorporation was used to determine cell proliferation following Roche's *in situ* cell proliferation kit, FLUOS protocol. Sample cells (1×10^6 cells) were incubated at 37°C with 10 μM BrdU for one hour then harvested and washed with PBS. Cells without BrdU incubation were used as negative controls. The cell pellets were resuspended with 500 μl 1× PBS, injected into 5 ml fixative solution (containing 3 volumes of PBS solution with 7 volumes of absolute ethanol) and incubated at 4°C for 40 minutes. Cells were washed with 1× PBS and resuspended in 500 μl freshly made 2 N HCl with 0.5% Triton-X-100 denaturation solution and incubated at room temperature for 15 minutes. Cells were washed with 1× PBS, pre-blocked with 1× PBS with 0.5% BSA at room temperature for 30 minutes, resuspended in 200 μl incubation buffer (1× PBS contains 0.5% BSA and 0.1% Tween 20) with 0.5 μg/ml anti-BrdU-FLUOS antibody and incubated at room temperature for 40 minutes followed by washing with 1× PBS three times. Propidium iodide (1 μg/ml) was added to perform cell cycle analysis using Beckman Coulter EPICS XL-MCL benchtop flow cytometer.

OE or KD clones with their controls were tested for analysis of variance. When the analysis of variance was significantly different, Student t-test was then used to test the difference between two clones. p values less than 0.05 were considered significant.

Apoptosis assay

TUNEL (TdT-mediated dUTP-X nick end labeling) assay was used to detect the apoptosis levels in different cell lines using the *in situ* cell death detection kit from Roche Applied Science following manufacturer's protocol. Cells were harvested and adjusted to 1×10^7 cells/ml. Cells were fixed with freshly prepared 2% paraformaldehyde in 1× PBS at room temperature for 30 minutes. Cells were washed with 2 mls 1× PBS, resuspended in 500 µl 0.1 M sodium citrate and permeablized at 70°C for 30 minutes. Cells were then washed with 2 mls 1× PBS twice, followed by blocking non-specific binding with 0.5% BSA in 1× PBS at room temperature for 15 minutes. Cell pellets were resuspended in 25 µl TUNEL reaction mixture (containing nucleotide mixture in reaction buffer and terminal deoxynucleotidyl transferase) and incubated at 37°C for 60 minutes. Cells incubated with reaction buffer without the terminal deoxynucleotidyl transferase were used as negative controls for analysis. Samples were washed twice with 1× PBS and resuspended in a final volume of 1 ml 1× PBS and analyzed using Beckman Coulter EPICS XL-MCL benchtop flow cytometer. The same statistical tests were used as in the proliferation assay.

Western blot analysis

Western blot analysis was used to confirm treacle level changes and investigate possible downstream gene product expression level changes in different cell lines. Cells were lysed on ice for 15 minutes in 10 mM Tris (pH7.5), 5 mM EDTA, 50 mM NaCl, 30 mM sodium pyrophosphate, 50 mM sodium fluoride, 0.4 mM sodium orthovanadate, 1%

Triton X-100 with the addition of 20 μl/ml protease inhibitor cocktail (Sigma). Lysed cells were sonicated and centrifuged at 4°C for 15 minutes to collect the supernatant. Whole cell lysates were separated on 6% (for treacle) or 10% (for all other proteins) PAGE-SDS gels. The protein was transferred to PVDF membrane (Bio-Rad). The membrane was incubated with the primary antibodies at a concentration of 0.3 μg/ml for treacle (Mogass et al., 2004), 0.2 μg/ml for c-myc and Tbx2 (Santa Cruz Biotechnology), 1.0 μg/ml for $p21^{WAF1/CIP1}$, $p19^{ARF}$, Ndrg1 and Mdm2 (Santa Cruz Biotechnology) and at a dilution of 1:10,000 for p53 (Calbiochem) and 1:10,000 for Cnbp (Abnova, Taiwan). Then the membranes were incubated with corresponding secondary antibodies at a dilution of 1:20,000 for treacle (Bio-Rad) and 1:10,000 for all others (Santa Cruz Biotechnology). The immune-complex was detected using Western Lightning chemiluminescence reagent plus (PerkinElmer) and exposed to X-ray film. The same membrane was stripped and then probed with a mouse monoclonal anti-α tubulin antibody at 0.3 μg/ml (Sigma–Aldrich). Spot densitometry was used for quantification of protein by normalization to α-tubulin. At least three independent Western blot analyses were used for each protein and average fold changes were calculated as relative changes to vector controls.

Results

Confirmation of microarray analysis data by real time quantitative PCR

Previously, we identified candidate Tcof1 downstream genes using microarray analysis by manipulating Tcof1 levels in a murine NB cell line N1E-115. By comparing

gene expression profiles in wildtype, Tcof1 overexpression or knockdown cells, 54 and 18 transcripts were identified to be positively (group 1) or negatively (group 2) correlated with Tcof1 expression respectively (Mogass et al., 2004). Five genes (Cnbp, Tbx2, Nolc1, Mapk14 and Ddx42) from group 1 and one gene (Ndrg1, N-myc downstream gene 1) from group 2 were chosen to perform quantitative real-time RT-PCR to validate microarray results. Cnbp, Nolc1, Tbx2 and Ndrg1 expression changes were confirmed to be the same as microarray analysis (Figure 6). Mapk14 and Ddx42 expression levels were down regulated with knockdown of Tcof1 but the overexpression of these genes in the Tcof1 overexpression cell line were not confirmed. N1E-115 transfected with vector only was used as a control in the quantitative real-time RT-PCR analysis to confirm that changes in gene expression were not the result of nonspecific cellular changes. After a literature review, transcription factors Cnbp and Tbx2 were chosen as the focus of this study and proposed Tcof1 pathways for regulating cell proliferation and death are shown in figure 5. Cnbp and Tbx2 are known to affect the cell cycle through the c-myc and p19-Mdm2/ $p21^{WAF/CIP}$ pathways respectively.

Characterization of cell growth and proliferation

The Tcof1 overexpression clone used in the microarray studies was lost during cryopreservation. The full length *Tcof1* cDNA was therefore used to generate additional Tcof1 overexpression clones for this study. Stable Tcof1 knockdown cell lines were generated by the pSuperRNAi system using previously identified siRNA oligo targets. After screening knockdown (KD) and overexpression (OE) clones, we identified several

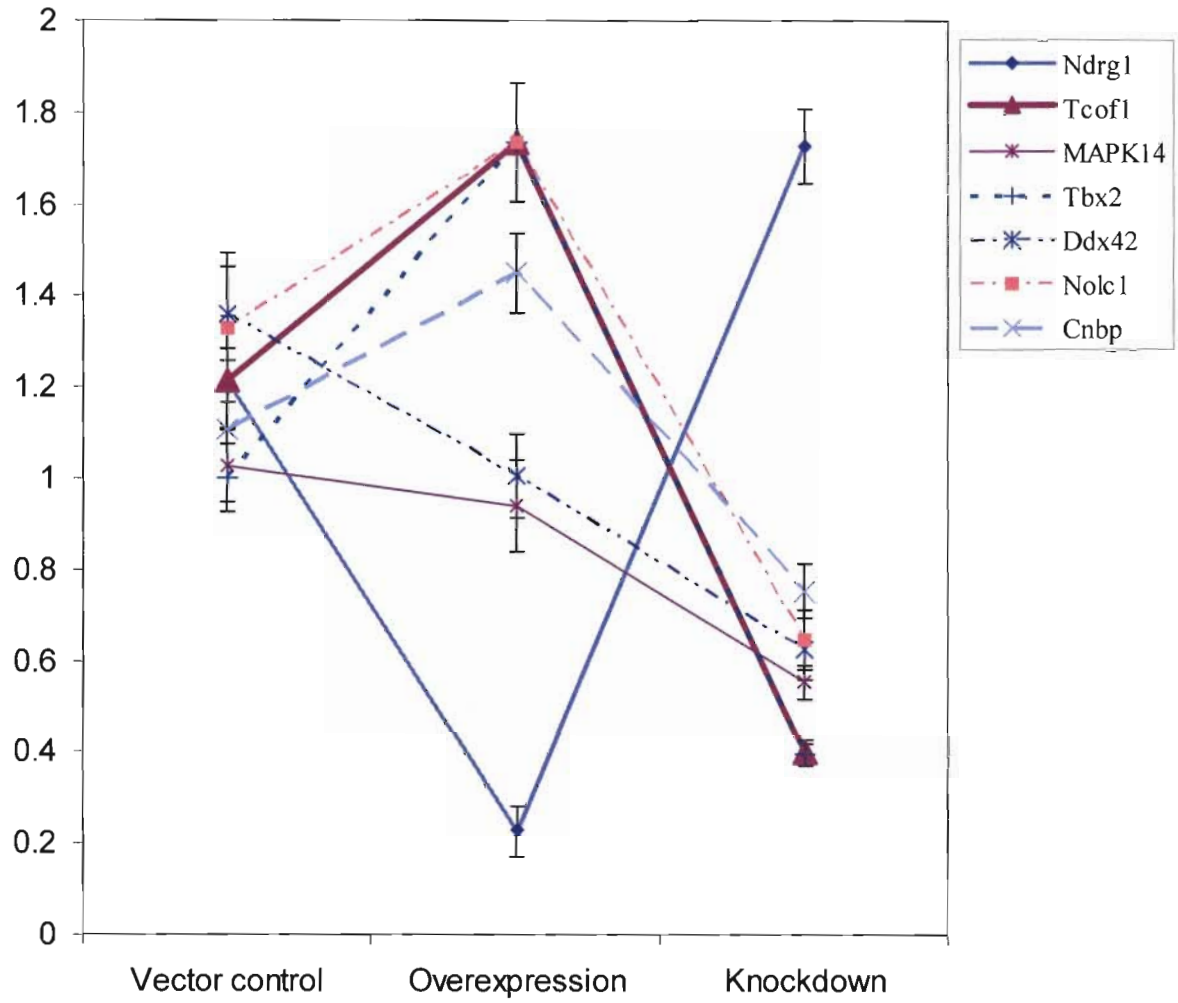

Figure 6 Real time quantitative RT-PCR analysis results. The x-axis shows different treatment groups of N1E-115 cells and the y-axis shows relative gene expression levels when compared to wildtype NB cells. Gene expression levels were normalized with GAPDH expression. Tcof1 is shown to be downregulated in knockdown cells and overexpressed in overexpression cells. Tcof1 expression is slightly elevated in the vector only control. Tbx2, Nolc1, and Cnbp expression are positively correlated with Tcof1 expression while Ndrg1 expression is negatively correlated with Tcof1 expression. Mapk14 and Ddx42 expression are decreased with knockdown of Tcof1 but not increased with Tcof1 overexpression.

independent stably transfected N1E-115 cell lines that express higher or lower treacle compared to parental cells or clones transfected with vector controls (Figure 7). Two cell lines of each, OE9 and OE39 for overexpression and KD16 and KD17 for knockdown, were used for all of the following experiments (Figure 7). Parental N1E-115 (WT) and two corresponding vector controls, DT3 for overexpression and SP21 for knockdown, were included as controls. Both DT3 and SP21 have slightly increased Tcof1 levels compared to N1E-115, which may be caused by the effects of the selection medium in which they are cultured.

Cell growth curves were originally generated by counting cell numbers for six consecutive days starting with 1×10^4 cells in T25 flasks (Figure 8). Vector control cells have reduced cell numbers than wildtype NB cells, probably because of the effects of the selection medium in which vector control cells are cultured. Interestingly, both overexpression and knockdown of treacle cause a significant reduction in cell numbers when compared with vector controls and parental cells, which suggests an optimal Tcof1 level is required for cell growth. Additionally, cells grown in log phase were used to generate cell growth curves by counting cell numbers every three days (Figure 9). Cell numbers at the low end of log phase (5×10^4) were used as the starting plating density. Similar results were observed for OE39, KD16 and KD17. OE9 grows at a similar rate as OE39 during the first week in culture, but at a faster rate than OE39 but still slower than vector control DT3 after a week. Some cellular changes may have occurred in OE9 to compensate for the detrimental effects of treacle overexpression on cells over time.

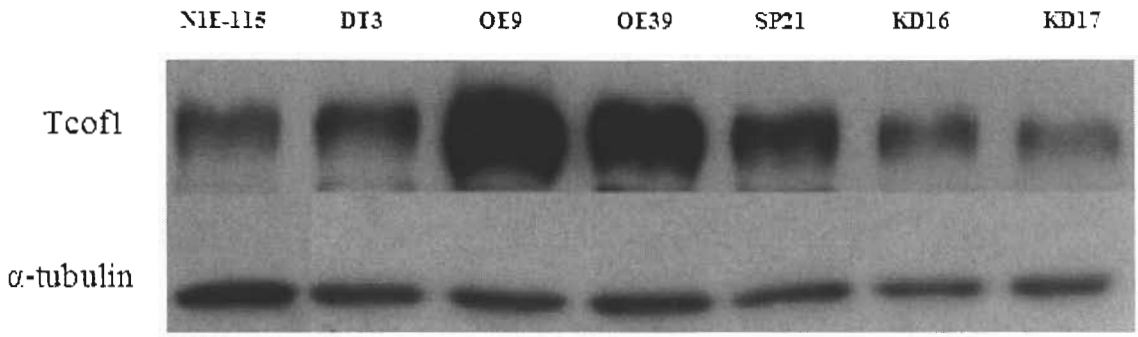

Average fold changes:	2.68	2.24		0.63	0.57
Standard Deviation:	0.38	0.37		0.07	0.16

Figure 7 Representative Western blot results using anti-treacle and anti-α-tubulin antibodies. OE9 and OE 39 are two Tcof1 overexpression cell lines. DT3 is the vector control cell line for OE clones. KD16 and KD17 are two Tcof1 knockdown cell lines. SP21 is the vector control cell line for KD clones. Both DT3 and SP21 have slightly increased Tcof1 levels compared to N1E-115. The numbers below the figure are calculated from three independent experiments. The fold changes are relative fold changes compared to their corresponding controls.

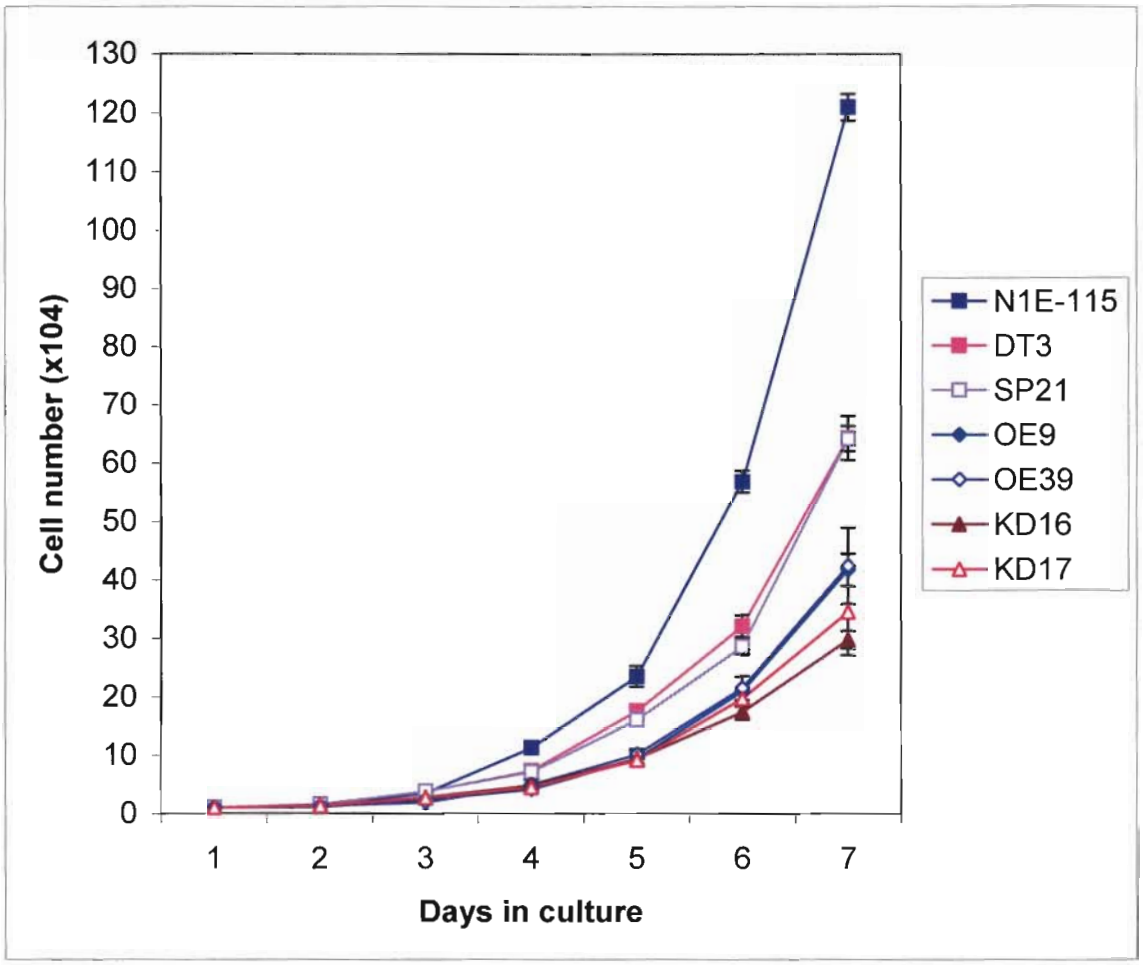

Figure 8 Cell growth curves. The X-axis represents days in culture. The Y-axis shows cell numbers. Vector control cells have reduced cell numbers than wildtype NB cells. Both overexpression and knockdown of treacle cause reduced cell numbers when compared with vector controls and parental cells.

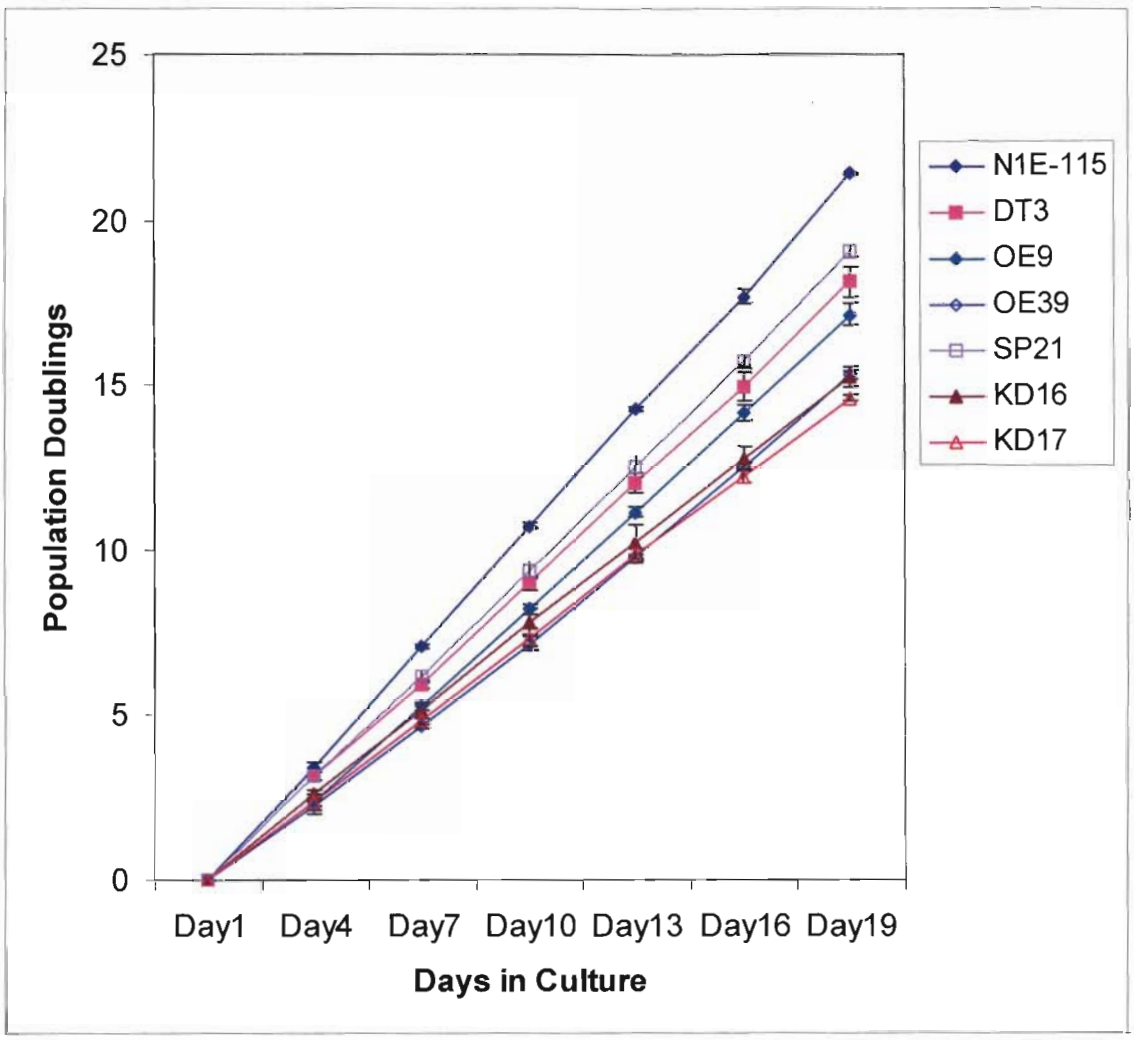

Figure 9 Cell growth curves generated with cells grown in log phase. The X-axis represents days in culture. The Y-axis represents cell population doublings. Both overexpression and knockdown of treacle cause reduced cell numbers when compared with vector controls and parental cells.

BrdU proliferation assays show a slightly smaller percentage of cells are in S phase of the cell cycle and a slightly increased percentage of cells in the G1 phase of the cell cycle in the OE39 cell line. The cell cycle distribution is not changed in OE9, which indicates the cell cycle distribution changes in OE39 may not be specific for overexpression of Tcof1. Both KD16 and KD17 show a significant reduction in DNA replication and increased percentage of cells in G1 and G2/M phases (Table 2; Figure 10). Our results indicate lower treacle levels reduce cell proliferation in NB cells while increased treacle levels do not affect cell proliferation in NB cells. These changes are not caused by nonspecific cellular changes because the proportion of cells in the different cell cycle phases is similar in vector control and parental NB cell lines.

Characterization of apoptosis levels

Heterozygous Tcof1 knockout mice show an increased apoptosis level in the prefusion neural folds, which is the site in which NC cells originate. NC cells are the major cell type that form the jaw and have the highest Tcof1 expression levels (Dixon et al., 2000). In this study, TUNEL assays were used to evaluate apoptosis levels in OE and KD clones. Both overexpression and knockdown of Tcof1 increase apoptosis levels significantly compared with vector controls and parental NB cells (Figure 11). The OE39 cell line, which grows slower than OE9, has significantly higher apoptosis levels than OE9. Vector control clones do not show an increase in apoptosis levels compared with wildtype NB cells, which indicates the increase in apoptosis in OE and KD clones is

Table 2 Percentage of cells in cell cycle stages.

	N1E-115	DT3	OE9	OE39	SP21	KD16	KD17
G1	34.24	33.82	35.44	40.27*	37.01	42.18*	45.51*
S	53.65	53.69	50.68	47.52*	51.06	34.02*	37.11*
G2/M	12.11	12.50	13.88	12.21	11.93	23.80*	17.38*

*: Significantly different from vector control.

A

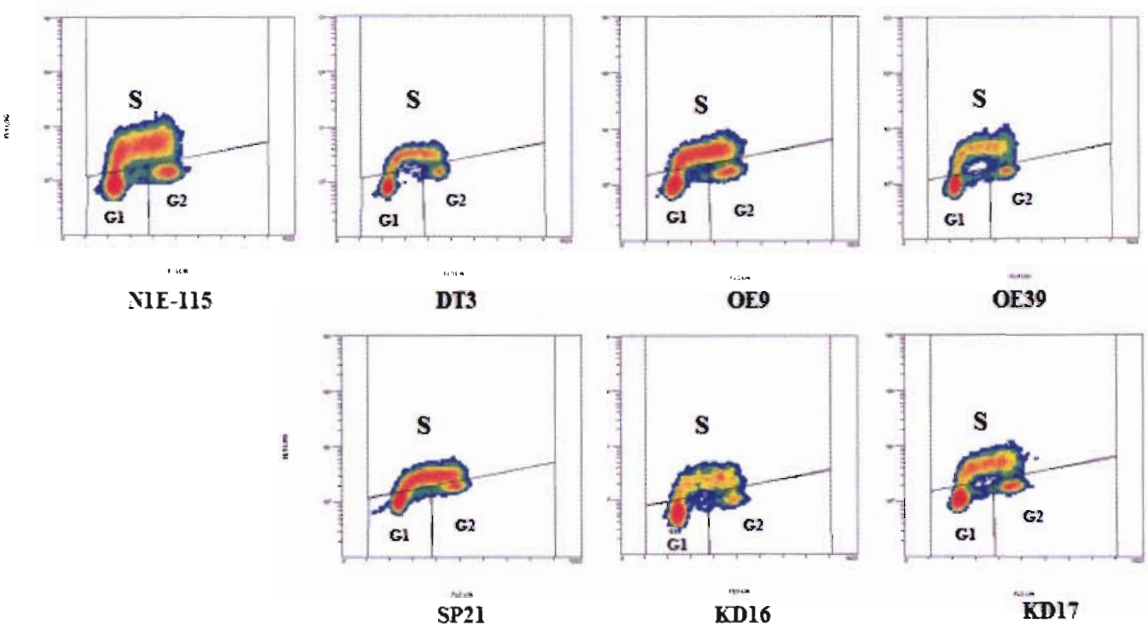

B

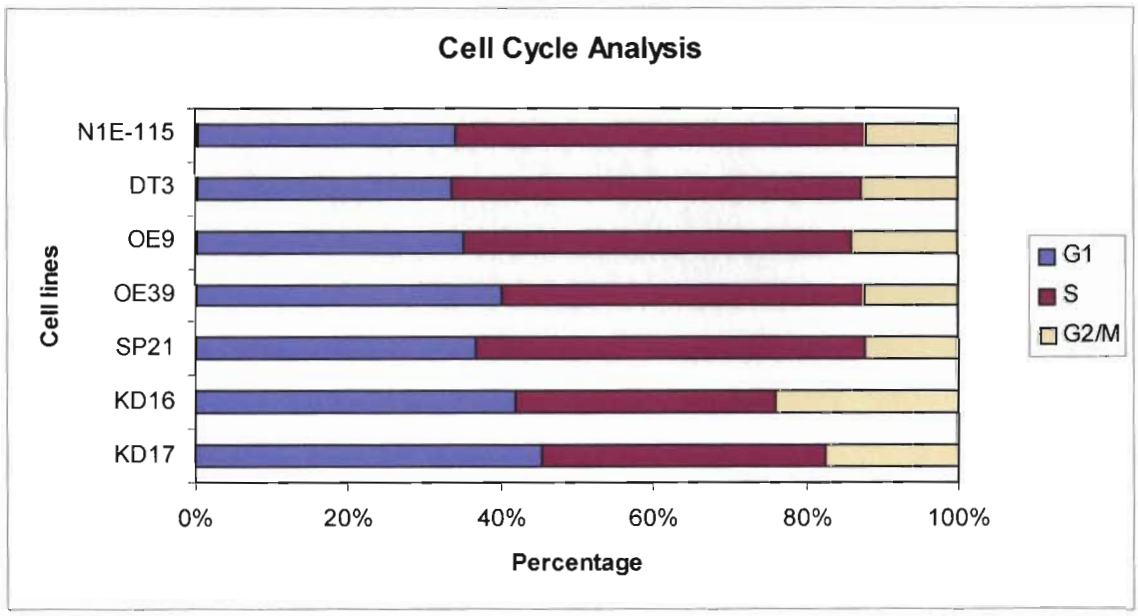

Figure 10 Cell cycle analysis results. A: Representative flow cytometry results. B: The X-axis shows the average proportion of cells in different cell cycle stages. The Y-axis indicates the different NB cell lines. Cell cycle distribution is not changed in DT3, OE9 and SP21. OE 39 has a slightly smaller percentage of cells in S phase of the cell cycle and a slightly increased percentage of cells in the G1 phase of the cell cycle. Both KD16 and KD17 show a significant reduction in DNA replication and increased percentage of cells in G1 and G2/M phases.

A

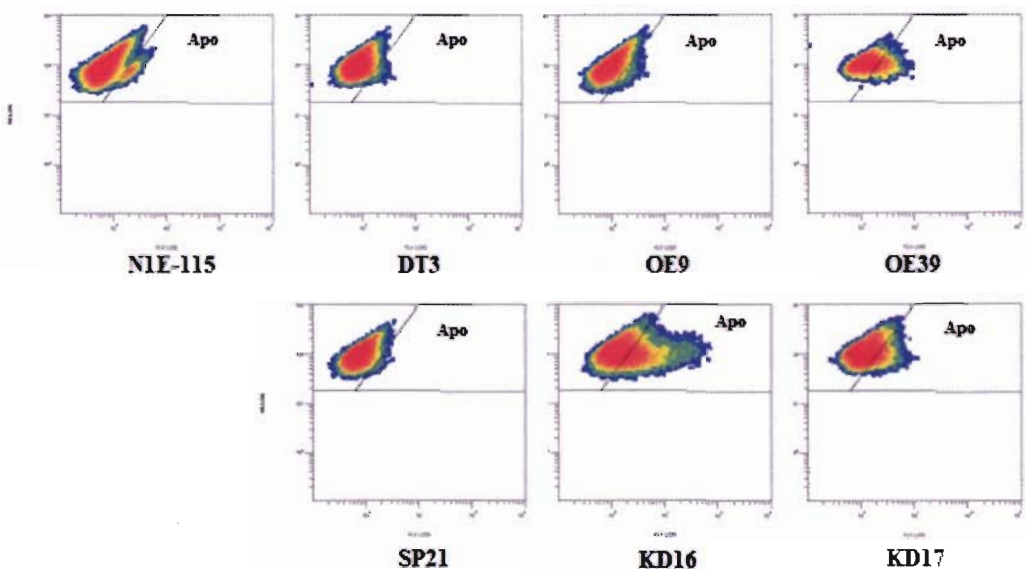

B

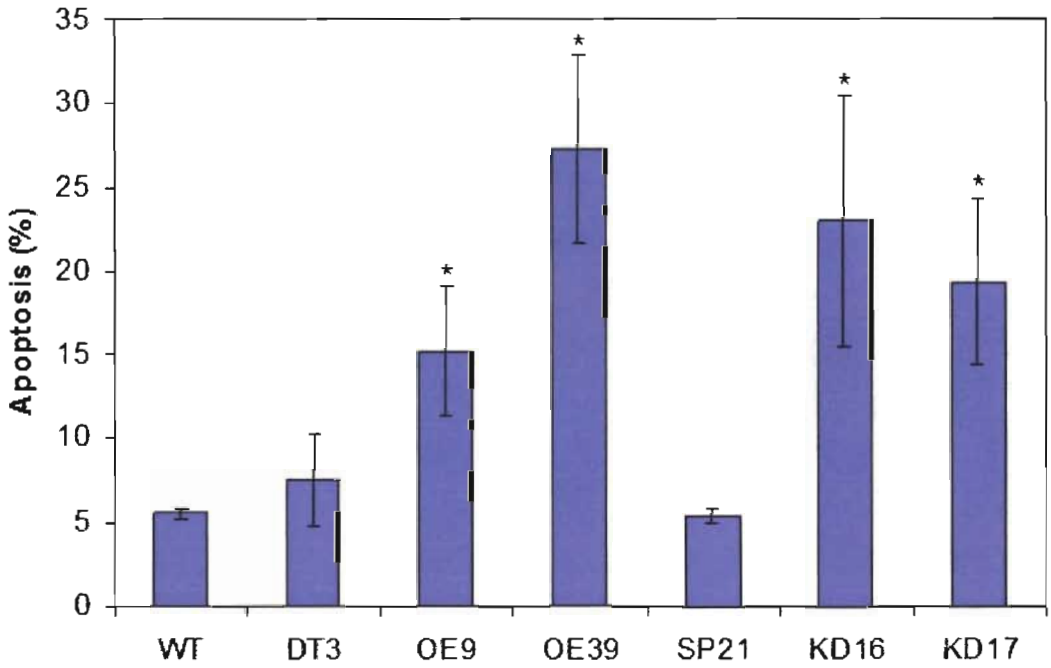

Figure 11 TUNEL assay results. A: Representative flow cytometry results. Apo: apoptosis cells. B: The X-axis shows different cell lines. The Y-axis shows the percentage of cells that are positive for apoptosis analysis. Stars indicate the apoptosis level is significantly different from controls. Vector control clones DT3 and SP21 have similar apoptosis levels compared with wildtype NB cells. Both overexpression and knockdown of Tcof1 increase apoptosis levels significantly compared with vector controls and parental NB cells.

caused by changes in treacle levels rather than nonspecific cellular changes during transfection. Our results indicate an optimal treacle level is also required for cell survival.

Western blot analysis to confirm candidate downstream genes

Previously, we identified *Cnbp* and *Tbx2* as downstream genes of *Tcof1* from a microarray analysis experiment comparing Tcof1 overexpression and knockdown NB cells to wild type (Mogass et al., 2004). Both genes share coordinate expression with Tcof1. The microarray analysis results of expression of proposed Cnbp/c-myc and Tbx2 pathway genes are shown in table 3.

In this study, Western blot analysis was used to detect Cnbp and its downstream targets c-myc and Ndrg1, and Tbx2 and its downstream targets $p19^{ARF}$ (Cdkn2d), Mdm2 and $p21^{WAF/CIP}$ (Cdkn1a) for protein level changes in OE and KD clones. Both OE clones show higher Cnbp levels without changes in c-myc levels, while both KD clones show lower Cnbp and c-myc levels (Figure 12). The c-myc downstream gene Ndrg1 levels are decreased in OE clones and not changed in KD clones compared with controls. The Tbx2 level is increased in OE39 but not in OE9 (the faster-growing cell line) and decreased in both KD clones (Figure 13). Surprisingly, Western blot analysis showed that $p19^{ARF}$, p53 and $p21^{WAF/CIP}$ protein levels are increased in OE clones and almost unchanged in KD clones (Figure 13). Mdm2 levels are not changed in OE and KD clones, which was expected because the regulation of Mdm2 is mainly through location changes.

Table 3 Microarray analysis results of Tcof1 downstream pathway genes

Gene	K vs. C	O vs. C	O vs. K
$p21^{WAF/CIP}$	0.85	1.02	0.96
$p19^{ARF}$	—	—	—
Mdm2	—	1.14	1.17
p53	—	1.25	1.41
c-myc	—	—	1.15

Numbers are average fold changes. K: NB cells with knockdown of Tcof1; O: NB cells with overexpression of Tcof1; C: Control wild type NB cells. — : No significant changes.

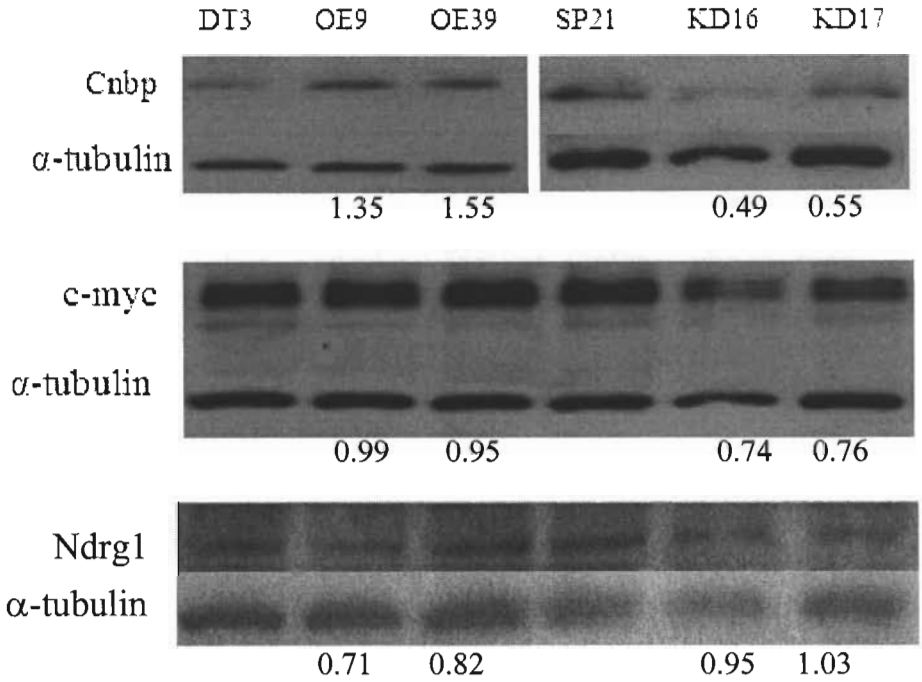

Figure 12 Representative Western blot analysis results show Cnbp, c-myc and Ndrg1 protein changes in different clones. Numbers are the average fold changes of the protein levels compared to vector controls. The Cnbp levels change coordinately with Tcof1. The c-myc levels are decreased in KD clones and increased in Tcof1 OE clones. The Ndrg1 levels are decreased in OE clones and not changed in KD clones compared with controls.

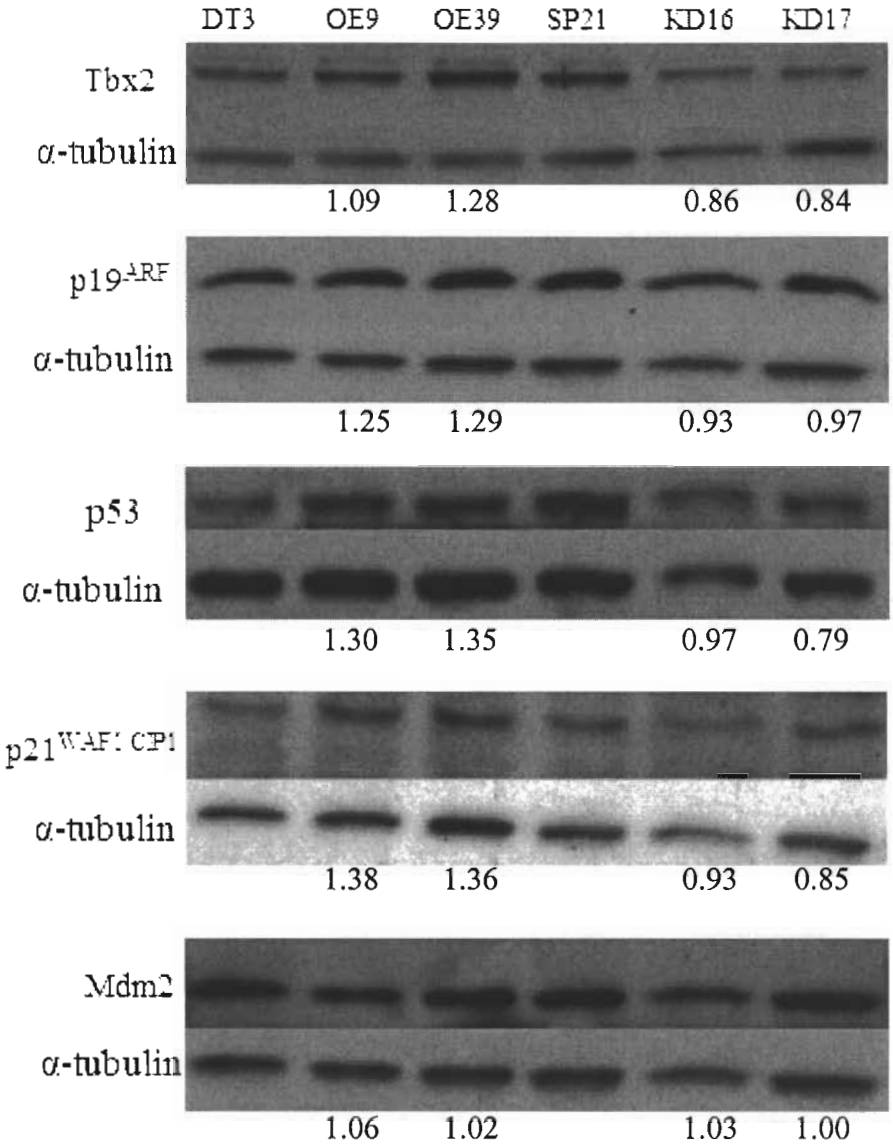

Figure 13 Representative Western blot analysis results of Tbx2, $p19^{ARF}$, p53, $p21^{WAF/CIP}$ and Mdm2 protein level changes in different clones. Numbers are the average fold changes of the protein levels compared to vector controls. The Tbx2 level is increased in OE39 but not in OE9 and decreased in both KD clones. The $p19^{ARF}$, p53 and $p21^{WAF/CIP}$ protein levels are increased in OE clones and not changed in KD clones. The Mdm2 levels are not changed with Tcof1.

In conclusion, overexpression of Tcof1 cause increased apoptosis without affecting cell proliferation and knockdown of Tcof1 cause reduced cell proliferation and increased apoptosis. Knockdown of Tcof1 results in reduced Cnbp and c-myc levels which may be responsible for the reduced cell growth in KD clones. Overexpression of Tcof1 results in increased $p19^{ARF}$, p53 and $p21^{WAF/CIP}$ levels, which may be responsible for the increased apoptosis levels in OE clones.

Discussion

Heterozygous Tcof1 knockout mice show an increased apoptosis level at highest Tcof1 expression sites (Dixon et al., 2000). SiRNA mediated down regulation of treacle level inhibits rRNA production (Valdez et al., 2004). Therefore, it was expected to see a decrease in cell growth and proliferation and an increase in apoptosis in Tcof1 knockdown clones. Surprisingly, overexpression of Tcof1 also causes an increase in apoptosis levels. An optimal Tcof1 level is evidently required for cells to survive and maintain proliferation.

OE9, which has higher treacle levels than OE39, has lower apoptosis levels than OE39 and correspondingly grows at a similar rate as OE39 during the first week in culture, then at a faster rate than OE39 over time. The difference in apoptosis levels cannot be explained by $p19^{ARF}$ and p53 level changes because their fold changes are similar in OE9 and OE39 compared to control. High levels of treacle seems to be harmful for cell survival. In order to survive, OE9 may have found some way which may include

other cellular changes to compensate for the detrimental effects of the highly overexpression of treacle on cells.

Knockdown of Tcof1 causes decreased expression in Cnbp. Cnbp, also called zinc finger protein 9 (ZNF9), is a highly conserved transcription factor with 7 zinc finger domains. Cnbp can bind the single strand CT element in the *c-myc* promoter region and enhance the transcription of *c-myc* (Michelotti et al., 1995; Shimizu et al., 2003). There is reduced expression of *c-myc* in the head region of Cnbp knockout mice (Chen et al., 2003). Myc family member c-myc is a basic helix-loop-helix leucine zipper (bHLH-Zip) transcription factor and known to bind to the bHLH-Zip protein Max to form heterodimers and regulate transcription. c-myc is well known for its potent oncogenic activity and ability to participate in most cellular activities including cell growth, proliferation, differentiation and apoptosis. Both *in vitro* and *in vivo* knockdown of c-myc expression in breast tumor cells result in decreased cell growth and increased apoptosis (Wang et al., 2005). Primary fibroblasts from c-myc knockout mice show reduced cell proliferation (Davis et al., 1993; Trumpp et al., 2001). Our study shows that Cnbp and c-myc are down regulated in Tcof1 knockdown clones. Knockdown of Tcof1 could cause decreased cell proliferation and increased apoptosis through down regulation of Cnbp and c-myc (Figure 14).

Overexpression of Tcof1 results in increased p53 and $p21^{WAF/CIP}$ (Cdkn1a, cyclin-dependent kinase inhibitor 1a) levels. The transcription factor p53 has been extensively studied and is known to respond to cellular stress, causing cell cycle arrest and apoptosis. Identified as a mediator of p53-induced growth arrest, $p21^{WAF/CIP}$ is known to bind to and

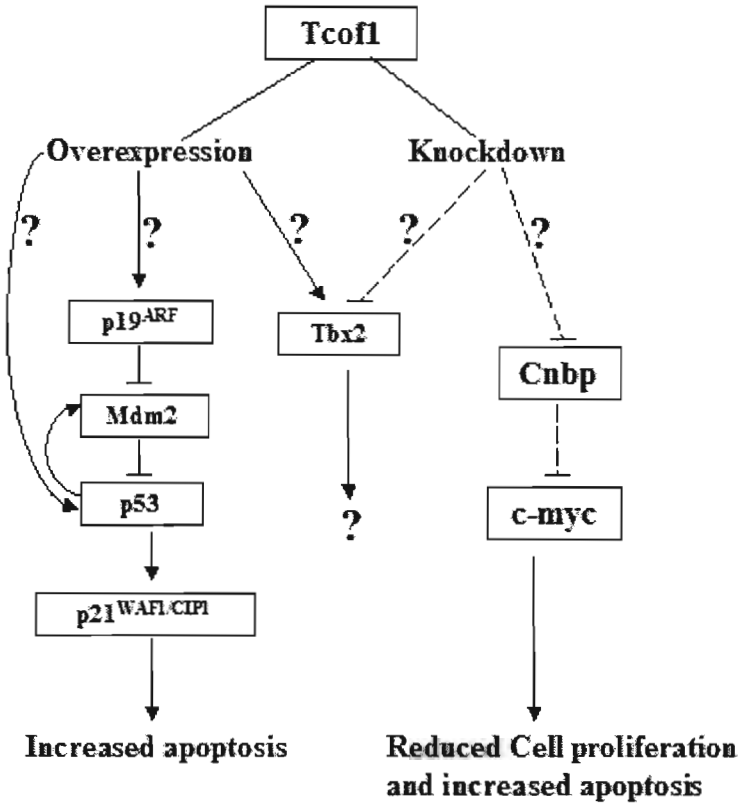

Figure 14 Tcof1 affect cell proliferation and apoptosis through different downstream pathways. Knockdown of Tcof1 causes decreased cell proliferation and increased apoptosis through down regulation of Cnbp and subsequent c-myc down regulation. Overexpression of Tcof1 causes increased apoptosis through up regulation of p53 and $p21^{WAF/CIP}$ directly or through up regulation of $p19^{ARF}$. ⟶ : Up regulate. – – –⊣: Down regulate. ——⊣ : Sequest or degradation. ?: unknown mechanism.

inactivate cyclin-dependent kinases required for cell cycle progression. It can also associate with proliferating nuclear antigen (PCNA) and directly inhibit DNA replication (reviewed by Dotto, 2000). As described in chapter one, tumor suppressor gene p53 is also suggested to be involved in the regulation of Pol I transcription therefore the regulation of ribosome biogenesis. Overexpression of Tcof1 could cause increased apoptosis through p53- $p21^{WAF/CIP}$ pathway (Figure 14). Unexpectedly, $p19^{ARF}$ is increased in Tcof1 overexpression clones. Overexpression of $p19^{ARF}$ can inhibit cyclin D1-cdk4 activity and cause G1 arrest in the cell cycle (Hirai et al., 1995), which could be responsible for the increased G1 phase in OE39. In addition, $p19^{ARF}$ can sequester Mdm2 from assisting in the degradation of p53, therefore increase the p53 level. Increased p53 can activate transcription of $p21^{WAF/CIP}$ and inhibit cell cycle progress at all stages and increase apoptosis through $p21^{WAF/CIP}$. While the increase of $p21^{WAF/CIP}$ could be due to increased p53, how Tcof1 up regulates $p19^{ARF}$ and p53 is still unclear and needs further investigation (Figure 14).

Tbx2 is a T box family transcription factor that can work as either an activator or repressor. Tbx2 is overexpressed in various cancer cells, including breast cancer, pancreatic cancer and melanoma, to maintain cell proliferation by repressing the activities of $p19^{ARF}$ (Cdkn2d) and $p21^{WAF1/CIP1}$ (Cdkn1a) (Lingbeek et al., 2002; Jacobs et al., 2000; Prince et al., 2004). The decreased amount of Tbx2 level in Tcof1 knockdown clones does not cause increased $p19^{ARF}$, $p21^{WAF1/CIP1}$ or p53 levels. The effects of decreased Tbx2 on cell proliferation and survival are not clear (Figure 14). Tbx2 levels are increased in one of the Tcof1 overexpressing clones OE39 but not OE9. This

indicates that a change in Tbx2 expression may not be specific to Tcof1 overexpression. On the other hand, Tbx2 expression could also be inhibited in OE9 by other cellular changes that has occurred in OE9.

Ndrg1 was identified as a gene negatively regulated with Tcof1 from our microarray experiments. However, in this study, Western blots show that Ndrg1 level is decreased in KD clones and not changed in OE clones. In our microarray experiment, siRNA technique was used to transiently inhibit treacle. There was complete silencing of treacle at 72 hours and cells behave like differentiated NB cells without treacle. Ndrg1 is usually up regulated in differentiated cells (Fotovati et al., 2006). In this study, stable knockdown of treacle were achieved using pSuperRNAi system. Because of the detrimental effects of reduced treacle level on cell growth, the lowest reduction we achieved in stable knockdown cell line is about 70% and cells do not behave like differentiated NB cells. That may explain why the Ndrg1 is not up regulated in KD clones. p53 has been shown to activate Ndrg1 and c-myc can inhibit the activity of Ndrg1 (Kurdistani et al., 1998; Shimono et al., 1999). While c-myc is not up regulated in OE clones, the increased p53 level does not cause increased Ndrg1 level in OE clones. There must be other factors regulating Ndrg1 level and needs further investigation.

In conclusion, this study shows an optimal Tcof1 level is required for cell proliferation and cell survival. Overexpression of Tcof1 causes increased apoptosis without affecting cell proliferation and knockdown of Tcof1 causes reduced cell proliferation and increased apoptosis. Knockdown of Tcof1 causes decreased cell proliferation and increased apoptosis through down regulation of Cnbp and subsequent

c-myc down regulation. Overexpression of Tcof1 causes increased apoptosis through up regulation of $p19^{ARF}$, p53 and $p21^{WAF/CIP}$.

Chapter 3: Creating and characterizing a murine model of Treacher Collins Syndrome (TCS)

Introduction

The creation and use of a murine model of human disease can provide many powerful approaches to the analysis of gene function. *Tcof1* heterozygous knockout mice were generated by replacing exon 1 of *Tcof1* with a neomycin-resistance cassette via homologous recombination in embryonic stem cells (Dixon et al., 2000). Tcof1 heterozygous mice with a mixed 129 and C57BL/6 (B6) background exhibit a generalized developmental delay and severe structural craniofacial abnormalities throughout development (Dixon et al., 2000). The phenotype of heterozygous mice overlaps TCS patients, including malformation of the maxilla, secondary palate, nasal complex and external ear and hypoplasia of the zygomatic arch, tympanic ring, middle ear ossicles and mandible, though structures in Tcof1 heterozygous mice are affected much more severely. The heterozygous mice die shortly after birth because they are unable to establish an airway due to severe craniofacial abnormalities, the lack of nasal passages and exencephaly. Perinatal lethality resulting from a comprised airway is rare in TCS patients. Exencephaly and anophthalmia (without eyes) have never been reported in TCS patients.

The penetrance and severity of craniofacial and other defects of Tcof1 heterozygous mice varies in different genetic backgrounds (Dixon and Dixon, 2004). Phenotypic variation includes severe facial defects and neonatal lethality in C57BL/6 (B6) or CBA/Ca and 129 mixed backgrounds to majority phenotypically normal in BALB/c or DBA/1 and 129 mixed backgrounds. Partial elimination of the *Tcof1* gene in mouse in a mixed B6/129 background is neonatal lethal, which circumvents further detailed analysis of the heterozygous and homozygous knockout mice on a homogenous background. Thus, a conditional knockout mouse model, which might more closely resemble human TCS, was generated using the Cre-lox system in this study.

Conventional knockout leads to the inactivation of the targeted gene in all tissues and development stages in targeted mice. More recently, conditional gene targeting approaches were developed to generate time- and/or tissue-specific knockout of the targeted gene. Conditional gene targeting approaches are especially useful when conventional knockout mice are embryonic or neonatal lethal which prevents further detailed analysis. Control of gene targeting in a time dependent manner allows the analysis of gene function at different development stages. Tissue specific inactivation of a gene gives further insight into the gene function in the targeted tissue (Müller, 1999).

The Cre-lox recombination system, which provides a powerful tool for gene targeting in mice, involves the use of a site specific recombinase, Cre, from bacteriophage P1 that recognizes and binds to a 34 bp long partly palindromic target sequence called loxP (locus of crossover x in P1). The 34 bp loxP site consists of two 13 bp inverted repeats, which are the binding sites for the Cre protein, and an 8 bp

asymmetric core region in which recombination occurs and decides the direction of the site. Cre recombinase has the ability to perform efficient recombination at loxP sites and excise or invert any sequence between two loxP sites of the same or opposite directions respectively (Sauer and Henderson, 1989).

The traditional knockout of the *Tcof1* gene in mice was generated by replacing exon 1 with a neomycin-resistance cassette, which indicates the elimination of exon 1 is sufficient for disrupting gene expression (Dixon et al., 2000). In this study, a tissue specific knockout mouse model was generated by the Cre-lox system. Targeted mice were generated with two loxP sites flanking exon 1 of *Tcof1* (floxed allele) and then crossed to commercially available transgenic mice that express Cre recombinase under the control of the Wnt1 promoter (Wnt1-Cre) (The Jackson Laboratory). Wnt1 is expressed in the central nervous system and early NC cell progenitors (Echelard et al., 1994, Dorsky et al., 1998). Wnt1-Cre transgenic mice have been widely used to generate mouse models with conditional targeted gene knockout in cranial and cardiac NC cells (Brault et al., 2001; Brewer et al., 2004; Dudas et al., 2004; Mori-Akiyama et al., 2003; Santagati et al., 2005).

The research objectives of this study are to generate a mouse line with a Tcof1 conditional allele, and to generate a TCS mouse model by inter-crossing the conditional allele mice with Wnt1-Cre transgenic mice. Analysis of the phenotype and downstream gene changes in this model as compared to control animals will give us further insight into the protein product function and disease pathogenesis.

Materials and methods

Construct

The targeting vector pTKLNCDL (a gift from Dr. Richard Mortensen) contains a neomycin-resistant gene (neo, positive selectable marker) adjacent to the cytosine deaminase (CD, negative selectable marker) gene. These markers have been floxed (flanked with loxP sites). Outside of the floxed region resides a thymidine kinase (TK, a second negative selectable marker) gene (Milstone et al., 1999). It was designed so that genomic fragments of the *Tcof1* gene need to be cloned into both sides of the floxed region (one in a NotI site and the other in a SalI site). The region to be deleted, exon 1 of *Tcof1*, needed to have another loxP site in its upstream sequence (Figure 15).

Since there is a lack of appropriate restriction enzyme sites, primers with NotI linkers (NotImHS1F: AAAGGAAAAAGCGGCCGCGTCACTGTATAGGTAGCCAT and NotImintron1R: AAGGAAAAAAGCGGCCGCGCCATTCTTGCTACTGAGAC) were designed using 5' upstream and intron 1 sequences to amplify a ~ 4.4 kb Not I fragment. Primers with SalI linkers (SalImintron1F: ACGCGTCGACGTCTCAGTAGCAAGAATGGC and SalImintron3R: ACGCGTCGACGAGTGACACTGAGCTCTTAG) were designed using intron 1 and intron 3 sequences to amplify a ~ 5.7 kb Sal I fragment. PCR was performed from 50 ng of a Tcof1 cosmid clone (cm7c2, isolated from a 129/sv strain genomic library from Dr. Jay Ellison) using Expand Long Template PCR System (Roche) according to manufacturer's instruction. The PCR products were TA cloned (Invitrogen) into PCR2.1-TOPO vector then sequenced to confirm the correct sequence. Previously, a loxP site was

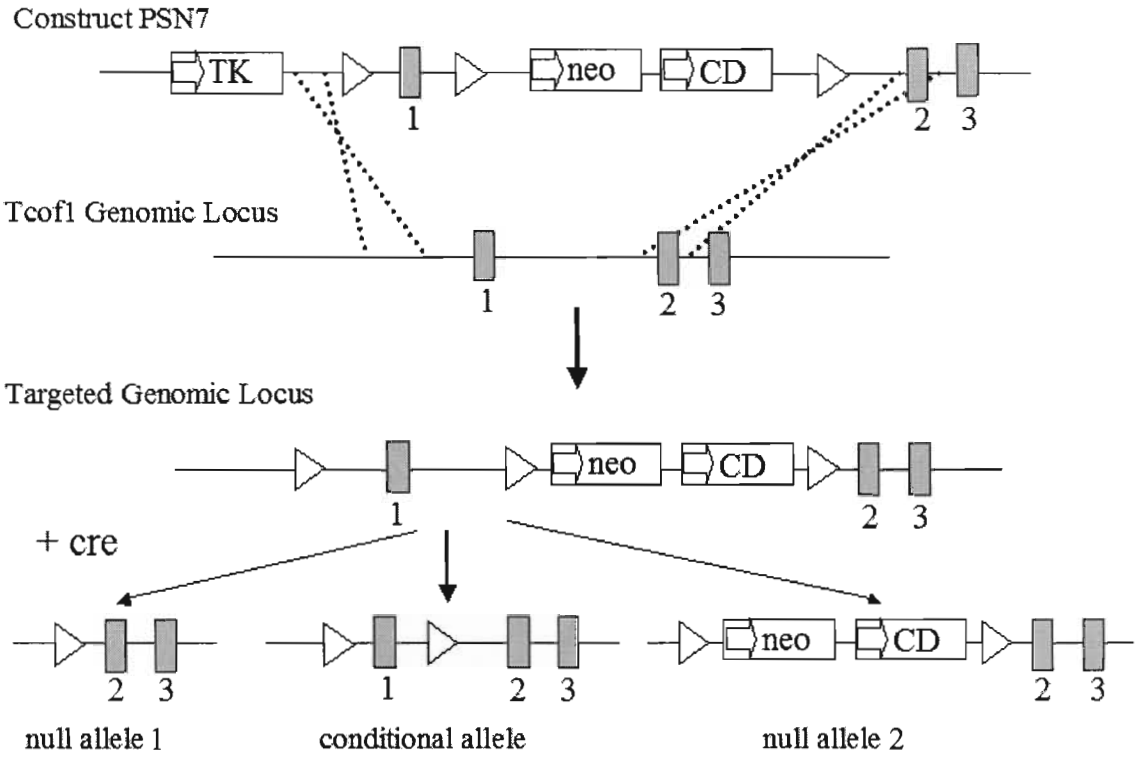

Figure 15 Generation of the *Tcof1* conditional allele. PSN7 is the construct we used to generate the conditional allele, which has the first three exons of *Tcof1*, a TK gene and a loxP site in the 5' of exon 1 and a floxed neo/CD cassette in intron 1. The construct PSN7 was electroporated into ES cells. After homologous recombination with the *Tcof1* genomic locus, a loxP site in the 5' region of exon 1 and a floxed neo/CD cassette in intron 1 will exist. Then the ES cell line was transiently transfected with pCMV-cre. There are three possible cre-mediated deletions. If the first and the third loxP sites are used, exon 1 and the neo/CD cassette will be deleted (null allele 1). If the second and the third loxP sites are used, this will result in a deletion of neo/CD cassette, leaving two loxP sites flanking exon 1. This construct was used to generate the conditional knockout mice. The last alternative, the first two loxP sites are used for recombination, then exon 1 will be deleted and the neo/CD cassette will remain (null allele 2). Numbered gray boxes represent *Tcof1* exons. Dashed lines represents the homologous recombination locations. ▷: loxP sites. TK: thymidine kinase gene; neo: neomycin-resistant gene; CD: cytosine deaminase gene.

inserted into the region 5' of exon 1 by PCR amplification of a PstI fragment of the same cosmid clone using primers with a loxP linker designed from *Tcof1* 5' upstream and intron 1 sequences and TA cloned into pBluescript (LoxPC).

The SalI fragment was cloned directly into SalI site of target vector pTKLNCDL. To insert a loxP site in the 5' of exon 1, the NotI fragment was subcloned from PCR2.1-TOPO vector into pBluescript (same vector as LoxPC). Then by digestion with BclI and partial digestion with NcoI, exon 1 was replaced with the exon 1 plus an upstream loxP site. The Not I fragment with 5' loxP site was then cloned into the Not I site of pTKLNCDL that contains the Sal I fragment. Direct sequencing was performed to confirm the desired direction and correct junction sequences.

Generating conditional allele mice

The PSN7 construct (Figure 15) was linearized by digesting with BstBI and run on an agarose gel to confirm complete linearization. The DNA was purified by phenol chloroform, precipitated with ethanol and resuspended in 10 mM Tris, pH 7.5, 0.1 mM EDTA. The DNA quality was confirmed by agarose gel electrophoresis. A total of 20 μg of DNA was electroporated by the Transgenic Mouse Facility at VCU into ~10×10^6 129/SvEv ES (HZ2.2) cells, a cell line that came from the same strain as the original genomic library. The cells were split and plated in 4 separate culture dishes and grown in nonselective media for 24 hours on a feeder layer of neomycin resistant cells (STO cells from ATCC, treated with mitomycin C). In three of the dishes, the media was changed and 180 μg/ml G418 and 2 mM of ganciclovir was added. A cell is viable when

homologous recombination occurs because of the positive selection on G418 (neo selection marker) and the negative selection on ganciclovir (TK selection marker) (Figure 15). However, the negative selection is not 100% effective because TK is often inactivated when randomly integrated into the genome. Approximately 8 days after selection, surviving clones were transferred into 96 well plates that containing feeder cells and expanded. When they were confluent, the cells were split and one set cryopreserved in 10% DMSO and the other expanded again for DNA extraction for genotyping to identify ES clones in which homologous recombination had occurred.

The ES cell line 1A5 that underwent homologous recombination was cultured and transiently transfected with 7 μg of pCMV-cre by electroporation. The cells were transferred into 96 well plates in duplicate. One set was grown in selection media with 180 μg/ml G418. Three possible cre-mediated deletions can occur (Figure 15). If the first and the third loxP sites are used, exon 1 and the neo/CD cassette will be deleted (null allele 1). This construct could be used to generate null mice. If the second and the third loxP sites are used, this will result in a deletion of neo/CD cassette, leaving two loxP sites flanking exon 1. This construct was used to generate the conditional knockout mice. The last alternative, the first two loxP sites are used for recombination, then exon 1 will be deleted and the neo/CD cassette will remain (null allele 2). The cells with the complete deletion and conditional allele are not viable under selection (Figure 15). Duplicate plating was used to expand the non-surviving clones from selection and genotyped for the conditional allele by PCR and Southern analysis.

Genotyping by PCR and Southern analysis

DNA was extracted from ES cells following a standard protocol obtained from the Transgenic Mouse Facility at VCU. For mouse genotyping, three weeks old pups were ear punched and the ear punch was used to extract DNA using the Wizard® Genomic DNA Purification Kit following manufacturer's protocol (Promega).

PCR analysis was used to detect the existence of the loxP sites in ES cells and mouse embryos. The PCR primers were designed around each loxP site (P1PCRF: GCACCAGACATCTGAACTGT and P1PCRR: AAGGCTAACCTAGCTCTGCCA for the 5' loxP site; mexon1F7: GTGTCAGCCCTCGGTTA and mTcof1ko-R: GGATCCTTCTTCACAGCACCA for the intron 1 loxP site) (Figure 16). PCR was performed with 50 ng mouse genomic DNA, 1× PCR buffer, 0.4 mM dNTP, 0.1 pmol/μl primers and 1u Taq polymerase (PGC scientific). The 12.5 μl reaction was denatured at 94°C for 2 min, then cycled at 94°C for 30 sec, 65°C for 30 sec, and 72°C for 30sec for 30 cycles, and then at 72°C for 7 min. PCR products were run on 6% acrylamide gels to visualize.

Southern analysis was used to confirm homologous recombination and identify the conditional allele. A probe from DNA upstream of exon 1 (5' probe) and another probe from genomic sequence around exon 4 (3' probe) were used for Southern analysis (Figure 16). The hybridization fragment sizes for wildtype allele was determined by Southern analysis using 129/SvEv mouse genomic DNA. Ten microliters of mouse genomic DNA was digested with EcoRV overnight at 37°C then separated on 0.9% agarose gel. The DNA was transferred overnight to Immobilon-Ny+ transfer membranes

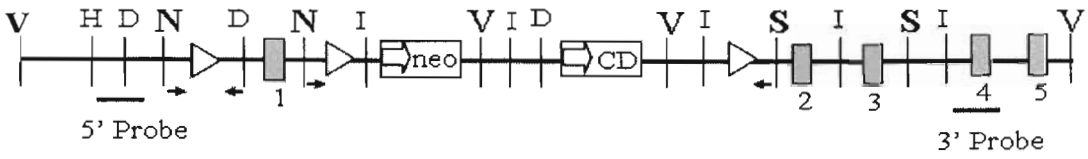

Figure 16 Restriction map of the targeted allele. Arrows represent PCR primers. H: HindIII; D: NdeI; N: NotI; I: EcoRI; V: EcoRV; S: SalI. —— : Southern probes. ▷: loxP sites. Numbered boxes are exons.

(Millipore) in 0.4 N NaOH transfer buffer. Membranes were rinsed for 15 minutes in 2× SSC, dried on filter paper and UV-crosslinked. Blots were washed in 0.2× SSC and 0.2% SDS at 65°C for 1 hour and pre-blocked in hybridization solution (50% formamide, 1× Denhardt solution, 0.5% SDS, 7.5% dextran sulfate, 5× SSC with 80 μg/ml salmon sperm DNA) for 24 hours at 65°C. Then membranes were hybridized with 50 ng of the DNA probe that was labeled by random primering with ^{32}P-dCTP overnight at 42°C. The following day, membranes were washed in 2× SSC/0.1% SDS, 1× SSC/0.1% SDS and 0.5× SSC/0.1% SDS each for 1 hour at 65°C. Membranes were exposed to X-ray film overnight at -70°C.

Karyotyping of ES cells

Karyotyping of mouse ES cells was performed following the protocol from Manipulating the Mouse Embryo Manual, the second edition (Hogan et al., 1994). ES cells were treated with 3 drops of 10 μg/ml colcemid for 20 minutes and harvested. Cells were resuspended in 4 ml 0.56% KCl and incubated at room temperature for 6 minutes. Cell pellets were fixed in 4 ml fresh absolute methanol:glacial acetic acid (3:1) fixative at room temperature and repeated three times. Cell pellets were resuspend in 200 μl fixative and dropped on slides. The slides were aged for 6 days and stained with Giemsa for G-banding analysis under microscope.

Mating scheme

To analyze our mouse model on a B6/129 background, Wnt1-Cre transgenic mice, which was on a Swiss Webster background, was crossed with C57BL/6 mice for at least 5 generations. Then hemizygous Wnt1-Cre mice were mated with homozygous conditional allele mice to generate conditional heterozygous knockout mice. Half of the offspring have the conditional heterozygous knockout allele, which includes the Wnt1-Cre transgene and one Tcof1 floxed allele (Figure 17A). Conditional heterozygous knockout males were then used to mate with homozygous floxed Tcof1 females to generate homozygous conditional knockout mice. Because Wnt1 is not expressed in germ cells, this mating scheme generates four different genotypes, ¼ conditional homozygous knockouts, ¼ conditional heterozygous knockouts and ½ heterozygous or homozygous floxed Tcof1 without Wnt1-Cre as controls (Figure 17B).

Cartilage staining

Cartilage staining was performed following the alcian blue cartilage staining protocol from Manipulating the Mouse Embryo Manual, the third edition (Gertsenstein et al., 2003) with slight modifications. Briefly, 12.5-14.5 dpc mouse embryos were dissected in 1× PBS and fixed in Bouin's solution (Sigma) for 2 hours at room temperature followed by washing in 70% ethanol with 0.1% NH_4OH for about 24 hours until embryos appeared white. Then embryos were equilibrated in 5% acetic acid for one hour twice at room temperature. Embryos were stained in 0.05% alcian blue in 5% acetic acid overnight at 4°C and additional 3 hours at room temperature followed by two

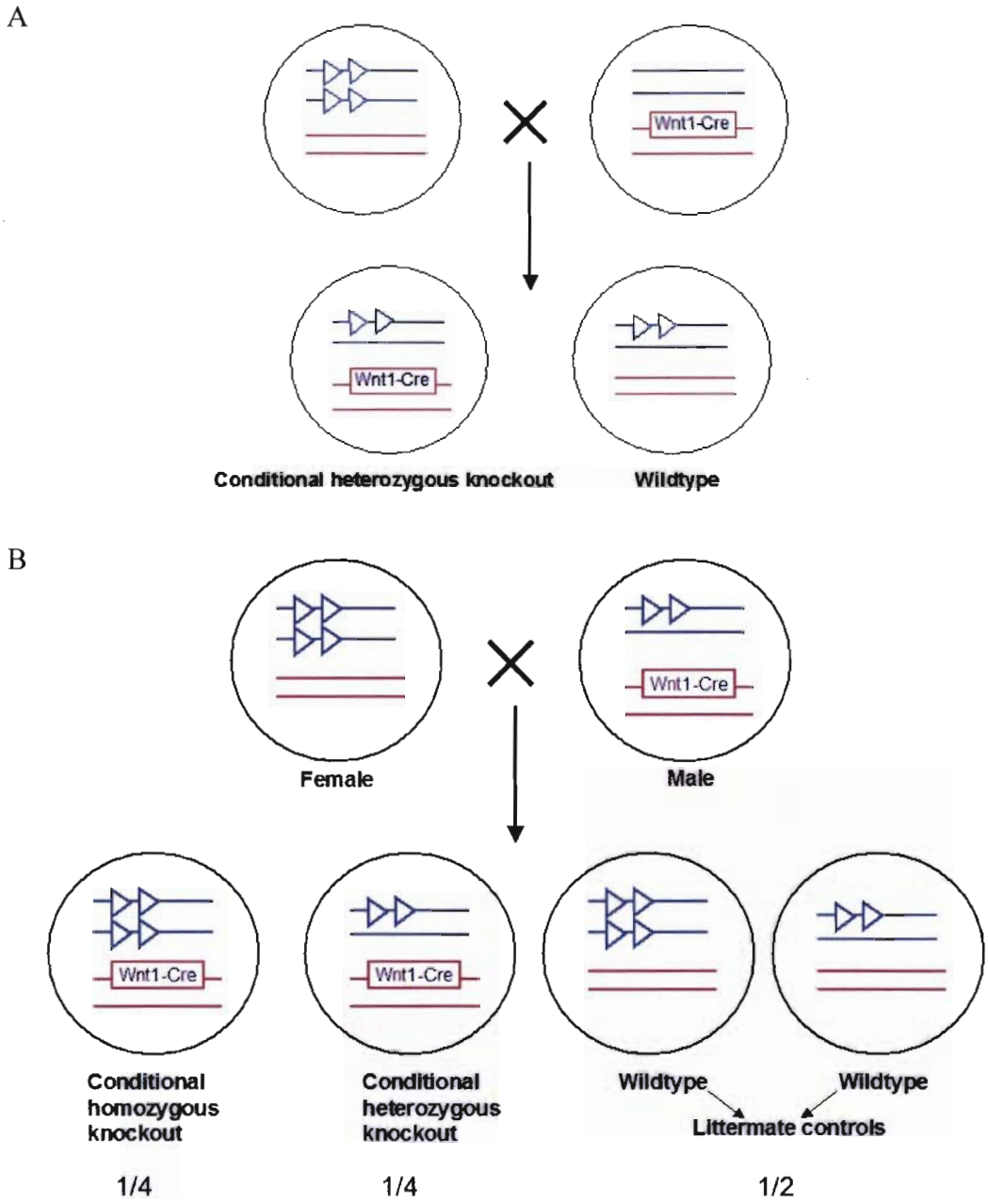

Figure 17 Mating schemes. A: The mating scheme for generating conditional heterozygous knockout mice. Homozygous conditional allele mice are crossed with Wnt1-Cre hemizygous mice and half of the offspring have the conditional heterozygous knockout allele. B: The mating scheme for generating conditional homozygous knockout mice. Homozygous conditional allele females are crossed with conditional heterozygous knockout males. This mating scheme generates four different genotypes, ¼ conditional homozygous knockouts, ¼ conditional heterozygous knockouts and ½ heterozygous or homozygous floxed Tcof1 without Wnt1-Cre as controls. ▷: loxP sites.

one-hour washes with 5% acetic acid and two one-hour washes with 100% methanol. Embryos were then cleared in BABB (1:2 benzyl alcohol to benzyl benzoate) overnight and photographed under a dissecting microscope for analysis.

Whole mount *in situ* hybridization

Candidate downstream gene, *Cnbp*, expression was investigated by whole mount *in situ* hybridization. A *Cnbp* cDNA clone was generated by RT-PCR essentially as described in chapter two using *Cnbp* cDNA primers mCnbpNativeF: GGGGACAAGTTTGTACAAAAAAGCAGGCTTAGAAGGAGATAGAACCATGAG CAGCAACGAATGCTTCAAG and mCnbpNativeR: GGGGACCACTTTGTACAAGAAAGCTGGGTCTTAGGCTGTAGCCTCAATTGTG CA. PCR was performed with a 65°C annealing temperature and 30 cycles using AccuPol Taq polymerase (PGC scientific). The PCR product was TA cloned into pBluescript and sequenced to confirm the correct sequence and determine insert direction.

Mouse embryos were dissected out in 1× PBS and fixed in 4% paraformaldehyde in PBS overnight at 4°C. Whole mount *in situ* hybridization was performed by Dr. Rita Shiang following the protocol obtained from the June 1996 Cold Spring Harbor Mouse Course.

Results

Generating homozygous conditional allele mice

A mouse genomic cosmid library was previously screened with a *Tcof1* full-length cDNA. The library was constructed using an EcoRII partial digestion of genomic DNA from a 129/Sv strain cloned into the pWE15 vector (Dr. J. Ellison). One positive clone containing the *Tcof1* gene was identified and the presence of the *Tcof1* gene was confirmed by PCR. The gene encompasses ~18.5 kb. Fragments of the cosmid clone were subcloned into pBluescript and ~ 14 kb of genomic DNA was sequenced including 2.7 kb upstream of exon 1 to intron 6. A restriction map of the mouse genomic region has been constructed (Figure 16) and used to design our construct.

After transfection with the target construct PSN7, ES cells were grown on selection medium, a total of 186 ES clones which survived selection were picked and DNA extracted to screen for homologous recombination by Southern blot analysis. When mouse genomic DNA was digested with EcoRV, the 5' probe hybridized to a ~23 kb band from a wildtype allele and a ~15.6 kb (7.4 kb smaller) band from the correctly targeted allele; the 3' probe hybridized to a ~ 23 kb band from a wildtype allele and ~9.6 kb band from the correctly targeted allele (Figure 18A,B). Four out of 186 clones screened had homologously recombined. PCR analysis was performed on the four clones, 1A5, 1G12, 2D2, and 2E6, to examine the presence of the loxP site upstream of exon 1. The existence of the 5' loxP site generates a 468 bp PCR product while the wildtype

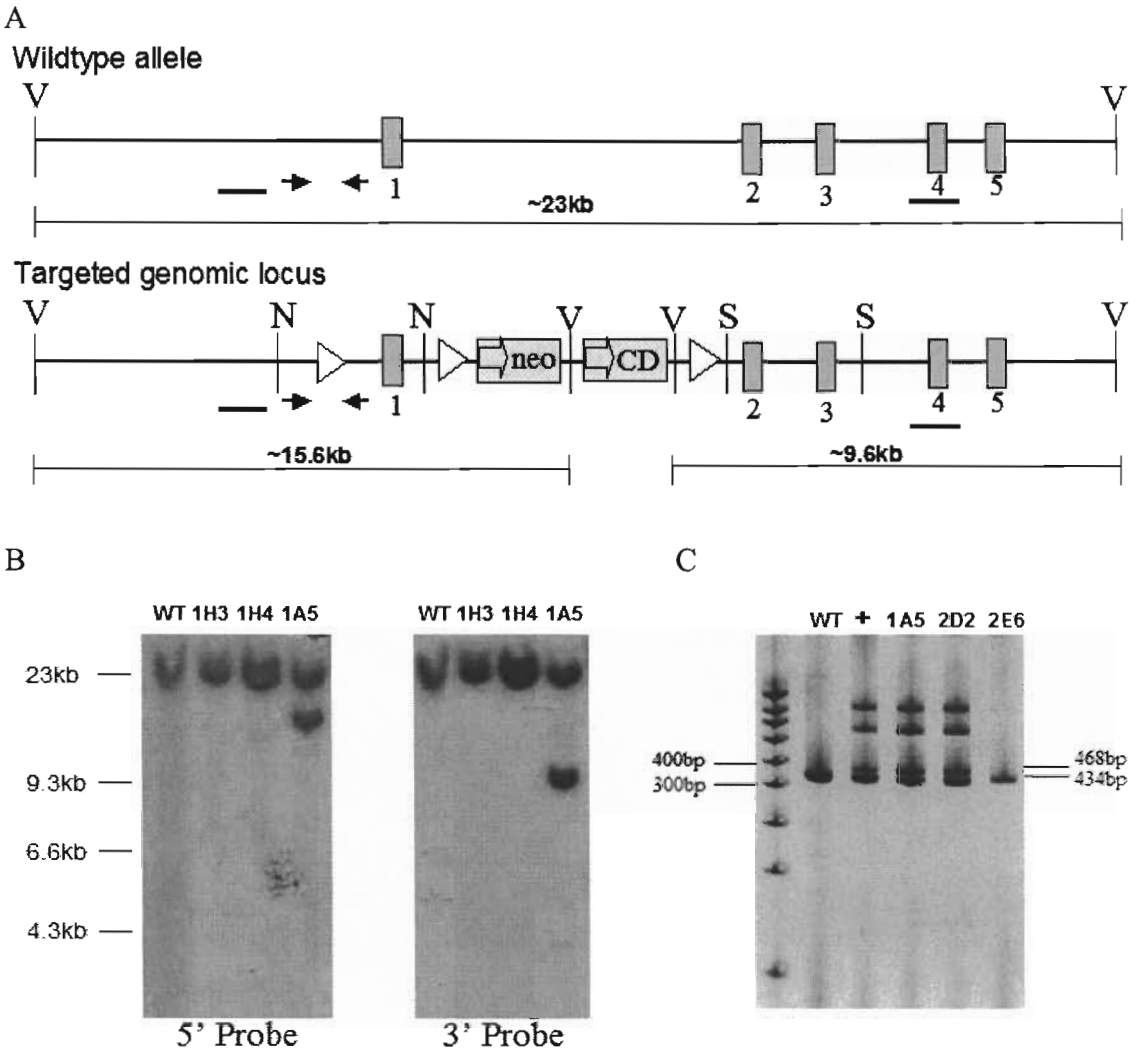

Figure 18 Southern and PCR analysis results. A: The restriction map of the target region. The wildtype and targeted alleles will generate different size bands on Southern blots using the EcoRV restriction enzyme. The PCR products will indicate the existence of the 5' loxP site. Arrows represent PCR primers. Bars represent Southern probes. N: NotI; V: EcoRV; S: SalI. B: Representative Southern analysis result for screening homologous recombination in representative clones. When mouse genomic DNA is digested with EcoRV, the 5' probe hybridized to a ~23 kb band from a wildtype allele and a ~15.6 kb band from the correctly targeted allele; the 3' probe hybridized to a ~ 23 kb band from a wildtype allele and ~9.6 kb band from the correctly targeted allele. C: Representative 5' loxP site PCR analysis result. The existence of the 5' loxP site generates a 468 bp PCR product while the wildtype allele generates a 434 bp product. There are two non-specific larger bands amplified in some of the positive clones. WT: DNA from wildtype 129 mouse. +: positive control.

allele generates a 434 bp product (Figure 18C). All lines except 2E6 retained the 5' loxP site.

One of the correctly targeted clones 1A5 was used for transient transfection with pCMV-cre to remove selection markers neo and CD from the ES cell genome. Twelve out of 96 clones were not G418 resistant and were tested for the existence of the conditional allele. In correctly targeted conditional allele clones, no genomic DNA should be deleted. The only difference between the conditional allele and the wildtype allele are two loxP sites that flank exon 1, which does not change the Southern analysis pattern (Figure 19A,B). PCR analysis was used to confirm the existence of both the 5' and the intron 1 loxP sites (Figure 19C). In a correctly targeted conditional allele, the existence of the intron 1 loxP site generates a 646 bp PCR product while the wildtype allele generates a 397 bp product. The size difference is caused by insertion of a part of the vector sequence (from the second loxP site in the vector to SalI site) into the mouse genome. Three out of twelve non-G418 resistant clones have the conditional allele; seven clones have the null allele 1 and two are found to be false positives for selection. All three ES clones containing the conditional allele have a normal karyotype (Figure 20).

Two clones, 1A5-N-1 and 1A5-N-3, were used to perform injections into blastocysts from C57BL/6 (B6) mice to generate chimeras. Three chimeric males from each line were used to set up mating with B6 females. The agouti coat color from the 129/SvEv ES cells is dominant over B6 black coat color, which facilitates the identification of pups derived from the 129/SvEv ES cells. Twenty seven pups (100%)

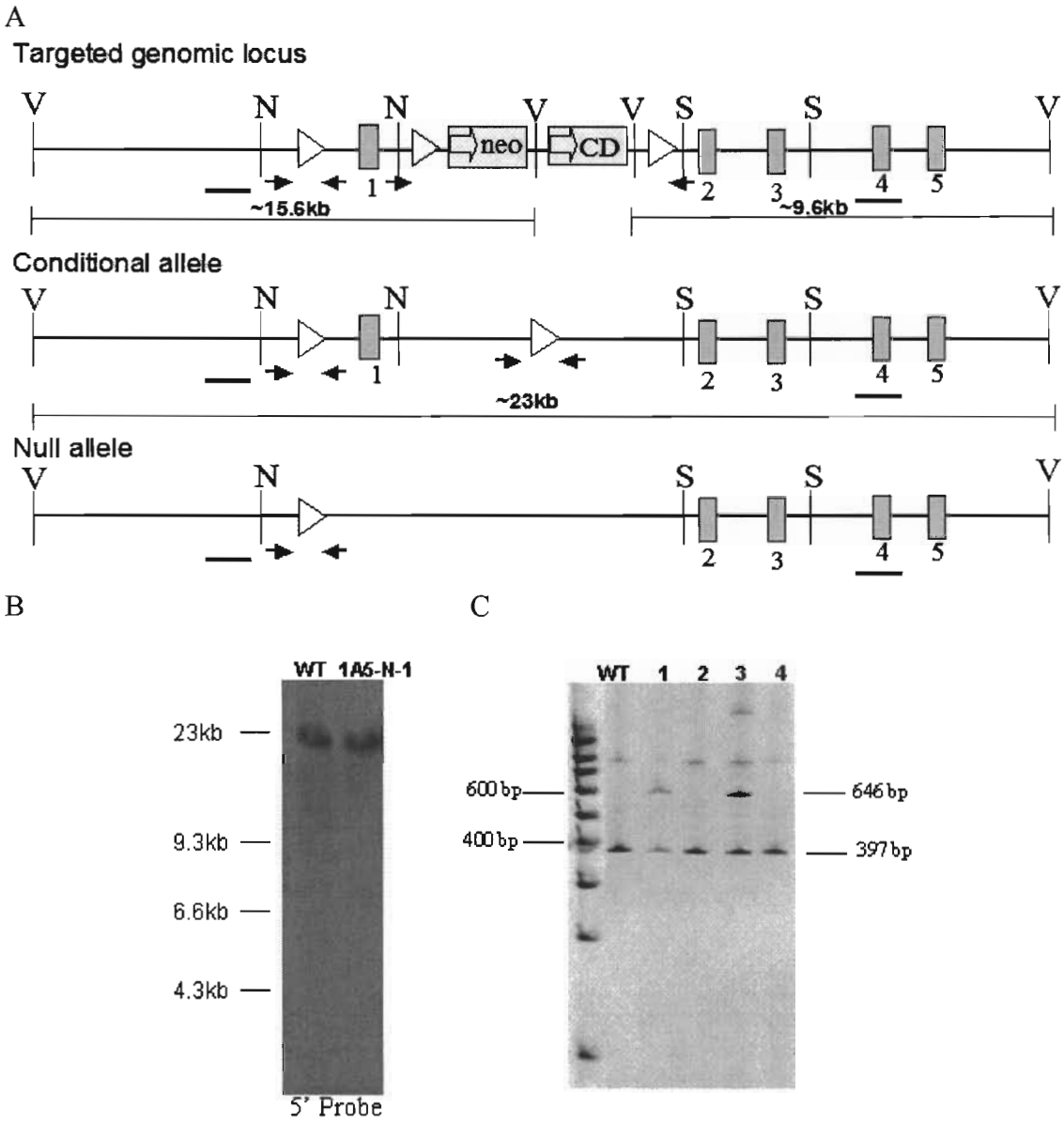

Figure 19 Southern and PCR analysis results of screening for the conditional allele. A: The restriction map of the target region. The wildtype and conditional alleles will generate same size bands on Southern blots using the EcoRV restriction enzyme. Arrows represent PCR primers. Bars represent Southern probes. N: NotI; V: EcoRV; S: SalI. B: Representative Southern analysis result for conditional allele. When mouse genomic DNA was digested with EcoRV, both the 5' and the 3' probes hybridized to a ~23 kb band from the conditional allele or the null allele. Clone 1A5-N-1 shows a Southern pattern indicative of the conditional allele which is indistinguishable from wildtype allele. C: Representative PCR result of the intron 1 loxP site. The existence of the intron 1 loxP site generates a 646 bp PCR product while the wildtype allele generates a 397 bp product. WT: DNA from wildtype 129 mouse. 1-4: 1A5-N-1 to 1A5-N-4.

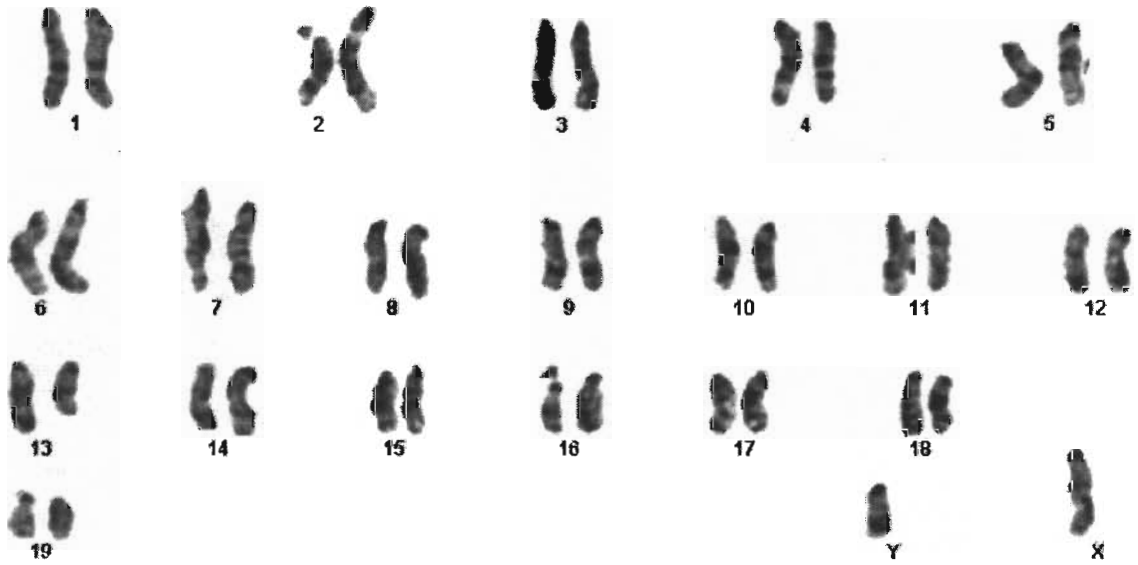

Figure 20 Representative normal mouse embryonic stem cell karyotype for 1A5-N-1. Chromosomes are arranged in pairs and the chromosomal number is indicated below each pair.

from the 1A5-N-1 line and forty three pups (68.3%) from the 1A5-N-3 line were agouti (Table 4). Half of the agouti offspring were heterozygous for the conditional allele (floxed Tcof1). Heterozygous floxed Tcof1 mice were mated to each other to generate homozygous floxed Tcof1 mice. Both heterozygous and homozygous floxed Tcof1 mice are viable, fertile and phenotypically normal.

Generating conditional knockout mice

Because genetic background has a major effect on the phenotype of Tcof1 knockout mice, Wnt1-Cre transgenic mice were transferred to a B6 background from the original Swiss-Webster background by crossing with B6 for at least 5 generations. Homozygous floxed Tcof1 mice were mated with Wnt1-Cre mice to generate conditional heterozygous knockout mice. Conditional heterozygous knockout mice are viable, fertile, of normal size and have no physical or behavioral abnormalities. This result was unexpected because the traditional heterozygous knockout causes neonatal lethality with severe craniofacial abnormalities. Because Wnt1 is expressed in early NC progenitor cells, this finding suggests that the expression of Tcof1 in other tissue/cells and/or at an earlier time is important for mouse craniofacial development.

Conditional heterozygous knockout mice (heterozygotes) were then used to mate with homozygous floxed Tcof1 mice to generate conditional homozygous knockout mice (homozygotes). Because no homozygous knockout pups were identified at birth, embryos were dissected at different embryonic days to determine the timing of embryonic lethality and to study the phenotype. The embryo dissection results are

Table 4 Chimera offspring germline transmission summaries

Cell Line	Chimera	Total Pups	Agouti Pups	Percentage
	#10	7	7	100%
1A5-N-1	#11	2	2	100%
	#18	18	18	100%
	#23	28	25	89%
1A5-N-3	#24	32	15	47%
	#25	3	3	100%

summarized in Table 5. The morphology of homozygotes is indistinguishable from heterozygotes and wildtype littermates on embryonic day 8 to 9.5 (E8-E9.5). At E10.5, the homozygotes displayed smaller first and second BAs compared to controls (Figure 21A). The telencephalon appeared larger in homozygotes than controls, which may be a secondary change due to the defects in the BAs. From E11.5-E13.5, homozygotes show obvious defects in craniofacial development and an abnormal exposed forebrain (Figure 21B; Figure 22A). The maxillary and mandible prominences are severely underdeveloped. The medial nasal prominence does not fuse at the midline. There is often abnormal blood vessel distribution in the cranial region in homozygotes. The blood vessels in the head region in homozygotes appear to be enlarged (Figure 21B, Figure 22A). The homozygotes die from around E12.5, which further supports cardiovascular system defects. Two embryos that survived until E14.5 did not develop normal craniofacial structures, with only remnants of maxillary and mandible prominences (Figure 22B; Figure 23). The forebrain appears smaller and the embryo has abnormal external ears. Eye development appears unaffected. By E15.5, most embryos examined were absorbed and no homozygotes were detected at E18.5. The mutant phenotype appears consistent from two independent lines 1A5-N-1 and 1A5-N-3. The occurrence of embryo lethality varies from E12.5 to E15.5, which may be caused by the lack of homogeneity in the genetic background, as some of the embryos may retain 1% Swiss Webster background.

Table 5 Embryos genotypes

d.p.c.	-/- (1/4)	+/- (1/4)	+/+ (1/2)	Unknown	Total
8.5	13	4	18	–	35
9.5	12	15	40	5	72
10.5	10	11	14	2	37
11.5	7	3	4	–	14
12.5	12/13*	16	46	–	75
13.5	4/6**	9	20	–	35
14.5	2/10**	12	17	–	39
15.5	0/9**	16	10	–	35
18.5	0**	5	19	–	24

-/-: Conditional homozygous knockout; +/-: Conditional heterozygous knockout; +/+: Wildtype. (1/4): expected frequency. *: The number after slash is the total embryos genotyped; the number before slash is the number of the embryos not absorbed. **: The ratio of the homozygotes is significantly different than expected ratio ¼.

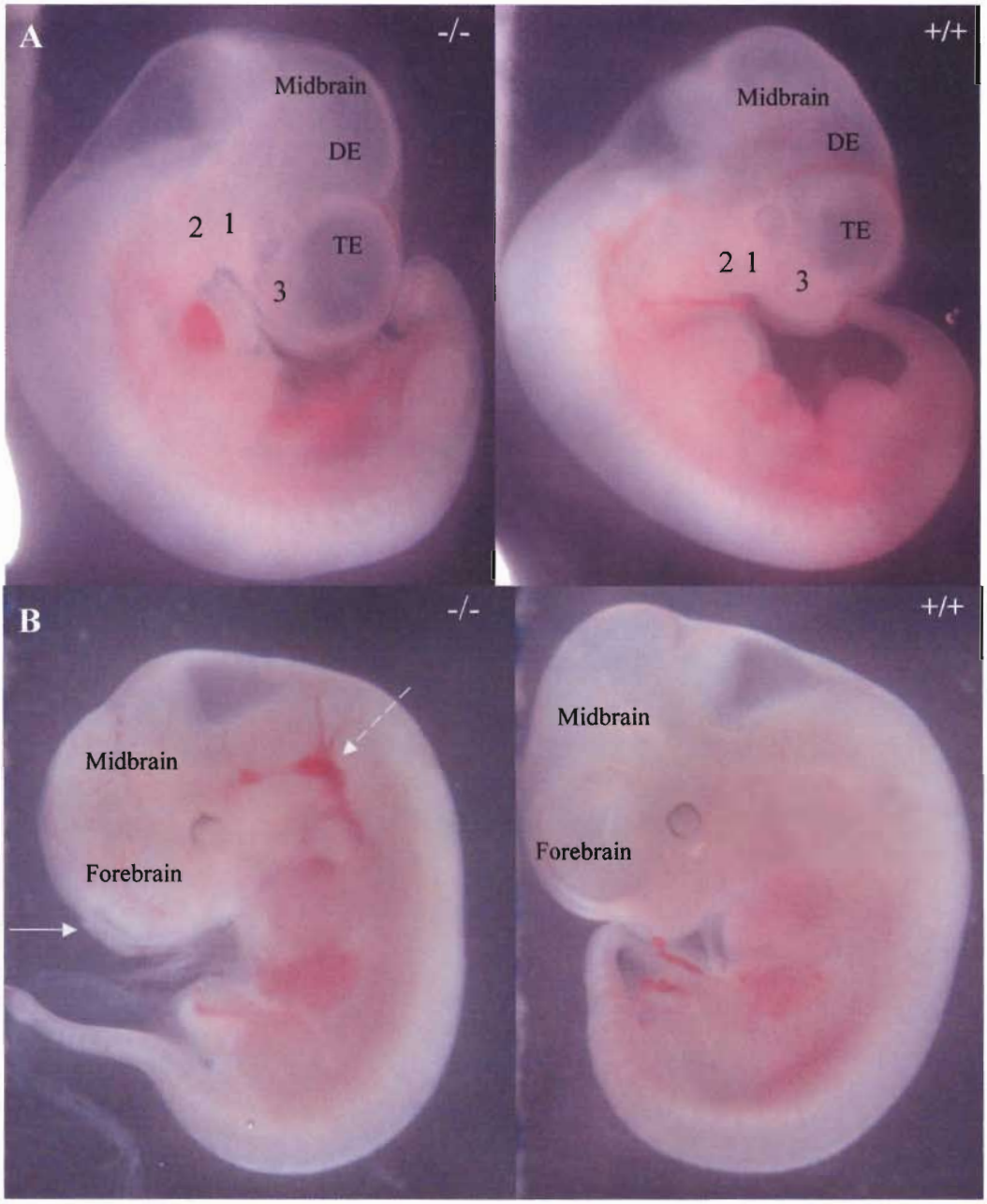

Figure 21 Craniofacial and forebrain defects in Tcof1 homozygous mutants. A: E10.5 embryos. At E10.5, the homozygotes displayed smaller first and second BAs compared to controls. B: E11.5 embryos. At E11.5, homozygotes show obvious defects in craniofacial development, an abnormal exposed forebrain and blood vessel abnormalities. The solid arrow points to the exposed forebrain. The broken arrow points to the enlarged blood vessel. Embryos are photographed in 1×PBS. -/-: conditional homozygous knockouts. +/+: wildtype controls. TE: Telencephalon; DE: Diencephalon; 1: 1st BA; 2: 2nd BA; 3: Frontonasal region.

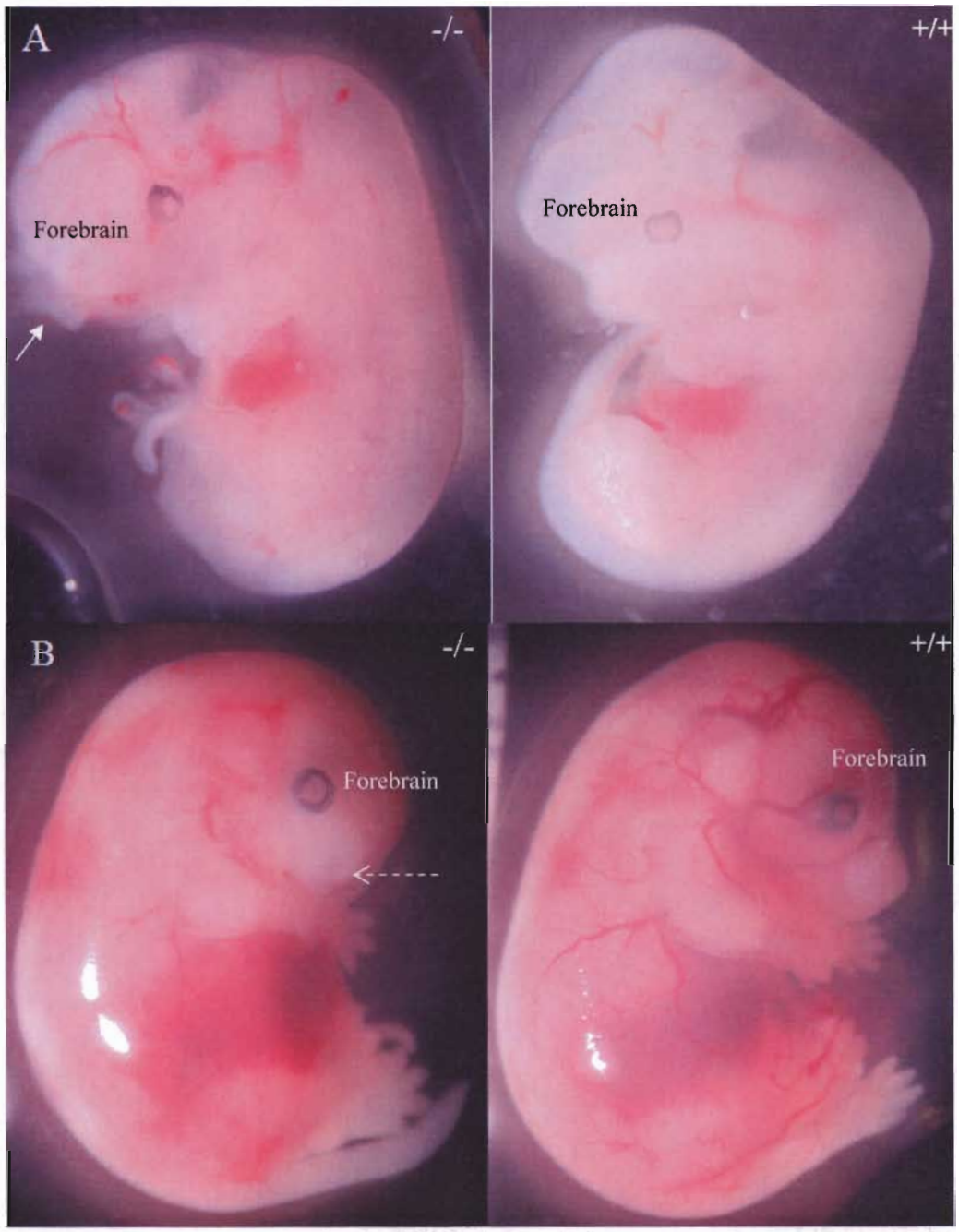

Figure 22 Craniofacial and forebrain defects in Tcof1 homozygous mutants. A: E12.5 embryos. At E12.5, homozygotes show obvious defects in craniofacial development and an abnormal exposed forebrain. The solid arrow points to the exposed forebrain. B: E14.5 embryos. At E14.5, homozygotes show severely underdeveloped maxillary and mandible prominences and smaller forebrain. The broken arrow shows that the medial nasal prominence does not fuse at the midline. Embryos are photographed in 1×PBS. -/-: conditional homozygous knockouts. +/+: wildtype controls.

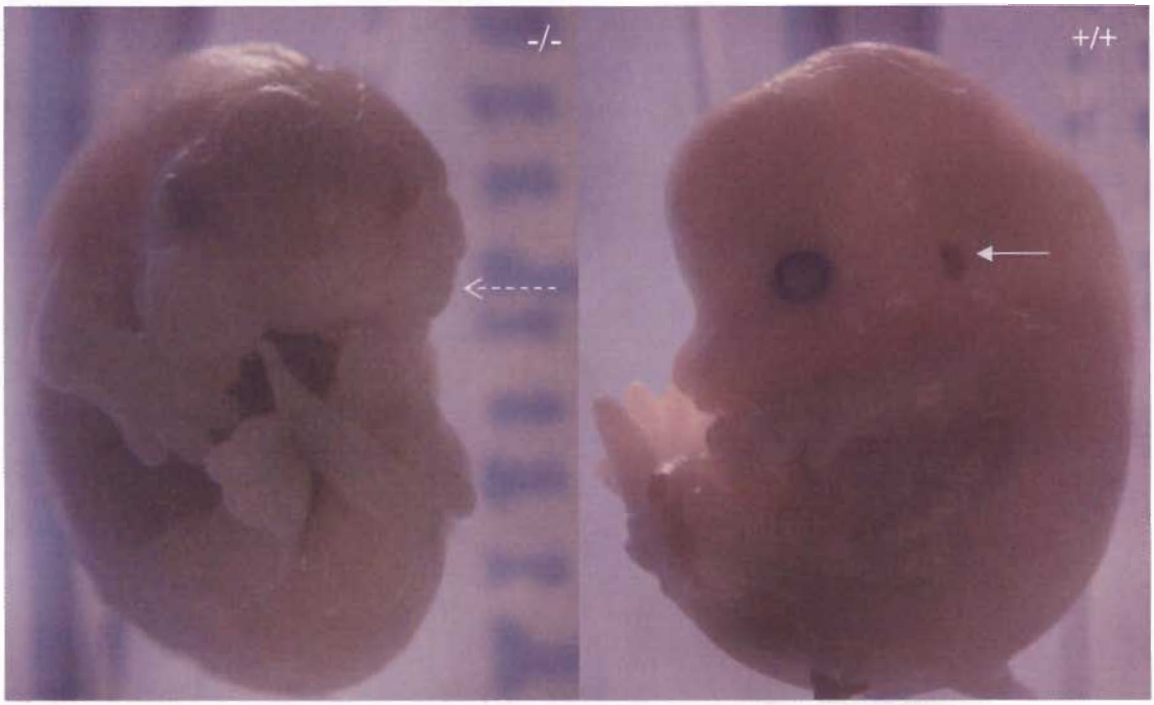

Figure 23 Absence of craniofacial development in E14.5 Tcof1 homozygous mutant. Homozygotes show severely underdeveloped maxillary and mandible prominences. The medial nasal prominence does not fuse at the midline. The solid arrow shows the normal development of external ear in control embryo. The broken arrow shows that the medial nasal prominence does not fuse at the midline. Embryos are fixed with Bouin's fixative. -/-: conditional homozygous knockouts. +/+: wildtype controls.

Cartilage development defects in Tcof1 homozygotes

To further investigate cartilage development, E12.5-E14.5 embryos were dissected and stained with alcian blue, which revealed severe cartilage defects in the craniofacial region. Meckel's cartilage is derived from the first BA and provides the template for mandible development. The majority of Meckel's cartilage disappears in the mandible while a persisting portion forms the malleus and incus middle ear ossicles. The second BA cartilage, Reichert's cartilage, gives rise to the third middle ear ossicle (stapes) and the styloid process of the temporal bone and part of the hyoid bone. From E12.5, Meckel's cartilage starts to develop in heterozygotes and wildtype littermates but not in homozygotes mutants (Figure 24). At E13.5-E14.5, Meckel's and Reichert's cartilages are well formed in controls and absent in the homozygotes (Figures 25-27). Later at E13.5, other cartilages in the head region including the nasal capsule and septal cartilage start to develop in all the controls and some of the homozygotes. The external ear cartilage seems unaffected in the homozygotes. Limb and spinal cartilages development is unaffected in the mutants (Figure 28). These findings suggest Tcof1 is essential for first and second BA cartilages development.

Down regulation of *Cnbp* expression in Tcof1 homozygotes

As described in chapter two, Cnbp was identified as a *Tcof1* downstream gene using an *in vitro* model. Here, we tested the Cnbp expression changes in the Tcof1 homozygous mutant. Wildtype littermates were used as controls. At E9.5, two of the three homozygotes examined show no expression of Cnbp in the first and second BAs

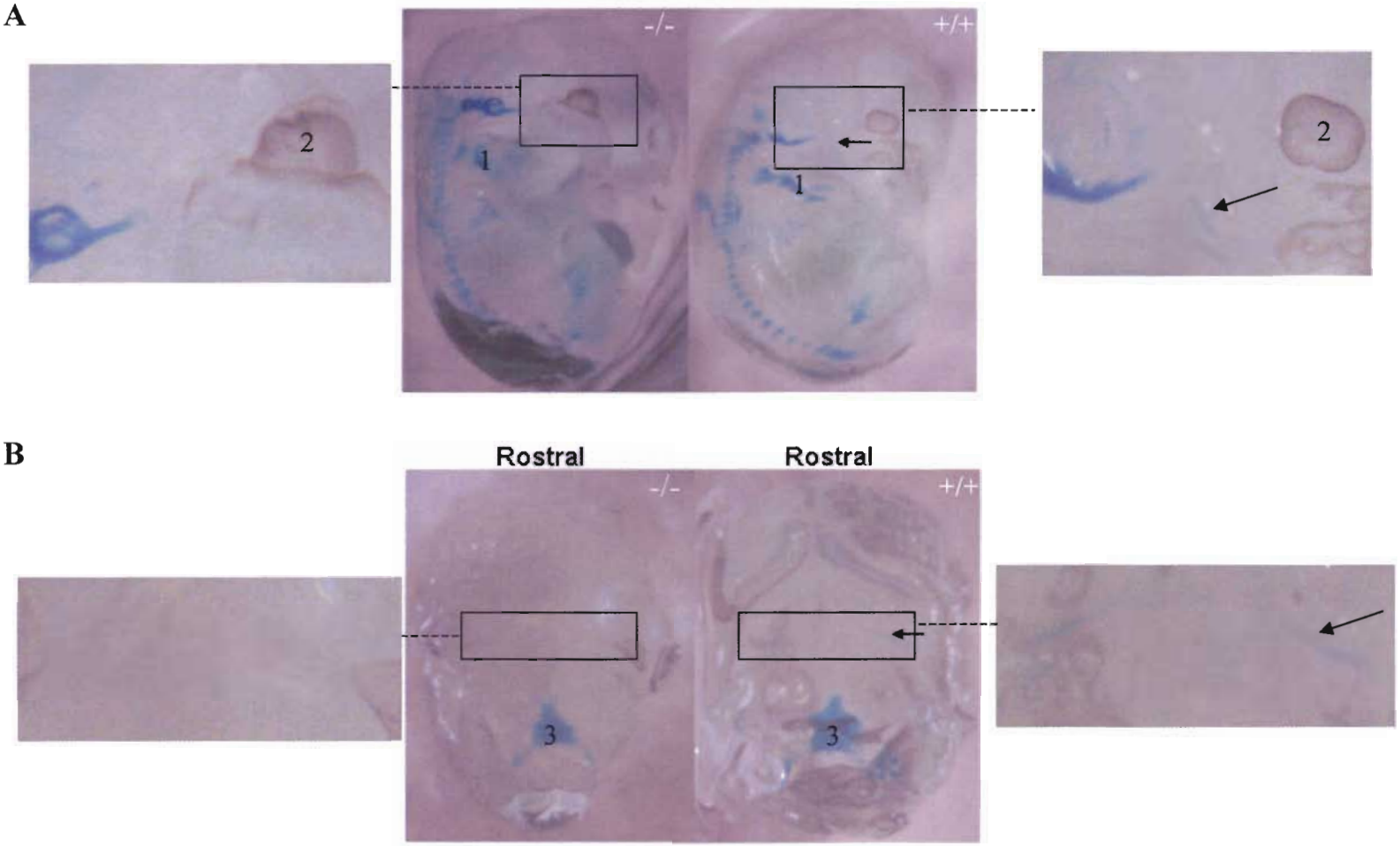

Figure 24 Absence of the Meckel's cartilage development in E12.5 Tcof1 homozygotes. A: lateral view of the whole embryos. B: ventral view of the head. These views also include close up views of the region where the Meckel's cartilage forms. Arrows show the Meckel's cartilage. 1: upper limbs. 2: eyes. 3: spine. -/-: conditional homozygous knockouts. +/+: wildtype controls.

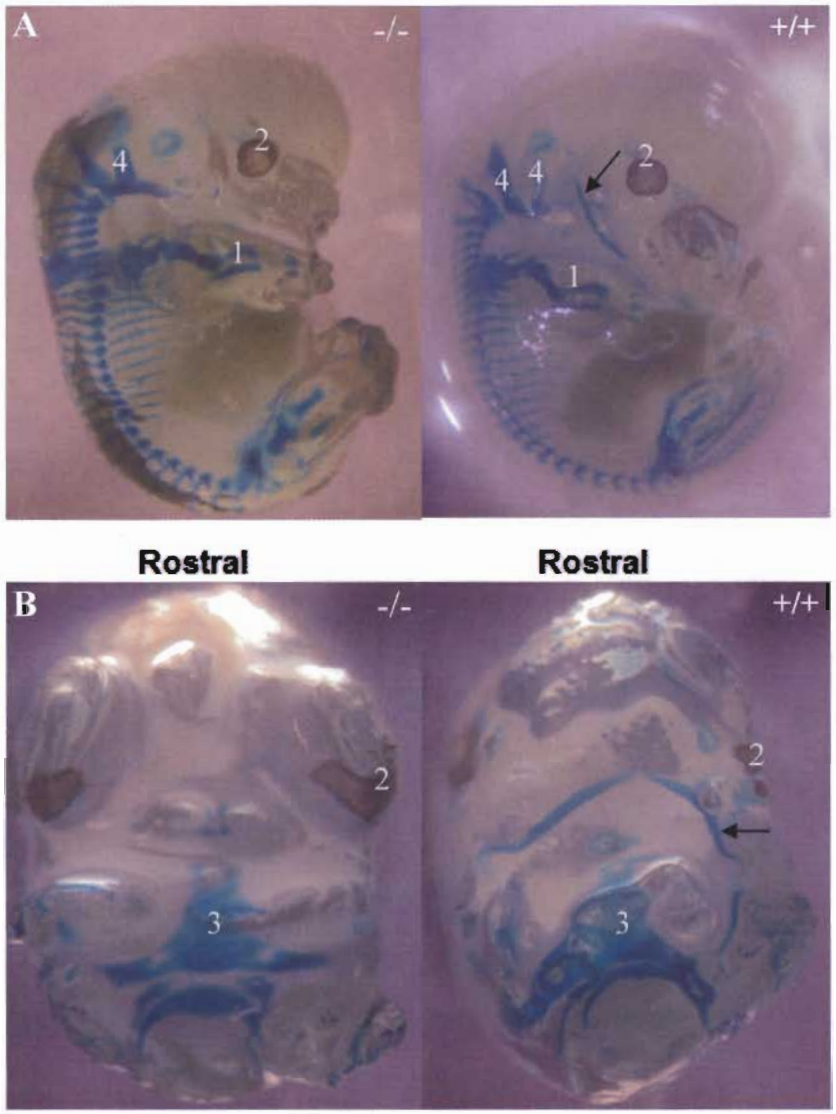

Figure 25 Absence of the Meckel's cartilage development in E13.5 Tcof1 homozygotes. A: lateral view of the whole embryos. B: ventral view of the head. -/-: conditional homozygous knockout. +/+: wildtype control. Arrows show the Meckel's cartilage. 1: upper limbs. 2: eyes. 3: spine. 4: Basiooccipital cartilages.

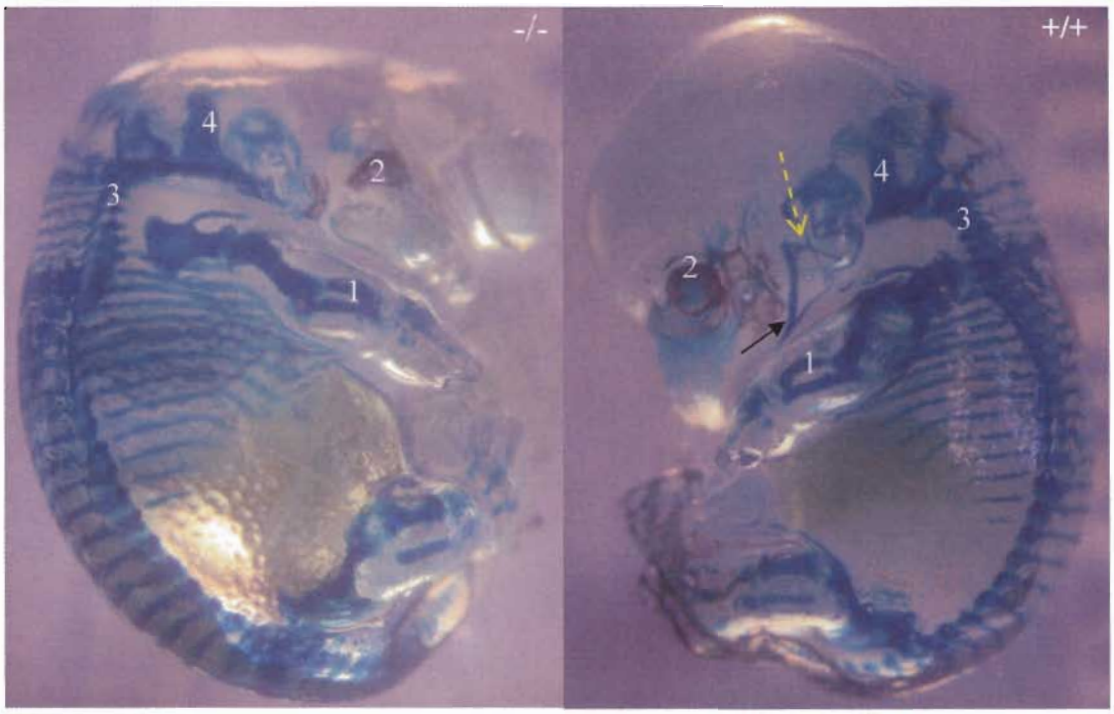

Figure 26 Absence of the Meckel's and Rechert's cartilage development in E13.5 Tcof1 homozygotes. -/-: conditional homozygous knockout. +/+: wildtype control. The solid arrow shows the Meckel's cartilage. The broken arrow shows the Rechert's cartilage. 1: upper limbs. 2: eyes. 3: spine. 4: Basiooccipital cartilages.

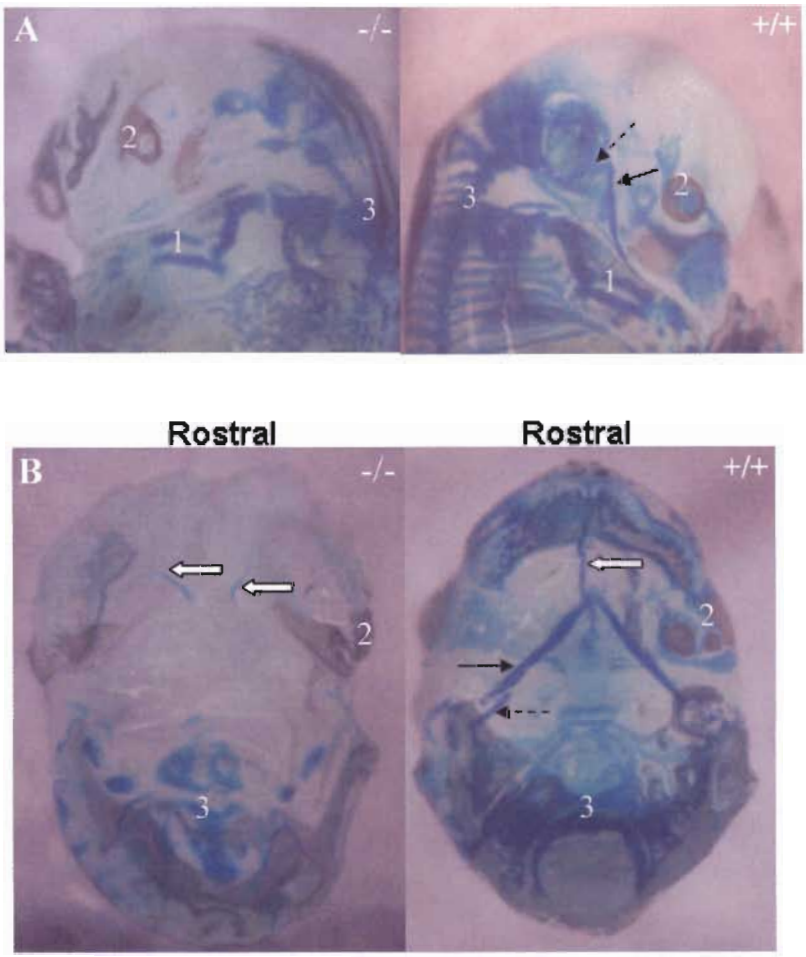

Figure 27 Absence of the Meckel's and Rechert's cartilage development in E14.5 Tcof1 homozygotes. A: lateral view of the head region of the embryos. B: ventral view of the head. -/-: conditional homozygous knockout. +/+: wildtype control. The solid arrow shows the Meckel's cartilage. The broken arrow shows the Rechert's cartilage. The white arrow shows the nasal septal cartilage. 1: upper limbs. 2: eyes. 3: spine.

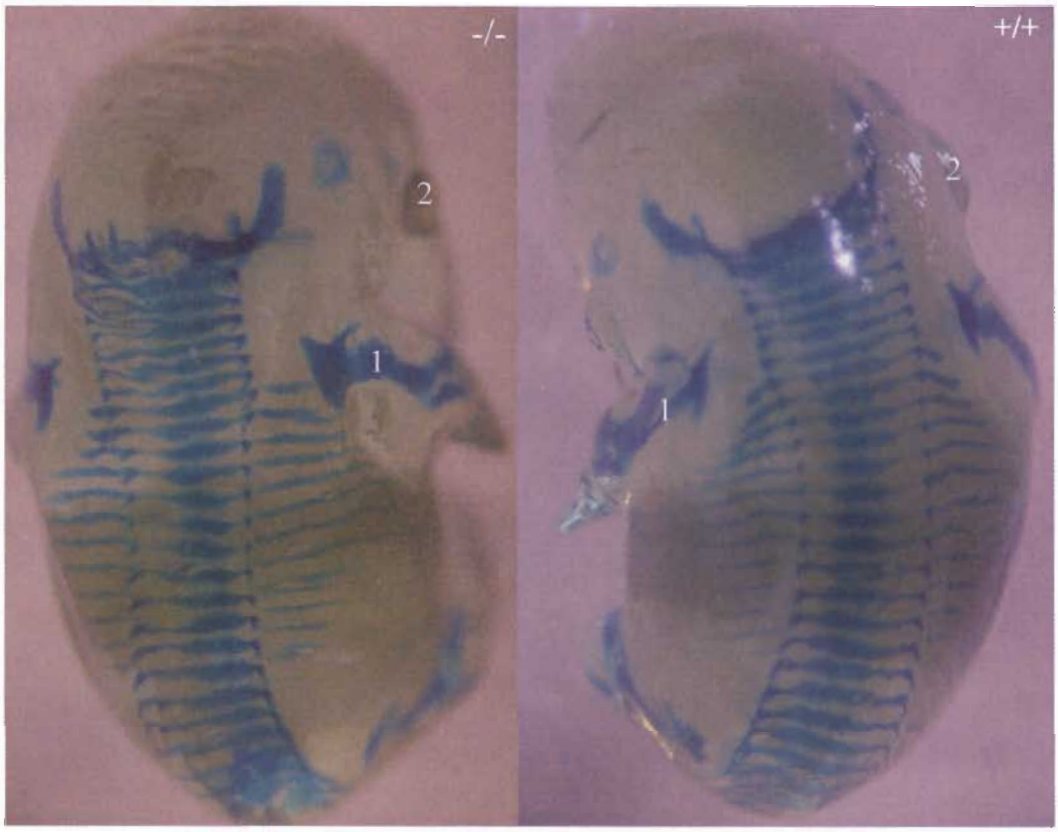

Figure 28 Normal limb and spinal cartilages development in E13.5 Tcof1 homozygotes. -/-: conditional homozygous knockout. +/+: wildtype control. 1: upper limbs. 2: eyes.

while one embryo shows almost normal Cnbp expression compared to controls (Figure 29). At E10.5 to E11.5 embryos, Cnbp expression in the craniofacial region is reduced in more severely affected embryos which did not develop craniofacial structure (Figure 29). Cnbp expression in the limb buds is not affected in any of the embryos examined. Our results give further *in vivo* evidence of Cnbp being downstream gene of *Tcof1*. The lack of Cnbp expression in some of the embryos may be also caused by the lack of the craniofacial tissues which normally expression Cnbp. On the other hand, the difference in the Cnbp expression in the homozygotes may also be caused by the slight difference in background and can be tested on homozygotes in a B6 background in the future.

Discussion

The complete knockout of Tcof1 expression in Wnt1 expressing cells causes severe abnormalities in mouse craniofacial development. The homozygous deleted mice have much smaller first and second BAs and later no signs of the developing first and second arch cartilages. The first and second arch Meckel's and Rechert's cartilages are required for the development of mandible and middle ear ossicles. TCS patients usually have abnormalities in mandible and middle ear ossicle development. Cleft palate, which affects the secondary palate, is another common symptom observed in TCS patients. The secondary palate structure comes from the maxillary prominence. The abnormal development of the maxillary prominence in homozygotes can cause abnormal secondary palate development. The phenotype of conditional homozygous knockout overlaps with

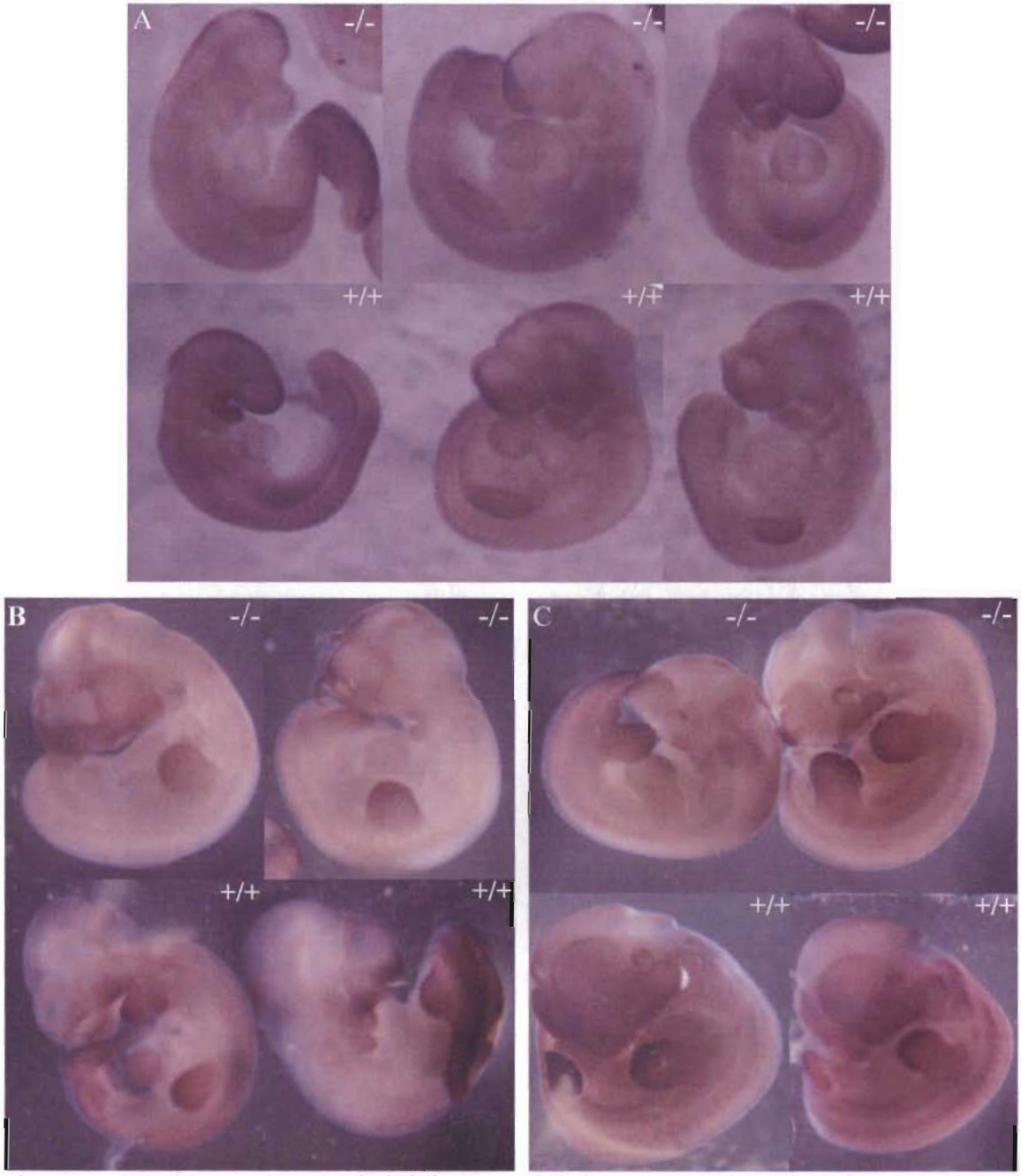

Figure 29 Whole mount *in situ* hybridization of *Cnbp* expression in Tcof1 homozygotes. Cnbp expression in the craniofacial region is reduced in more severely affected embryos which did not develop craniofacial structure. Cnbp expression in the limb buds is not affected in any of the embryos examined. A: E9.5 embryos. Two homozygotes on the left show no expression of Cnbp in the first and second BAs, while the one on the right shows almost normal Cnbp expression compared to controls. B: E10.5 embryos; C: E11.5 embryos. -/-: conditional homozygous knockouts. +/+: wildtype controls.

TCS patients including abnormal maxillary, mandible and external/middle ear, which gives further evidence for the fundamental role of Tcof1 in craniofacial development.

TCS is an autosomal dominant disease. The traditional heterozygous knockout mice are neonatal lethal in a mixed 129/B6 background. So it was surprising to observe that heterozygous mice with Tcof1 knocked out in NC cells are phenotypically normal. As early as embryonic day 7.5, Wnt1 is expressed in the midbrain and hindbrain regions of the prefusion neural fold where cranial and cardiac NC cells originate (Echelard et al., 1994). NC cells have been thought to be the main cell population affected in TCS patients. As reviewed in chapter one, NC cells and paraxial mesoderm provide the basic structure for craniofacial development but can only correctly develop when the coordinated reciprocal signals from the ectoderm, mesoderm and endoderm are present. Endoderm is indispensable for NC cell derived bone development. The conditional allele mice have also been crossed with CMV-Cre mice in a mixed 129/B6/BALB/c background. Preliminary data show homozygous knockout mice are also embryonic lethal from around E12.5 and have more severely affected phenotype including abnormalities in neural tube fusion, craniofacial, ear and eye development. Our findings suggest that Tcof1 expression in other tissues, most likely the endoderm, at an earlier time in development may also be important for craniofacial development.

As shown in chapter two, knockdown of Tcof1 in NB cells causes decreased expression of Cnbp. Cnbp is a highly conserved transcription factor with 7 zinc finger domains. Human and mouse Cnbp protein are 100% identical suggesting a fundamental role during development. Cnbp shows strong expression in the midbrain, hindbrain, first

and second BAs, limb buds and somites during mouse development (Shimizu et al., 2003; Chen et al., 2003). Cnbp homozygous knockout mice display severe forebrain and craniofacial defects and die around E10.5. About 40% of Cnbp heterozygous knockout mice die perinatally with forebrain, eye and mandible defects resembling Tcof1 knockout mice (Chen et al., 2003). Our Tcof1 knockout mouse model shows reduced Cnbp level in some of the homozygotes detected by whole mount *in situ* hybridization. Apparently, Cnbp play very important roles during craniofacial development. After Wnt1-Cre mice are transferred to a homogeneous B6 background, they will be crossed with our conditional allele mice and the Cnbp level will be examined with whole mount *in situ* hybridization. We will be able to distinguish whether the variation of Cnbp expression in our homozygotes is caused by a difference in backgrounds.

In conclusion, our conditional homozygous knockout mice show an overlapping phenotype with human TCS patients, including maxillary, mandible and external ear abnormalities. Tcof1 expression is required for mouse craniofacial development and embryo survival. Cnbp appears to be down regulated in Tcof1 conditional knockout mice.

Chapter 4: Discussion

An optimal level of Tcof1 is required for cell growth and survival

Most of the mutations identified in TCS patients introduce a premature stop codon into the protein product treacle (Splendore et al., 2005). The result of these mutations is most likely to be a severe reduction in the level of mRNA produced from the mutant allele through the nonsense mediated mRNA decay mechanism (reviewed by Behm-Ansmant I and Izaurralde E, 2006). The reduced transcript level will likely cause a reduction in the protein product level as well. Because treacle interacts with hNop56 and UBF and down regulation of treacle expression inhibits rDNA transcription, Tcof1 has been suggested to be involved in ribosome biogenesis, which is linked to cell cycle control and cell growth regulation (Hayano et al., 2003; Valdez et al., 2004; Gonzales et al., 2005). Therefore, it is important to investigate the cellular effects caused by knockdown of Tcof1, and it is interesting to see how overexpression of Tcof1 affects cell growth and survival as well.

Heterozygous Tcof1 knockout mice show an increased apoptosis level at highest Tcof1 expression sites (Dixon et al., 2000). SiRNA mediated down regulation of treacle level inhibits rRNA production (Valdez et al., 2004). Therefore, it was expected to see a decrease in cell growth and proliferation and an increase in apoptosis in Tcof1 knockdown clones. Surprisingly, overexpression of Tcof1 also causes an increase in

apoptosis level. An optimal Tcof1 level is evidently required for cells to survive and maintain proliferation.

About 30% reduction of treacle levels caused reduced NB cell proliferation and increased apoptosis. Reduced treacle levels will probably cause reduced cell proliferation and increased apoptosis in NC cells during development. Examination of the cell proliferation and apoptosis levels in the developing craniofacial region of the heterozygous and homozygous knockout mice will give us further insights of the effects of Tcof1 on cell growth *in vivo*.

Homozygous conditional knockout mouse model shows overlapping phenotype with TCS patients and traditional heterozygous knockout mouse model

The complete knockout of Tcof1 expression in Wnt1 expressing cells causes severe abnormalities in mouse craniofacial development. The homozygous deleted mice have much smaller first and second BAs and later no signs of the developing first and second arch cartilages. These are probably caused by reduced cell numbers within the cell populations in the BAs. Since the knockdown of treacle (30% reduction) in NB cells causes decreased cell proliferation and increased apoptosis levels, the complete deletion of Tcof1 is probably more detrimental to cell growth.

Comparisons of phenotypes in TCS patients and the two knockout mice models are shown in table 6. TCS patients usually have abnormalities in mandible and middle ear ossicles development. Traditional heterozygous knockout mice have smaller and shorter mandibles and hypoplastic middle ear ossicles (Dixon et al., 2000). The first and second

Table 6 Comparisons of phenotypes in TCS patients and knockout mice

Structures	TCS patients	Traditional heterozygous knockout mice (Dixon et al, 2000)	Conditional homozygous knockout mice
Mandible	Hypoplasia	Smaller and shorter	No sign of development
Maxillary	Hypoplasia	Hypoplasia	Hypoplasia
Zygomatic arch	Hypoplasia	Hypoplasia	Unable to examine
Nasal process	Normal development	Failed to develop, lack of nasal pit and nasal passages	Developed without fusion in the face midline
Secondary Palate	Cleft palate	Disorganized	No sign of development
External ear	Malformed or malposed	Low-set-cup-shaped	Absent or malformed
Middle ear ossicles	Malformed	Hypoplastic	Unable to examine
Eye	Lateral downward slanting eyes with coloboma and lack of eyelashes	Anophthalmia	Appears normal
Brain	Normal development	Exencephaly from rostral neuropore, hypoplastic forebrain and midbrain	Normal neural tube closure, hypoplastic forebrain

arch Meckel's and Rechert's cartilages are required for the development of mandible and middle ear ossicles. Our conditional homozygotes show no sign of the developing Meckel's cartilage. This will likely cause the lack of development of the mandible and middle ear ossicles, which are more severely affected than in TCS patients and traditional heterozygous mice. There are similar maxillary and external ear defects in TCS patients, heterozygous knockout mice and conditional homozygous knockout mice. Cleft palate is another common symptom observed in TCS patients. The primary palate is derived from the medial nasal prominence, which does not fuse in the midline of the face in the conditional homozygotes. The result of this is cleft lip, which is not observed in TCS patients and heterozygous knockout mice. The secondary palate structure comes from the maxillary prominence. The abnormal development of the maxillary prominence in homozygotes can cause abnormal secondary palate development. The result of this is cleft palate, which is also observed in TCS patients and heterozygous knockout mice. Traditional heterozygous knockout mice have exencephaly and anophthalmia, which are not observed in TCS patients and our conditional homozygotes (Dixon et al., 2000). Both TCS patients and traditional heterozygous knockout mice have hypoplastic zygomatic arch. The zygomatic arch was not examined in our homozygotes because most of them died before the zygomatic arch develops.

The phenotype of traditional heterozygous knockout mice overlaps TCS patients, though structures in Tcof1 heterozygous mice are affected much more severely. The heterozygous mice die shortly after birth because they are unable to establish an airway due to severe craniofacial abnormalities, the lack of nasal passages and exencephaly.

Perinatal lethality resulting from a comprised airway is rare in TCS patients. Exencephaly and anophthalmia have never been reported in TCS patients. The difference between the heterozygous knockout mice and patients may be caused by the difference in treacle expression pattern in human and mice. Mouse treacle may have broader expression and is important for brain and eye development as well as craniofacial development, while human treacle expression may be more restricted to developing craniofacial structures. Other modifier genes in human can also compensate for the effects of low treacle expression level on brain and eye development.

The phenotype of conditional homozygous knockout mice overlaps with TCS patients and traditional heterozygous knockout mice including abnormal maxillary, mandible and external/middle ear. These structures are more severely affected in our model since treacle is completely deleted in our model in these regions while the traditional knockouts and patients still have half of the normal treacle level. In our model, treacle is only deleted in NC cells when Wnt1 is expressed, while in the traditional knockout model treacle is deleted from the beginning of embryo development and in all the tissues. So the tissues affected in our model are more restricted to the tissues affected in TCS patients, which indicates that our model better resemble TCS patients.

Heterozygous conditional knockout mice are phenotypically normal

TCS is an autosomal dominant disease. The traditional heterozygous knockout mice are neonatal lethal in a mixed 129/B6 background. So it is surprising to observe that heterozygous mice in the same background with Tcof1 knocked out in NC cells are

phenotypically normal. In the conditional heterozygous knockout mice, treacle is specifically deleted only in NC cells when Wnt1 is expressed, while in the traditional knockout mice treacle is deleted from the beginning of embryo development in all the tissues. As early as embryonic day 7.5, Wnt1 is expressed in the midbrain and hindbrain regions of the prefusion neural fold where cranial and cardiac NC cells originate (Echelard et al., 1994). Treacle expression earlier than E7.5 may be important for NC cell induction and development. By the time treacle is deleted in the conditional heterozygous knockout mice, critical events may already occurred for normal craniofacial development. Whole mount *in situ* hybridization with Tcof1 in the knockout mice will give us more information about when Tcof1 is deleted.

Another explanation is that another cell population is also important for craniofacial development and it expands and compensates for the loss of NC cells. NC cells have been thought to be the main cell population affected in TCS patients. As reviewed in chapter one, NC cells and paraxial mesoderm provide the basic structures for craniofacial development but can only correctly develop when the coordinated reciprocal signals from the ectoderm, mesoderm and endoderm are present. Endoderm is indispensable for NC cell derived bone development (Piotrowski and Nusslein-Volhard, 2000). High Tcof1 expression has been detected in embryonic day 8.5 in the prefusion neural folds. Examination of *Tcof1* expression in whole mount and cross sections in earlier embryos will give us further insights into the importance of Tcof1 in cells other than NC cells and its importance for craniofacial development. We can also cross our conditional allele mice with another transgenic mouse line that has Cre under the control of a promoter

having specific endothelial expression, such as Tek-Cre mice (The Jackson Laboratory). Analyzing the phenotype of offspring of this cross and comparing them to the traditional heterozygous knockout mice and homozygotes in this study will give us further information about the physiological function of Tcof1 during development.

It is also possible that the recombination between the loxP sites to delete exon 1 of Tcof1 does not occur 100% in the conditional allele under the action of Cre. If that is the case, then the treacle level may be higher than 50% in the conditional heterozygous knockout mice, which could be enough for normal craniofacial development. The conditional allele mice have also been crossed with CMV-Cre mice in a mixed 129/B6/BALB/c background. Cre is likely to be expressed everywhere during early embryogenesis under the control of CMV. Heterozyous knockout mice from this crossing are phenotypically normal, which is not surprising because traditional knockout mice are phenotypically normal with the same background. Preliminary data show homozygous knockout mice are also embryonic lethal from around E12.5 and have more severely affected phenotype including abnormalities in neural tube fusion, craniofacial, ear and eye development. These homozygous knockout mice have same tissues affected as traditional heterozygous knockout mice with more severe phenotype, which suggests the deletion of Tcof1 occurs efficiently.

Our findings suggest that Tcof1 expression in NC cells or other tissues, most likely the endoderm, at an earlier time in development is important for craniofacial development.

Tcof1 regulates cell proliferation and apoptosis through the Cnbp-c-myc pathway

Knockdown of Tcof1 causes decreased expression in Cnbp. Cnbp, also called zinc finger protein 9 (ZNF9), is a highly conserved transcription factor with 7 zinc finger domains. Human and mouse Cnbp protein are 100% identical suggesting a fundamental role during development. Cnbp shows strong expression in the midbrain, hindbrain, first and second branchial arches, limb buds and somites during mouse development (Shimizu et al., 2003; Chen et al., 2003). A CCTG expansion in intron 1 of Cnbp is responsible for myotonic dystrophy 2 (Liquori et al., 2001). However, Cnbp homozygous knockout mice display severe forebrain and craniofacial defects and die around E10.5. About 40% of Cnbp heterozygous knockout mice die perinatally with forebrain, eye and mandible defects resembling Tcof1 knockout mice (Chen et al., 2003). Cnbp can bind the single strand CT element in the *c-myc* promoter region and enhance the transcription of *c-myc* (Michelotti., 1995; Shimizu et al., 2003). There is reduced expression of c-myc in the head region of Cnbp knockout mice (Chen et al., 2003).

Myc family member c-myc is a basic helix-loop-helix leucine zipper (bHLH-Zip) transcription factor and known to bind to the bHLH-Zip protein Max to form heterodimers and regulate transcription. c-myc is well known for its potent oncogenic activity and ability to participate in most cellular activities including cell growth, proliferation, differentiation and apoptosis. Both *in vitro* and *in vivo* knockdown of c-myc expression in breast tumor cells result in decreased cell growth and increased apoptosis (Wang et al., 2005). During mouse development, c-myc has a high level of expression in the craniofacial region. Homozygous c-myc knockout mice are embryonic

lethal before E10.5 and have severely reduced body and multiple organ (including bone) size. Heterozygous c-myc knockout mice also have smaller body size. Reduced cell number rather than smaller cell size causes the smaller organs and body sizes. Primary fibroblasts from c-myc knockout mice show reduced cell proliferation (Davis et al., 1993; Trumpp et al., 2001).

Our *in vitro* study shows that Cnbp and c-myc are down regulated in Tcof1 knockdown clones. Knockdown of Tcof1 could cause decreased cell proliferation and increased apoptosis through down regulation of Cnbp and c-myc (Figure 14). *Tcof1* knockout mouse model shows reduced *Cnbp* level in some of the homozygotes detected by whole mount *in situ* hybridization. Apparently, Cnbp and c-myc play very important roles during craniofacial development. To further investigate this, a *Cnbp* cDNA clone can be transfected into the Tcof1 knockdown clones to generate stably transfected cell lines, in which rescue of the decreased cell proliferation and increased apoptosis phenotype would confirm the effects of Cnbp on cell growth and survival. Furthermore, Cnbp transgenic mice can be mated to our Tcof1 knockout mouse model, in which rescue of the phenotype would also confirm the importance of Cnbp on craniofacial development.

The specific pathway through which treacle affects Cnbp is not clear. Treacle may act as a transcription factor and affects Cnbp transcription directly. Treacle is localized to the nucleolus. During mitosis when the nucleolus disassociates, Treacle may come in contact with the *Cnbp* promoter region. This can be tested by gel shift assays using the *Cnbp* promoter region as a probe. Treacle could also act through other transcription

factors and indirectly affect *Cnbp* transcription. Another possible explanation would be that treacle affects the stability of Cnbp. Treacle may directly bind to Cnbp and prevent it from degradation.

Treacle could regulate Cnbp/c-myc levels to maintain cell proliferation and inhibit apoptosis in BAs to preserve enough cells for later in development. After Wnt1-Cre mice are transferred to a homogeneous B6 background, they will be crossed with our conditional allele mice and the Cnbp level will be examined with whole mount *in situ* hybridization. We will be able to distinguish whether the variation of Cnbp expression in our homozygotes is caused by a difference in backgrounds.

Recently, c-myc/Max heterodimers have been shown to interact with ribosomal DNA and activate RNA Pol I transcription in vitro, which suggests c-myc may also regulate ribosomal biogenesis (Arabi et al., 2005). SiRNA mediated down-regulation of treacle expression inhibits rRNA production (Valdez et al., 2004). Treacle may also regulate ribosome biogenesis by regulating c-myc expression levels through Cnbp in addition to interacting with hNop56 and UBF.

Tcof1 and Tbx2

Tbx2 is a T box family transcription factor that can work as either an activator or repressor. Tbx2 is overexpressed in various cancer cells, including breast cancer, pancreatic cancer and melanoma, to maintain cell proliferation by repressing the activities of $p19^{ARF}$ (Cdkn2d) and $p21^{WAF1/CIP1}$ (Cdkn1a) (Lingbeek et al., 2002; Jacobs et al., 2000; Prince et al., 2004). Tbx2 has also been shown to repress the expression of the

gap junction protein, connexin 42, in osteoblastic-like cells suggesting that it may be involved in bone development (Chen et al., 2004). Together with other T box family members, Tbx2 is involved in heart, eye and limb development. Tbx2 is also expressed highly in the maxillary and mandible prominences during mouse development. Tbx2 knockout mouse models show craniofacial abnormalities (Chen et al., 2003; Harrelson et al., 2004).

In our study, the decreased Tbx2 levels in Tcof1 knockdown clones indicates that Tbx2 may be important for Tcof1 function during development. The decreased amount of Tbx2 protein in Tcof1 knockdown clones does not cause an increase in $p19^{ARF}$, $p21^{WAF1/CIP1}$ or p53 levels. Tbx2 knockout mice also show normal levels of $p19^{ARF}$, $p21^{WAF1/CIP1}$ and p53 expression (Harrelson et al., 2004). So it is unlikely that reduced Tbx2 inhibits cell proliferation and increases apoptosis through down regulation of $p19^{ARF}$ or $p21^{WAF1/CIP1}$ during development. Tbx2 may work through regulating transcription of other genes, like connexin 42, to affect bone development. Tcof1 may regulate Tbx2 and its downstream gene levels to ensure normal craniofacial skeleton development. *Tbx2* expression can be tested by whole mount *in situ* hybridization in knockout mouse model to confirm its functional connection with Tcof1. Tbx2 transgenic mice can also be used to mate with our Tcof1 knockout mouse model. Rescue of the phenotype will also confirm the importance of Tbx2 on craniofacial development.

Tbx2 levels are increased in one of the Tcof1 overexpression clone OE39 but not OE9. This indicates that a change in Tbx2 expression may not be specific to Tcof1 overexpression. A high level of treacle is harmful for cell growth. In order to survive,

OE9, which has higher treacle level than OE39, may have found a way through other cellular changes to compensate for the detrimental effects of the high overexpression of treacle on cells. Tbx2 expression could also be inhibited in OE9 by these cellular changes that has occurred in OE9. Tbx2 levels can be examined in additional Tcof1 overexpression clones to confirm the specificity of the Tbx2 overexpression as the result of Tcof1 overexpression.

Overexpression of Tcof1 affects cell proliferation and apoptosis through the p19-Mdm2-p53-p21 pathway

Overexpression of Tcof1 results in increased p53 and $p21^{WAF/CIP}$ (Cdkn1a, cyclin-dependent kinase inhibitor 1a) protein levels. The transcription factor p53 has been extensively studied and is known to respond to cellular stress, causing cell cycle arrest and apoptosis. Identified as a mediator of p53-induced growth arrest, $p21^{WAF/CIP}$ is known to bind to and inactivate cyclin-dependent kinases required for cell cycle progression. It can also associate with proliferating nuclear antigen (PCNA) and directly inhibit DNA replication (reviewed by Dotto, 2000). Tumor suppressor gene p53 is also suggested to be involved in the regulation of Pol I transcription. Immunofluorescence studies have shown that p53 is localized to both the nucleoplasm and the nucleolus (Rubbi and Milner, 2000). Immunoprecipitation shows that p53 binds to SL1 and inhibits SL1 and UBF interaction. *In vitro* transcription assays show that p53 inhibits human Pol I transcription activity (Zhai and Comai, 2000). In addition, several ribosomal proteins, such as RPL26 and nucleolin, have been shown to increase p53 level by increasing

translation of p53 or stabilizing p53, which links p53 function with ribosome biogenesis as well (Takagi et al., 2005).

Overexpression of Tcof1 could cause increased apoptosis through p53- $p21^{WAF/CIP}$ pathway (Figure 14). It was expected that increased Tbx2 level in Tcof1 overexpression clones would have reduced $p19^{ARF}$ level since Tbx2 is known to inhibit the transcription of $p19^{ARF}$ (Cdkn2d). Surprisingly, $p19^{ARF}$ is also increased in Tcof1 overexpression clones. Overexpression of $p19^{ARF}$ can inhibit cyclin D1-cdk4 activity and cause G1 arrest in the cell cycle (Hirai et al., 1995), which could be responsible for the increased G1 phase in OE39 cells. In addition, $p19^{ARF}$ can sequester Mdm2 from assisting in the degradation of p53 and increase the p53 level. Increased p53 can activate transcription of $p21^{WAF/CIP}$ and inhibit cell cycle progress at all stages and increase apoptosis through p21. While the increase of $p21^{WAF/CIP}$ could be due to increased p53, how Tcof1 up regulates $p19^{ARF}$ and p53 is still unclear and needs further investigation. Tcof1 may act as a transcription factor which affects their transcription directly or indirectly through other transcription factors. Another possible explanation would be that Tcof1 affects the stability of $p19^{ARF}$ and p53.

Embryonic lethality in conditional homozygotes suggests additional functions of Tcof1 during development

Tcof1 has a high level of expression in the developing craniofacial region and a generally low level of expression in a variety of other tissues. Conditional homozygous knockout mice die from around embryonic day 12.5. Such an early embryonic lethality is

usually caused by defects in the cardiovascular system, hematopoietic cells or placenta development.

There is often abnormal blood vessel distribution in the cranial region in homozygotes. The blood vessels in the head region in homozygotes appear to be enlarged. Whether this defect is primary or secondary to craniofacial developmental defects also needs further investigation. India ink injection into embryonic heart can be used to help visualize abnormal distribution of blood vessels. The reason for the blood vessels abnormalities is not clear, but suggesting cardiovascular system defects.

c-myc homozygous knockout mice die around E10.5 because of defects in primitive hematopoiesis which result in a pale yolk sac (Trumpp et al., 2001). Although c-myc has been shown to be down regulated with Tcof1 in neuroblastoma cells, our homozygote embryos do not show a pale yolk sac. Whether hematopoiesis is affected in our mouse model needs further investigation.

Another possible explanation for embryonic lethality in the homozygotes is through Tbx2. Tbx2 is required to repress chamber differentiation during heart development. Tbx2 homozygous knockout mouse die by E14.5 due to cardiovascular defects (Harrelson et al., 2004). Tbx2 is down regulated with knockdown of Tcof1 *in vitro*. Conditional homozygous embryos have a heart beat, but whether cardiac cells develop and differentiate correctly is not clear. They may die from heart defects caused by ablation of Tbx2 expression in the heart, which can be examined by histology and *in situ* hybridization studies with embryonic heart.

Future studies

The mechanism that Tcof1 affects Cnbp, Tbx2, p53 and $p19^{ARF}$ levels are not clear. Immunofluorescence localization study can be used to examine whether any of these proteins colocalize with Tcof1. Immunoprecipitation assays can be used to detect interaction between Tcof1 and these proteins. Colocalization and direct interaction with any of these proteins will provide more information about cellular function of treacle.

Knockdown of Tcof1 causes increased apoptosis and an increased percentage of cells in G2/M as well as G1 phase. This cannot be fully explained by down regulation of c-myc because c-myc is known to cause cell cycle arrest in G2/M phase (Ushmorov et al., 2005). Other Tcof1 candidate downstream cell cycle control genes like Bclaf1 (BCL2-associated transcription factor 1), and Rasa1 (RAS p21 protein activator 1) can be tested in knockdown clones by Western blot analysis to identify additional genes Tcof1 is associated with to regulate cell proliferation and apoptosis. Tcof1 is localized to the nucleolus and involved in rDNA transcription and pre-rRNA methylation. Nucleolar protein Nolc1 (Nucleolar and coiled-body phosphoprotein 1) and RNA processing protein Ddx42 (DEAD box polypeptide 42) are also identified as Tcof1 candidate downstream genes and their down regulation in Tcof1 knockdown cells has been confirmed by real-time PCR. Western blot analysis can also be used to confirm protein level changes. Any downstream genes confirmed by Western blot analysis can also be tested in our knockout mouse model by whole mount *in situ* hybridization to investigate their relationship with Tcof1 *in vivo*.

Knockdown of Tcof1 causes reduced cell proliferation and increased apoptosis. BrdU proliferation and TUNEL assays can also be performed on whole mount or tissue sections of conditional knockout mouse embryos to confirm the cellular effects of Tcof1 *in vivo*. Different cell type markers can be used to determine which cell type has decreased proliferation and increased apoptosis.

Histological analyses of our conditional homozygous knockout mouse embryos will also give us further information about the affected structures. Early NC cell specific markers AP2, Hfh2 and Slug can be used to trace the NC cell migration and determine if the migration is affected as well.

After determining the cell types in which Tcof1 is expressed using *in situ* hybridization on early mouse embryo tissue sections, we can breed our conditional allele mice with another transgenic mouse line that has Cre under the control of a promoter having specific expression in the identified cell type. Analyzing the phenotype of offspring from this crossing and comparing them to the traditional heterozygous knockout mice and homozygotes in this study will give us further information about the physiological function of Tcof1 during development.

Conclusions

In conclusion, this study shows an optimal Tcof1 level is required for cell proliferation and cell survival. Overexpression of Tcof1 causes increased apoptosis without affecting cell proliferation and knockdown of Tcof1 causes reduced cell proliferation and increased apoptosis. Knockdown of Tcof1 may cause decreased cell

proliferation and increased apoptosis through down regulation of Cnbp and subsequent c-myc down regulation. Overexpression of Tcof1 may cause increased apoptosis through up regulation of $p19^{ARF}$, p53 and $p21^{WAF/CIP}$.

Tcof1 conditional knockout mice show craniofacial abnormalities resembling TCS patients, but do not show the full phenotype observed in traditional knockout mice, which indicates that Tcof1 functions in tissues other than NC cells during mouse development. The abnormalities may arise from having reduced cell numbers during development due to reduced *Cnbp* expression. Without normal Tcof1 expression in the developing craniofacial region, Cnbp and c-myc may be down regulated. Abnormal craniofacial development may be caused by reduced cell numbers as the result of reduced cell proliferation and increased apoptosis.

List of References

List of References

Allende JE, Allende CC. (1995) Protein kinases. 4. Protein kinase CK2: an enzyme with multiple substrates and a puzzling regulation. *FASEB J.* 9(5):313-323. Review.

Arabi A, Wu S, Ridderstrale K, Bierhoff H, Shiue C, Fatyol K, Fahlen S, Hydbring P, Soderberg O, Grummt I, Larsson LG, Wright AP. (2005) c-Myc associates with ribosomal DNA and activates RNA polymerase I transcription. *Nat Cell Biol.* 7(3):303-310.

Bachetti T, Borghini S, Ravazzolo R, Ceccherini I. (2005) An in vitro approach to test the possible role of candidate factors in the transcriptional regulation of the RET proto-oncogene. *Gene Expr.* 12(3):137-149.

Batlle E, Sancho E, Franci C, Dominguez D, Monfar M, Baulida J, Garcia De Herreros A. (2000) The transcription factor snail is a repressor of E-cadherin gene expression in epithelial tumour cells. *Nat Cell Biol.* 2(2):84-89.

Behm-Ansmant I, Izaurralde E (2006) Quality control of gene expression: a stepwise assembly pathway for the surveillance complex that triggers nonsense-mediated mRNA decay. *Genes Dev.* 20(4):391-398.

Bernardi R, Pandolfi PP. (2003) The nucleolus: at the stem of immortality. *Nat Med.* 9(1):24-25.

Brault V, Moore R, Kutsch S, Ishibashi M, Rowitch DH, McMahon AP, Sommer L, Boussadia O, Kemler R. (2001) Inactivation of the beta-catenin gene by Wnt1-Cre-mediated deletion results in dramatic brain malformation and failure of craniofacial development. *Development.* 128(8):1253-1264.

Brewer S, Feng W, Huang J, Sullivan S, Williams T. (2004) Wnt1-Cre-mediated deletion of AP-2alpha causes multiple neural crest-related defects. *Dev Biol.* 267(1):135-152.

Cairns C, McStay B. (1995) Identification and cDNA cloning of a xenopus nucleolar phosphoprotein, xNopp180, that is the homolog of the rat nucleolar protein Nopp140. *J Cell Sci.* 108 (Pt 10):3339-3347.

Cano A, Perez-Moreno MA, Rodrigo I, Locascio A, Blanco MJ, del Barrio MG, Portillo F, Nieto MA. (2000) The transcription factor snail controls epithelial-mesenchymal transitions by repressing E-cadherin expression. *Nat Cell Biol.* 2(2):76-83.

Cesi V, Giuffrida ML, Vitali R, Tanno B, Mancini C, Calabretta B, Raschella G. (2005) C/EBP alpha and beta mimic retinoic acid activation of IGFBP-5 in neuroblastoma cells by a mechanism independent from binding to their site. *Exp Cell Res.* 305(1):179-189.

Chai Y, Jiang X, Ito Y, Bringas P Jr, Han J, Rowitch DH, Soriano P, McMahon AP, Sucov HM. (2000) Fate of the mammalian cranial neural crest during tooth and mandibular morphogenesis. *Development.* 127(8):1671-1679.

Chen HK, Pai CY, Huang JY, Yeh NH. (1999) Human Nopp140, which interacts with RNA polymerase I: implications for rRNA gene transcription and nucleolar structural organization. *Mol Cell Biol.* 19(12):8536-8546.

Chen W, Liang Y, Deng W, Shimizu K, Ashique AM, Li E, Li YP. (2003) The zinc-finger protein CNBP is required for forebrain formation in the mouse. *Development.* 130(7):1367-1379.

Chen JR, Chatterjee B, Meyer R, Yu JC, Borke JL, Isales CM, Kirby ML, Lo CW, Bollag RJ. (2004) Tbx2 represses expression of Connexin43 in osteoblastic-like cells. *Calcif Tissue Int.* 74(6):561-573.

Collins ET. (1900) Cases with symmetrical congenital notches in the outer part of each lid and defective development of the malar bones. *Trans. Ophthalmol. Soc. UK,* 20,190-192.

Compton SA, Elmore LW, Haydu K, Jackson-Cook CK, Holt SE. (2006) Induction of nitric oxide synthase-dependent telomere shortening after functional inhibition of Hsp90 in human tumor cells. *Mol Cell Biol.* 26(4):1452-62.

Couly G, Creuzet S, Bennaceur S, Vincent C, Le Douarin NM. (2002) Interactions between Hox-negative cephalic neural crest cells and the foregut endoderm in patterning the facial skeleton in the vertebrate head. *Development.* 129(4):1061-1073.

Creuzet S, Couly G, Vincent C, Le Douarin NM. (2002) Negative effect of Hox gene expression on the development of the neural crest-derived facial skeleton. *Development.* 129(18):4301-4313.

Creuzet S, Schuler B, Couly G, le Douarin NM. (2004). Reciprocal relationships between Fgf8 and neural crest cells in facial and forebrain development. *Proc Natl Acad Sci U S A.* 101(14):4843-4847.

Davis AC, Wims M, Spotts GD, Hann SR, Bradley A. (1993) A null c-myc mutation causes lethality before 10.5 days of gestation in homozygotes and reduced fertility in heterozygous female mice. *Genes Dev.* 7(4):671-682.

Dixon MJ, Read AP, Donnai D, Colley A, Dixon J, Williamson R. (1991) The gene for Treacher Collins syndrome maps to the long arm of chromosome 5. *Am J Hum Genet.* 49(1):17-22.

Dixon MJ, Dixon J, Houseal T, Bhatt M, Ward DC, Klinger K, Landes GM. (1993) Narrowing the position of the Treacher Collins syndrome locus to a small interval between three new microsatellite markers at 5q32-33.1. *Am J Hum Genet.* 52(5):907-914.

Dixon MJ. (1996) Treacher Collins Syndrome. *Hum. Mol. Genet.* 5 Spec No:1391-1396. Review.

Dixon MJ. (1996) Treacher Collins Syndrome. *J.Med. Genet* 32(10):806-808.

Dixon J, Edwards SJ, Anderson I, Brass A, Scambler PJ, Dixon MJ. (1997) Identification of the complete coding sequence and genomic organization of the Treacher Collins Syndrome gene. *Genome Res.* 7(3):223-234.

Dixon J, Brakebusch C, Fässler R, Dixon MJ. (2000) Increased levels of apoptosis in the prefusion neural folds underlie the craniofacial disorder, Treacher Collins syndrome. *Hum. Mol. Genet.* 9(10):1473-1480.

Dixon J, Dixon MJ. (2004) Genetic background has a major effect on the penetrance and severity of craniofacial defects in mice heterozygous for the gene encoding the nucleolar protein Treacle. *Dev Dyn*. 229(4):907-914.

Dorsky RI, Moon RT, Raible DW. (1998) Control of neural crest cell fate by the Wnt signalling pathway. *Nature*. 396(6709):370-373.

Dotto GP. (2000) p21(WAF1/Cip1): more than a break to the cell cycle? *Biochim Biophys Acta*. 1471(1):M43-56. Review.

Dudas M, Sridurongrit S, Nagy A, Okazaki K, Kaartinen V. (2004) Craniofacial defects in mice lacking BMP type I receptor Alk2 in neural crest cells. *Mech Dev*. 121(2):173-182.

Dunn KJ, Williams BO, Li Y, Pavan WJ. (2000) Neural crest-directed gene transfer demonstrates Wnt1 role in melanocyte expansion and differentiation during mouse development. *Proc Natl Acad Sci U S A*. 97(18):10050-10055.

Eames BF, Sharpe PT, Helms JA. (2004) Hierarchy revealed in the specification of three skeletal fates by Sox9 and Runx2. *Dev Biol.* 274(1):188-200.

Echelard Y, Vassileva G, McMahon AP. (1994) Cis-acting regulatory sequences governing Wnt-1 expression in the developing mouse CNS. *Development.* 120(8):2213-2224.

Edward SJ, Gladwin AJ, Dixon MJ. (1997) The mutational spectrum in Treacher Collins Syndrome reveals a predominance of mutations that create a premature-termination codon. *Am J Hum Genet.* 60(3):515-524.

Emes RD, Ponting CP. (2001) A new sequence motif linking lissencephaly, Treacher Collins and oral-facial-digital type 1 syndromes, microtubule dynamics and cell migration. *Hum Mol Genet.* 10(24):2813-2820.

Fotovati A, Fujii T, Yamaguchi M, Kage M, Shirouzu K, Oie S, Basaki Y, Ono M, Yamana H, Kuwano M. (2006) 17Beta-estradiol induces down-regulation of Cap43/NDRG1/Drg-1, a putative differentiation-related and metastasis suppressor gene, in human breast cancer cells. *Clin Cancer Res.* 12(10):3010-3018.

Gall JG. (2000) Cajal bodies: the first 100 years. *Annu Rev Cell Dev Biol.* 16:273-300. Review.

Garcia-Castro MI, Marcelle C, Bronner-Fraser M. (2002) Ectodermal Wnt function as a neural crest inducer. *Science*. 297(5582):848-851.

Gavrieli Y, Sherman Y, Ben-Sasson SA. (1992) Identification of programmed cell death in situ via specific labeling of nuclear DNA fragmentation. *J Cell Biol.* 119(3):493-501.

Gertsenstein M, Vintersten K, Behringer R. (2003) *Manipulating the Mouse Embryo: a Laboratory Manual.* 3rd edition. Cold Spring Harbor Laboratory.

Gladwin AJ, Dixon J, Loftus SK, Edwards S, Wasmuth JJ, Hennekam RCM, Dixon MJ. (1996) Treacher Collins Syndrome may result from insertions , deletion or splicing mutations, which introduce a termination codon into the gene. *Hum Mol Genet.* 5(10):1533-1538.

Gonzales B, Yang H, Henning D, Valdez BC. (2005) Cloning and functional characterization of the Xenopus orthologue of the Treacher Collins syndrome (TCOF1) gene product. *Gene*. 359:73-80.

Gonzales B, Henning D, So RB, Dixon J, Dixon MJ, Valdez BC. (2005) The Treacher Collins syndrome (TCOF1) gene product is involved in pre-rRNA methylation. *Hum Mol Genet.* 14(14):2035-2043.

Gorlin RJ, Cohen Jr MM, Levin LS. (1990) *Syndromes of the head and neck.* Ed Oxford University Press, Oxford.

Hannan KM, Brandenburger Y, Jenkins A, Sharkey K, Cavanaugh A, Rothblum L, Moss T, Poortinga G, McArthur GA, Pearson RB, Hannan RD. (2003) mTOR-dependent regulation of ribosomal gene transcription requires S6K1 and is mediated by phosphorylation of the carboxy-terminal activation domain of the nucleolar transcription factor UBF. *Mol Cell Biol.* 23(23):8862-8877.

Harrelson Z, Kelly RG, Goldin SN, Gibson-Brown JJ, Bollag RJ, Silver LM, Papaioannou VE. (2004) Tbx2 is essential for patterning the atrioventricular canal and for morphogenesis of the outflow tract during heart development. *Development.* 131(20):5041-5052.

Haworth KE, Islam I, Breen M, Putt W, Makrinou E, Binns M, Hopkinson D, Edwards Y. (2001) Canine TCOF1; cloning, chromosome assignment and genetic analysis in dogs with different head types. *Mamm Genome.* 12(8):622-629.

Hayano T, Yanagida M, Yamauchi Y, Shinkawa T, Isobe T, Takahashi N. (2003) Proteomic analysis of human Nop56p-associated pre-ribosomal ribonucleoprotein complexes. Possible link between Nop56p and the nucleolar protein treacle responsible for Treacher Collins syndrome. *J Biol Chem.* 278(36):34309-34319.

Heix J, Zomerdijk JC, Ravanpay A, Tjian R, Grummt I. (1997) Cloning of murine RNA polymerase I-specific TAF factors: conserved interactions between the subunits of the species-specific transcription initiation factor TIF-IB/SL1. *Proc Natl Acad Sci U S A.* 94(5):1733-1738.

Heix J, Vente A, Voit R, Budde A, Michaelidis TM, Grummt I. (1998) Mitotic silencing of human rRNA synthesis: inactivation of the promoter selectivity factor SL1 by cdc2/cyclin B-mediated phosphorylation. *EMBO J.* 17(24):7373-7381.

Hirai H, Roussel MF, Kato JY, Ashmun RA, Sherr CJ. (1995) Novel INK4 proteins, p19 and p18, are specific inhibitors of the cyclin D-dependent kinases CDK4 and CDK6. *Mol Cell Biol.* 15(5):2672-2681.

Hogan B, Beddington R, Costantini F and Lacy E. (1994) *Manipulating the Mouse Embryo: a Laboratory Manual.* 2nd edition. Cold Spring Harbor Laboratory.

Isaac C, Yang Y, Meier UT. (1998) Nopp140 functions as a molecular link between the nucleolus and the coiled bodies. *J Cell Biol.* 142(2):319-329.

Isaac C, Marsh KL, Paznekas WA, Dixon J, Dixon MJ, Jabs EW, Meier UT. (2000) Characterization of the Nucleolar Gene Product, treacle, in Treacher Collins Syndrome. *Mol Biol Cell.* 11(9):3061-3071.

Jabs EW, Li X, Coss CA, Taylor EW, Meyers DA, Weber JL. (1991) Mapping the Treacher Collins syndrome locus to 5q31.3----q33.3. *Genomics.* 11(1):193-198.

Jacobs JJ, Keblusek P, Robanus-Maandag E, Kristel P, Lingbeek M, Nederlof PM, van Welsem T, van de Vijver MJ, Koh EY, Daley GQ, van Lohuizen M. (2000) Senescence bypass screen identifies TBX2, which represses Cdkn2a (p19(ARF)) and is amplified in a subset of human breast cancers. *Nat Genet.* 26(3):291-299.

Jegalian BG, De Robertis EM. (1992) Homeotic Transformations in the Mouse Induced by Overexpression of a Human Hox3.3 Transgene. *Cell.* 71(6):901-910.

Jiang X, Iseki S, Maxson RE, Sucov HM, Morriss-Kay GM. (2002) Tissue origins and interactions in the mammalian skull vault. *Dev Biol.* 241(1):106-116.

Jones KL, Smith DW, Harvey MAS, Hall BD, Quan L. (1975) Older paternal age and fresh gene mutation: data on additional disorders. *J. Pediat.* 86(1):84-88.

Jones NC, Farlie PG, Minichiello J, Newgreen DF. (1999) Detection of an appropriate kinase activity in branchial arches I and II that coincides with peak expression of the Treacher Collins syndrome gene product, treacle. *Hum Mol Genet.* 8(12): 2239-2245.

Klein J, Grummt I. (1999) Cell cycle-dependent regulation of RNA polymerase I transcription: the nucleolar transcription factor UBF is inactive in mitosis and early G1. *Proc Natl Acad Sci U S A*.96(11):6096-6101.

Kurdistani SK, Arizti P, Reimer CL, Sugrue MM, Aaronson SA, Lee SW. (1998) Inhibition of tumor cell growth by RTP/rit42 and its responsiveness to p53 and DNA damage. *Cancer Res*. 58(19):4439-4444.

LaBonne C, Bronner-Fraser M. (1998) Neural crest induction in Xenopus: evidence for a two-signal model. *Development*. 125(13):2403-2414.

Labosky PA, Kaestner KH. (1998) The winged helix transcription factor Hfh2 is expressed in neural crest and spinal cord during mouse development. *Mech Dev*. 76(1-2):185-190.

Lammer EJ, Chen DT, Hoar RM, Agnish ND, Benke PJ, Braun JT, Curry CJ, Fernhoff PM, Grix AJ Jr, Lott IT, Richard JM, and Sun SC. (1985) Retinoic acid embryopathy. *N Engl J Med* 313: 837–841.

Lewis JL, Bonner J, Modrell M, Ragland JW, Moon RT, Dorsky RI, Raible DW. (2004) Reiterated Wnt signaling during zebrafish neural crest development. *Development*. 131(6):1299-1308.

Li D, Meier T, Dobrowolska G, Krebs EG. (1997) Specific interaction between Casein Kinase 2 and the nucleolar protein Nopp140. *J Biol Chem.* 272(6):3773-3779.

Lingbeek ME, Jacobs JJ, van Lohuizen M. (2002) The T-box repressors TBX2 and TBX3 specifically regulate the tumor suppressor gene p14ARF via a variant T-site in the initiator. *J Biol Chem.* 277(29):26120-26127.

Liquori CL, Ricker K, Moseley ML, Jacobsen JF, Kress W, Naylor SL, Day JW, Ranum LP. (2001) Myotonic dystrophy type 2 caused by a CCTG expansion in intron 1 of ZNF9. *Science.* 293(5531):864-867.

Marchant L, Linker C, Ruiz P, Guerrero N, Mayor R. (1998) The inductive properties of mesoderm suggest that the neural crest cells are specified by a BMP gradient. *Dev Biol.* 198(2):319-329.

Marszalek B, Wojcicki P, Kobus K, Trzeciak WH. (2002) Clinical features, treatment and genetic background of Treacher Collins syndrome. *J Appl Genet.* 43(2):223-233.

Marsh KL, Dixon J, Dixon MJ, (1998) Mutation in the Treacher Collins syndrome gene lead to mislocalization of the nucleolar protein treacle. *Hum Mol Genet.* 7(11),1795-1801.

Mayor R, Morgan R, Sargent MG. (1995) Induction of the prospective neural crest of Xenopus. *Development*. 121(3):767-777.

Meier UT and Blobel G. (1992) Nopp140 shuttles on tracks between nucleolus and cytoplasm. *Cell*. 70(1):127-138.

Meier U.T. (1996) Comparison of the rat nucleolar protein nopp140 with its yeast homolog SRP40. Differential phosphorylation in vertebrates and yeast. *J Biol Chem.* 271(32):19376-19384.

Miau L, Chang C, Tsai W, Lee S. (1997) Identification and characterization of a nucleolar phosphoprotein, Nopp140, as a transcription factor. *Mol Cell Biol*. 17(1):230-239.

Michelotti EF, Tomonaga T, Krutzsch H, Levens D. (1995) Cellular nucleic acid binding protein regulates the CT element of the human c-myc protooncogene. *J Biol Chem.* 270(16):9494-9499.

Milstone DS, Bradwin G, Mortensen RM. (1999) Simultaneous Cre catalyzed recombination of two alleles to restore neomycin sensitivity and facilitate homozygous mutations. *Nucleic Acids Res*. 27(15):e10.

Mogass M, York TP, Li L, Rujirabanjerd S, Shiang R. (2004) Genomewide analysis of gene expression associated with Tcof1 in mouse neuroblastoma. *Biochem Biophys Res Commun*. 325(1):124-132.

Monsoro-Burq AH, Fletcher RB, Harland RM. (2003) Neural crest induction by paraxial mesoderm in Xenopus embryos requires FGF signals. *Development*. 130(14):3111-3124.

Monsoro-Burq AH, Wang E, Harland R. (2005) Msx1 and Pax3 cooperate to mediate FGF8 and WNT signals during Xenopus neural crest induction. *Dev Cell*. 8(2):167-178.

Moore KL, Persaud TVN. (1993) *The Developing Human, Clinically Oriented Embryology*. 5th ed. Philadelphia: W. B. Saunders Company.

Mori-Akiyama Y, Akiyama H, Rowitch DH, de Crombrugghe B. (2003) Sox9 is required for determination of the chondrogenic cell lineage in the cranial neural crest. *Proc Natl Acad Sci U S A*. 100(16):9360-9365.

Müller U. (1999) Ten years of gene targeting: targeted mouse mutants, from vector design to phenotype analysis. *Mech. of Develop.* 82:3-21.

Nazar RN. (2004) Ribosomal RNA processing and ribosome biogenesis in eukaryotes. *IUBMB Life*. 56(8):457-465. Review.

Neave B, Holder N, Patient R. (1997) A graded response to BMP-4 spatially coordinates patterning of the mesoderm and ectoderm in the zebrafish. *Mech Dev.* 62(2):183-195.

Nichols DH. (1986) Formation and distribution of neural crest mesenchyme to the first pharyngeal arch region of the mouse embryo. *Am J Anat.* 176(2):221-231.

Noden DM. (1983). The embryonic origins of avian cephalic and cervical muscles and associated connective tissues. *Am J Anat.* 168(3):257-276.

Osumi-Yamashita N, Ninomiya Y, Doi H, Eto K. (1994) The contribution of both forebrain and midbrain crest cells to the mesenchyme in the frontonasal mass of mouse embryos. *Dev Biol.* 164(2):409-419.

Pai CY, Chen HK, Sheu HL, Yeh NH. (1995) Cell-cycle-dependent alterations of a highly phosphorylated nucleolar protein p130 are associated with nucleologenesis. *J Cell Sci.* 108 (Pt 5):1911-1920.

Parr BA, Shea MJ, Vassileva G, McMahon AP. (1993) Mouse Wnt genes exhibit discrete domains of expression in the early embryonic CNS and limb buds. *Development.* 119(1):247-261.

Paznekas WA, Zhang N, Gridley T, Jabs EW. (1997) Mouse TCOF1 is expressed widely, has motifs conserved in nucleolar phosphoproteins, and maps to chromosome 18. *Biochem Biophys Res Commun.* 238(1):1-6.

Pederson T. (1998) The plurifunctional nucleolus. *Nucleic Acids Res.* 26(17):3871-3876. Review.

Piotrowski T, Nusslein-Volhard C. (2000) The endoderm plays an important role in patterning the segmented pharyngeal region in zebrafish (Danio rerio). *Dev Biol.* 225(2):339-356.

Posnick JC and Ruiz RL. (2000) Treacher Collins syndrome: current evaluation, treatment, and future directions. *Cleft Palate Craniofac J.* 37(5):434.

Poswillo D. (1975) The pathogenesis of the Treacher Collins syndrome (mandibulofacial dysostosis). *Br J Oral Surg.* 13(1):1-26.

Prince S, Carreira S, Vance KW, Abrahams A, Goding CR. (2004) Tbx2 directly represses the expression of the p21(WAF1) cyclin-dependent kinase inhibitor. *Cancer Res.* 64(5):1669-1674.

Rovin S, Dachi SF, Borenstein DB, Cotter WB. (1964) Mandibulofacial dysostosis, a familial study of five generations. *J Pediatr.* 65:215-221.

Rubbi CP, Milner J. (2000) Non-activated p53 co-localizes with sites of transcription within both the nucleoplasm and the nucleolus. *Oncogene.* 19(1):85-96.

Rujirabanjerd S, Winokur ST, Shiang R. (1999) Characterization of the murine homolog of the Treacher Collins Syndrome gene product, treacle. 49th Annual Meeting of the American Society of Human Genetics, San Francisco, California.

Rujirabanjerd S. (2003) *Characterization of the Treacher Collins Syndrome (TCOF1) gene and its gene product, Treacle.* Unpublished Doctoral Dissertation, Virginia Commonwealth University, Richmond.

Sakai D, Tanaka Y, Endo Y, Osumi N, Okamoto H, Wakamatsu Y. (2005) Regulation of Slug transcription in embryonic ectoderm by beta-catenin-Lef/Tcf and BMP-Smad signaling. *Dev Growth Differ.* 47(7):471-482.

Santagati F, Minoux M, Ren SY, Rijli FM. (2005) Temporal requirement of Hoxa2 in cranial neural crest skeletal morphogenesis. *Development.* 132(22):4927-4936.

Santoro R, Grummt I. (2001) Molecular mechanisms mediating methylation-dependent silencing of ribosomal gene transcription. *Mol Cell.* 8(3):719-725.

Sauer B, Henderson N. (1989) Cre-stimulated recombination at loxP-containing DNA sequences placed into the mammalian genome. *Nucleic Acids Res.* 17(1):147-161.

Savagner P, Yamada KM, Thiery JP. (1997) The zinc-finger protein slug causes desmosome dissociation, an initial and necessary step for growth factor-induced epithelial-mesenchymal transition. *J Cell Biol.* 137(6):1403-1419.

Savagner P, Karavanova I, Perantoni A, Thiery JP, Yamada KM. (1998) Slug mRNA is expressed by specific mesodermal derivatives during rodent organogenesis. *Dev Dyn.* 213(2):182-187.

Serbedzija GN, Bronner-Fraser M, Fraser SE. (1992) Vital dye analysis of cranial neural crest cell migration in the mouse embryo. *Development.* 116(2):297-307.

Shimizu K, Chen W, Ashique AM, Moroi R, Li YP. (2003) Molecular cloning, developmental expression, promoter analysis and functional characterization of the mouse CNBP gene. *Gene.* 307:51-62.

Shimono A, Okuda T, Kondoh H. (1999) N-myc-dependent repression of ndr1, a gene identified by direct subtraction of whole mouse embryo cDNAs between wild type and N-myc mutant. *Mech Dev.* 83(1-2):39-52.

Shows KH, Ward C, Summers L, Li L, Ziegler GR, Hendrickx AG, Shiang R. (2006) Reduced TCOF1 mRNA level in a rhesus macaque with Treacher Collins-like syndrome: further evidence for haploinsufficiency of treacle as the cause of disease. *Mamm Genome.* 17(2):168-177.

Smith TK, Nylander KD, Schor NF. (1998) The roles of mitotic arrest and protein synthesis in induction of apoptosis and differentiation in neuroblastoma cells in culture. *Brain Res Dev Brain Res.* 105(2):175-180.

So RB, Gonzales B, Henning D, Dixon J, Dixon MJ, Valdez BC. (2004) Another face of the Treacher Collins Syndrome (TCOF1) gene: identification of additional exons. *Gene.* 328:49-57.

Soriano P. (1997) The PDGF alpha receptor is required for neural crest cell development and for normal patterning of the somites. *Development.* 124(14):2691-2700.

Spector DL. (1993) Macromolecular domains within the cell nucleus. *Annu Rev Cell Biol.* 9:265-315. Review.

Splendore A, Fanganiello RD, Masotti C, Morganti LSC, Passos-Bueno MR. (2005) TCOF1 Mutation Database: Novel Mutation in the Alternatively Spliced Exon 6A and Update in Mutation Nomenclature. *Hum Mutat.* 25(5):429-434.

Stefanovsky VY, Pelletier G, Hannan R, Gagnon-Kugler T, Rothblum LI, Moss T. (2001) An immediate response of ribosomal transcription to growth factor stimulation in mammals is mediated by ERK phosphorylation of UBF. *Mol Cell.* 8(5):1063-1073.

Sulik KK, Johnston MC, Smiley SJ, Speight HS, Jarvis BE. (1987) Mandibulofacial dysostosis (Treacher Collins syndrome): a new proposal for its pathogenesis. *Am J Med Genet.* 27(2):359-372.

Swiatek PJ, Gridley T. (1993) Perinatal lethality and defects in hindbrain development in mice homozygous for a targeted mutation of the zinc finger gene Krox20. *Genes Dev.* 7(11):2071-2084.

Takagi M, Absalon MJ, McLure KG, Kastan MB. (2005) Regulation of p53 translation and induction after DNA damage by ribosomal protein L26 and nucleolin. *Cell.* 123(1):49-63.

Teber OA, Gillessen-Kaesbach G, Fischer S, Bohringer S, Albrecht B, Albert A, Arslan-Kirchner M, Haan E, Hagedorn-Greiwe M, Hammans C, Henn W, Hinkel GK, Konig R,

Kunstmann E, Kunze J, Neumann LM, Prott EC, Rauch A, Rott HD, Seidel H, Spranger S, Sprengel M, Zoll B, Lohmann DR, Wieczorek D. (2004) Genotyping in 46 patients with tentative diagnosis of Treacher Collins syndrome revealed unexpected phenotypic variation. *Eur J Hum Genet.* 12(11):879-890.

Tollervey D, Lehtonen H, Jansen R, Kern H, Hurt EC. (1993) Temperature-sensitive mutations demonstrate roles for yeast fibrillarin in pre-rRNA processing, pre-rRNA methylation, and ribosome assembly. *Cell.* 72(3):443-457.

Trainor PA, Tan SS, Tam PP. (1994) Cranial paraxial mesoderm: regionalisation of cell fate and impact on craniofacial development in mouse embryos. *Development.* 120(9):2397-2408.

Trainor PA, Tam PP. (1995) Cranial paraxial mesoderm and neural crest cells of the mouse embryo: co-distribution in the craniofacial mesenchyme but distinct segregation in branchial arches. *Development.* 121(8):2569-2582.

Trainor PA. (2005) Specification of neural crest cell formation and migration in mouse embryos. *Semin Cell Dev Biol.* 16(6):683-693. Review.

Treacher Collins Syndrome Collaborative group. (1996) Positional cloning of a gene involved in the pathogenesis of Treacher Collins syndrome. *Nat Genet.* 12(2):130-136.

Trumpp A, Refaeli Y, Oskarsson T, Gasser S, Murphy M, Martin GR, Bishop JM. (2001) c-Myc regulates mammalian body size by controlling cell number but not cell size. *Nature*. 414(6865):768-73.

Tsai RY, McKay RD. (2002) A nucleolar mechanism controlling cell proliferation in stem cells and cancer cells. *Genes Dev*. 16(23):2991-3003.

Tuan JC, Zhai W, Comai L. (1999) Recruitment of TATA-binding protein-TAFI complex SL1 to the human ribosomal DNA promoter is mediated by the carboxy-terminal activation domain of upstream binding factor (UBF) and is regulated by UBF phosphorylation. *Mol Cell Biol.* 19(4):2872-2879.

Ushmorov A, Debatin KM, Beltinger C. (2005) Growth inhibition of murine neuroblastoma cells by c-myc with cell cycle arrest in G2/M. *Cancer Biol Ther*. 4(2):181-186.

Valdez BC, Henning D, So RB, Dixon J, Dixon MJ. (2004) The Treacher Collins syndrome (TCOF1) gene product is involved in ribosomal DNA gene transcription by interacting with upstream binding factor. *Proc Natl Acad Sci U S A*. 101(29):10709-10714.

Veitch E, Begbie J, Schilling TF, Smith MM, Graham A. (1999) Pharyngeal arch patterning in the absence of neural crest. *Curr Biol.* 9(24):1481-1484.

Voit R, Schnapp A, Kuhn A, Rosenbauer H, Hirschmann P, Stunnenberg HG, Grummt I. (1992) The nucleolar transcription factor mUBF is phosphorylated by casein kinase II in the C-terminal hyperacidic tail which is essential for transactivation. *EMBO J.* 11(6):2211-2218.

Wang YH, Liu S, Zhang G, Zhou CQ, Zhu HX, Zhou XB, Quan LP, Bai JF, Xu NZ. (2005) Knockdown of c-Myc expression by RNAi inhibits MCF-7 breast tumor cells growth in vitro and in vivo. *Breast Cancer Res.* 7(2):R220-228.

Wise CA, Chiang LC, Paznekas WA, Sharma M, Musy MM, Ashley JA, Lovett M, Jabs EW. (1997) TCOF1 gene encodes a putative nucleolar phosphoprotein that exhibits mutations in Treacher Collins Syndrome throughout its coding region. *Proc Natl Acad Sci U S A.* 94(7):3110-3115.

Wilson PA, Lagna G, Suzuki A, Hemmati-Brivanlou A. (1997) Concentration-dependent patterning of the Xenopus ectoderm by BMP4 and its signal transducer Smad1. *Development.* 124(16):3177-3184.

Winokur ST, Shiang R. (1998) The Treacher Collins syndrome (TCOF1) gene product, treacle, is targeted to the nucleolus by signals in its C-terminus. *Hum Mol Genet.* 7(12):1947-1952.

Wise CA, Chiang LC, Paznekas WA, Sharma M, Musy MM, Ashley JA, Lovett M, Jabs EW. (1997) TCOF1 gene encodes a putative nucleolar phosphoprotein that exhibits mutations in Treacher Collins Syndrome throughout its coding region. *Proc Natl Acad Sci U S A.* 94(7):3110-3115.

Yamauchi Y, Abe K, Mantani A, Hitoshi Y, Suzuki M, Osuzu F, Kuratani S, Yamamura K. (1999) A Novel Transgenic Technique That Allows Specific Marking of the Neural Crest Cell Lineage in Mice. *Dev Biol.* 212(1):191-203.

Zebarjadian Y, King T, Fournier MJ, Clarke L, Carbon J. (1999) Point mutations in yeast CBF5 can abolish in vivo pseudouridylation of rRNA. *Mol Cell Biol.* 19(11):7461-7472.

Zhai W, Comai L. (2000) Repression of RNA polymerase I transcription by the tumor suppressor p53. *Mol Cell Biol.* 20(16):5930-5938.

VITA

Lin Li was born on Jan 23, 1976 in Jinan, Shandong province, China and is a Chinese citizen. She graduated from Shandong Experimental Middle School in 1992. She received her Doctor in Medicine degree from Shandong Medical University, Jinan, China in 1997. She received a Master of Science degree in Genetics from Qingdao Medical School, Qingdao, China in 2000.